INVESTIGATION OF AERODYNAMIC AND STRUCTURAL FEATURES OF TWISTING TALL BUILDINGS

A THESIS SUBMITTED TO
THE GRADUATE SCHOOL OF NATURAL AND APPLIED SCIENCES
OF
MIDDLE EAST TECHNICAL UNIVERSITY

BY

SİNAN BİLGEN

IN PARTIAL FULFILLMENT OF THE REQUIREMENTS
FOR
THE DEGREE OF MASTER OF SCIENCE
IN
BUILDING SCIENCE IN ARCHITECTURE

SEPTEMBER 2019

Approval of the thesis:

INVESTIGATION OF AERODYNAMIC AND STRUCTURAL FEATURES OF TWISTING TALL BUILDINGS

submitted by **SİNAN BİLGEN** in partial fulfillment of the requirements for the degree of **Master of Science in Building Science in Architecture Department Department, Middle East Technical University** by,

Prof. Dr. Halil Kalıpçılar
Dean, Graduate School of **Natural and Applied Sciences** _____

Prof. Dr. Fatma Cânâ Bilsel
Head of Department, **Archicture** _____

Assist. Prof. Dr. Bekir Özer Ay
Supervisor, **Department of Architecture, METU** _____

Assoc. Prof. Dr. Nilay Sezer Uzol
Co-Supervisor, **Aerospace Engineering, METU** _____

Examining Committee Members:

Assoc. Prof. Dr. Mehmet Halis Günel
Department of Architecture, METU _____

Assist. Prof. Dr. Bekir Özer Ay
Department of Architecture, METU _____

Assoc. Prof. Dr. Nilay Sezer Uzol
Department of Aerospace Engineering, METU _____

Prof. Dr. Murat Altuğ Erberik
Department of Civil Engineering, METU _____

Prof. Dr. Can Balkaya
Department of Civil Engineering, Beykent University _____

Date: 05.09.2019

I hereby declare that all information in this document has been obtained and presented in accordance with academic rules and ethical conduct. I also declare that, as required by these rules and conduct, I have fully cited and referenced all material and results that are not original to this work.

Name, Surname: Sinan Bilgen

Signature:

ABSTRACT

INVESTIGATION OF AERODYNAMIC AND STRUCTURAL FEATURES OF TWISTING TALL BUILDINGS

Bilgen, Sinan
Master of Science, Building Science in Architecture
Supervisor: Assist. Prof. Dr. Bekir Özer Ay
Co-Supervisor: Assoc. Prof. Dr. Nilay Sezer Uzol

September 2019, 108 pages

After decades of conventional shapes, irregular forms with complex geometries are getting more popular for form generation of tall buildings all over the world. This trend has recently brought out diverse building forms such as twisting tall buildings. This study investigates both the aerodynamic and structural features of twisting tall buildings through comparative analyses. Since twisting a tall building gives rise to additional complexities related with the form and structural system, lateral load effects become of greater importance on these buildings. The aim of this study is to analyze the inherent characteristics of these iconic forms by comparing the wind loads on twisting tall buildings with those on their prismatic twins. The prismatic twin of the twisting form was generated by removing the progressive rotation of the floors where the floor plan area and the story height kept the same. Through a case study research, aerodynamic analyses of an existing twisting tall building and its prismatic counterpart were performed, and the results have been compared. High-frequency base balance (HFBB) tests and synchronous pressure measurement tests on twisting and prismatic 3D models were performed to evaluate wind load effects. Comparisons of mean and maximum base moments with respect to different wind directions are performed together with the resultant moments. Performance-based analyses under investigation

have been evaluated in accordance with the aerodynamic loads obtained from HFBB tests. This way, base shear forces, story displacements, torsional moments and the distribution of loads on structural members are examined. Comparisons highlight that, the twisting form under investigation is aerodynamically better due to less wind loads both for along and across wind directions. Compared to the prismatic counterpart; twisting model is competitor in terms of roof drift and member forces due to relatively less wind loads on it but subjected to higher torsion levels.

Keywords: Twisting Tall Buildings, Aerodynamic Features, High-Frequency Base Balance Test, Synchronous Pressure Measurement Test, Structural Response

ÖZ

BURGULU YÜKSEK BİNALARIN AERODİNAMİK VE YAPISAL ÖZELLİKLERİNİN İNCELENMESİ

Bilgen, Sinan
Yüksek Lisans, Yapı Bilimleri
Tez Danışmanı: Dr. Öğr. Üyesi Bekir Özer Ay
Ortak Tez Danışmanı: Doç. Dr. Nilay Sezer Uzol

Eylül 2019, 108 sayfa

Geleneksel prizmatik formdaki yüksek yapılara alternatif olarak yakın dönemde ortaya çıkmış olan yenilikçi karmaşık geometrili tasarımların önemli örneklerinden biri de burgulu yüksek binalardır. Bu çalışmanın amacı burgulu yüksek yapıların doğasından gelen ilave karmaşıklık ve zorlukları, formun aerodinamik üstünlükleri ile birlikte değerlendirmektir. Çalışma kapsamında burgulu yüksek yapıların aerodinamik ve yapısal performansı incelenmiştir. Bu çalışmada burgu formlu ve prizmatik özdeş yüksek yapı tasarımları üzerinden zorluklar ve üstünlükler bir arada ele alınmıştır. Prizmatik özdeş model, burgulu modelin herhangi bir dönme veya burulmaya uğratılmadan konvansiyonel bir şekilde, başka bir deyişle bina katları boyunca değişime uğramadan yükseltilmesi yoluyla elde edilmiştir. Prizmatik ve burgu formlu yapı modellerinin yüksek frekanslı taban balans (YFTB) testleri ve eş zamanlı basınç ölçüm testleri yapılmıştır. Farklı rüzgâr açılarına göre ortalama ve maksimum taban momentlerinin karşılaştırılması bileşke moment ile birlikte dikkate alınmıştır. YFTB testlerinin sonucunda hesaplanan aerodinamik yükler yapısal analiz programına sokulmuş, kesit ve yükseklik açısından özdeş yapılar üzerindeki rüzgâr etkileri incelenmiştir. Sonuçlar ışığında, burgulu yapının hem rüzgâr etkilerini azaltma konusunda hem de bu yüklerin etkisi altında kesme kuvvetleri, moment ve kat

ötelenmesi konusunda daha avantajlı oldukları görülmüştür. Öte yandan burgulu bina modelinin daha fazla burulma momentine maruz kaldığı yapısal analizler sonucunda bulunmuştur.

Anahtar Kelimeler: Burgulu Yüksek Binalar, Aerodinamik Özellikler, Yüksek Frekanslı Taban Balans Testi, Eş Zamanlı Basınç Ölçüm Testi, Yapısal Davranış

To my beloved family

ACKNOWLEDGEMENTS

My first and deepest gratitude is to my thesis supervisor Assist. Prof. Dr. Bekir Özer Ay for encouragement, great guidance, limitless patience and sharing knowledge through the whole process. His contribution to the study is admirable. I also thank for the responses irrespective of time but whenever I needed. I sincerely feel lucky to know and to work with a mentor who inspires me.

I'm also grateful to my co-advisor Assoc. Prof. Dr. Nilay Sezer Uzol for her insightful comments and contribution not only to the thesis but also to the publication of ACE conference in İzmir. I'm deeply thankful to research assistant Ezgi Orbay for the contributions related to BAP research project and for conducting CFD analyses.

I would like to thank Assoc. Prof. Dr. Mehmet Halis Günel for his academic support and valuable feedbacks about the tall buildings.

Special thanks to my cousin Yasin Çevik and beloved friends Hamza Yanık, Emre Akyüz, Göktuğ Baysal and Faruk Kınacı for sharing their help.

I would like thank Prof. Dr. Oğuz Uzol for his support on using facilities at METUWIND and owe to acknowledge Dr. Yashar Ostovan for his guidance on measurements of wind tunnel tests. In addition, the author is also grateful to Prof. Dr. İrem Dikmen Toker, Prof. Dr. Arzu Gönenç Sorguç and MSc Serkan Ülgen for their support on use of equipment in METU Design Factory while the print out process of 3D models.

I would like to express my warmest thankfulness to my lovely parents and sisters for their prayers and moral supports.

Furthermore, this study has been partially developed within scientific research project, BAP-08-11-2016-064, funded by Middle East Technical University.

TABLE OF CONTENTS

LIST OF TABLES

TABLES

LIST OF FIGURES

FIGURES

LIST OF ABBREVIATIONS

ABL	Atmospheric Boundary Layer
ACI	American Concrete Institute
ASCE	American Society of Civil Engineers
CFD	Computational Fluid Dynamics
CTBUH	Council on Tall Buildings and Urban Habitat
HD	High Definition
HFBB	High-Frequency Base Balance
HFFB	High Frequency Force Balance
HFPI	High Frequency Pressure Integration
IABSE	International Association for Bridge and Structural Engineering
MEP	Mechanical, Electrical and Plumbing
METU	Middle East Technical University
METUWIND	METU Center for Wind Energy
PLA	Polylactic Acid
SEI	Structural Engineering Institute
SM-PPS	Synchronous multi-pressure scanning system
SOM	Skidmore, Owings & Merrill LLP
UC	Under Construction

CHAPTER 1

INTRODUCTION

This chapter presents a background information and the main argument of the study. These are followed by the aim and objectives, and contribution sections. The chapter finishes with the disposition of the thesis.

1.1. Background Information

The economic development that occurred at the end of nineteenth century led to a rapid population growth especially on the metropolises of United States of America. Limited buildable area on such a period of increased demand naturally resulted with a raise on real estate prices. As an inevitable solution to fulfill the requirements of that context, history of tall buildings started with the immergence of 55 m high Home Insurance Building (1885) in Chicago (Beedle, Ali, & Armstrong, 2007).

At the early stages of their emergence, they were generally designed for commercial reasons and used as office buildings. The main purpose here was to bring together the commercial activities in the city center and close to each other (Günel & Ilgın, 2014). In due time, functions of tall buildings are expanded to residential, hotel and mixed usages, their profitability and economic efficiency contributed to this variety. First examples of tall buildings were appeared in Chicago and then New York, thus they are called as American skyscraper, however, in time, they spread throughout the world with the aim of being the most iconic or the tallest building (Beedle et. al., 2007). In addition to that, tall buildings are constructed with many factors including but not limited to; less environmental damage, less land use and constructional cost efficiency (Alaghmandan, Bahrami, & Elnimeiri, 2014).

Correspondingly, tall buildings became an integral part of the urban context for metropolises all over the world in present-day. In fact, increasing number of tall buildings is an important indicator for future cities also.

In terms of architectural design, there is not any unanimity or constant specification for the definition of "tall building". It is a relative subject which changes according to place, building characteristics and time. A definite height or number of floors is not enough to define a building as tall. Council on Tall Buildings and Urban Habitat (CTBUH) – a Chicago based council, accepted as one of the most important multidisciplinary international organizations in the world involved with tall buildings and urban habitat – categorizes a building as tall if it has at least one of the following three characteristics (CTBUH, 2019):

i. Height relative to context (Figure 1.1, left panel)
ii. Proportion (Figure 1.1, right panel)
iii. Embracing technologies relevant to tall buildings

Figure 1.1. Height relative to context (left panel) and proportion (right panel) (CTBUH, 2019)

As depicted in Figure 1.1 (left panel), apart from the real height of a building, its comparative height to neighborhood is accepted as an indicative feature. A relative tall building of a suburb area may not be considered as tall in a city of high-risers. Accordingly, perception of tallness changes according to the relation between a building and high-rise characteristic of surrounding neighborhood.

In a similar way, proportion (Figure 1.1, right panel) is another characteristic influencing the perception of tallness. It is defined as the ratio of height to narrow width of the buildings. Aspect ratio (slenderness ratio) is the keyword for the proportion. Although a building with a relative height and small footprint can be defined as tall, a wide building with the same height may not be categorized as being tall due to its perception.

Emergence of tall buildings became possible through the origination of necessary technologies beforehand such as steel I-beam, reinforced concrete and safe elevators (Harbert, 2002). In other words, tall buildings are equipped with the technology of its own day. Regarding the last characteristic, CTBUH (2019) explains a tall building as: "a building containing technologies which may be attributed as being a product of "tall" (e.g., specific vertical transport technologies, structural wind bracing as a product of height, etc.)." Furthermore, Beedle et. al. (2007) make a very similar statement by saying:

> The tall building was defined earlier and can be described as a multistory building generally constructed using a structural frame, provided with high speed elevators, and combining extraordinary height with ordinary room spaces such as those found in low-rise buildings. In aggregate, it is physical, economic, and technological expression of city's power base and prestige, representing its private and public investments (p. 354).

Along with the above-mentioned characteristics, definition of tallness also changes in accordance with time. While the tallest building was only 55 m at one time, present days' next tallest building, Kingdom Tower of Jeddah which is under construction, will be 1000 m once it is completed in year 2021 (The Skyscraper Center, 2019a). As accepting today's remarkable heights, CTBUH (2019) defines sub-groups for the buildings over 300 m in height as "supertall" and over 600 m in height as "megatall" buildings.

In terms of structural design, it is simpler to define a building as tall, since the definition comes from the lateral loads. According to Taranath (2010), if the lateral loads which particularly are somehow determinant for the structural design and analyses of a building, it can be considered as tall. Depending upon the increase in height, wind becomes the dominant force naturally. Furthermore, Taranath (2010) claims that to identify a building as tall; "perhaps the dividing line should be drawn where the design of the structure moves from the field of statics into the field of structural dynamics". Similarly, Günel and Ilgın (2014) point out to the decisive role of wind loads for structural design of tall buildings which are generally unimportant for low-rise buildings. In fact, according to Günel and Ilgın (2014), wind loads are usually more critical than the seismic loads in terms of lateral drift for tall buildings.

From the emergence of Home Insurance Building to the present day, number of tall buildings increased incrementally, spread all over the world and have become innovative works of today's technology. Improvements in material, construction and computer aided technologies helped to the regeneration of iconic forms and advanced structural systems. In conjunction with this advancement progress, reachable heights are also increased dramatically (Gerometta, 2009). As of 2019 September, the completed tallest 10 buildings of the world are shown in Figure 1.2.

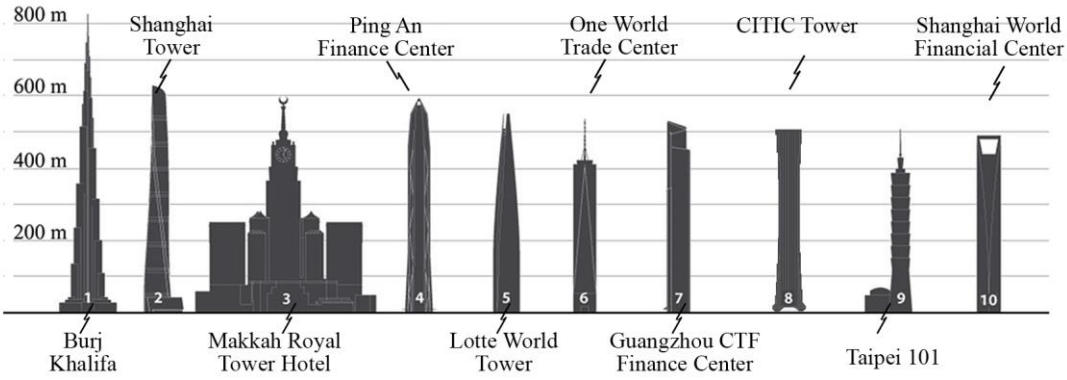

Figure 1.2. Tallest 10 buildings of the world (Adapted from the Skyscraper Center, 2019d)

Historical review of tall buildings is described in periods by various references. Although the number of phases vary from one author to another, fundamentals of contents are very similar to each other. In terms of external view, conventional rectangular boxes, in other words prismatic forms prevailed through the most part of those time phases. It doesn't matter either in the form of simple, modified or ornamented boxes (Alaghmandan et. al., 2014; Beedle et. al., 2007). However, since the early 2000s, both designers and investors are in an effort of creating distinctive design products. Thus, many different approaches appeared in the realm of tall buildings, a richness and multiplicity began to rule the present day's perception. Remarkably, irregular forms with complex geometries getting more popular for form generation of tall buildings around the world. Consequently, this recent trend has brought out diverse building forms, indeed which are designed to be iconic such as twisting, tilted and even free forms.

As stated above, twisting form is one of the most recent trends in the architecture of tall buildings. CTBUH (2016) defines a "twisting" tall building, in other saying "twisters" as "one that progressively rotate its floor plates or its facade as it gains height. Usually, but not always, each plate is shaped similarly in plan and is turned around a shared axis with a consistent number of degrees from the floor below". In addition to this, Vollers (2001, 2005, 2009) built and developed a morphological methodology to define complex shaped tall buildings. In this methodology, as well as subcategories exist, main classification for the buildings with twisted shapes is based on two forms; "twister" (Figure 1.3, on left) and the "tordo" (Figure 1.3, on right). According to Vollers (2001, 2005, 2009), "twister is a building with floors that lie horizontally rotated around a vertical axis. The axis usually lies in the center of the floor plan. Often there is a cylindrical core, around which floor wings lie". In twister, structural members or facade elements are placed helically through height and resulting in a non-orthogonal superstructure. On the other hand, Vollers (2001, 2005, 2009) define the tordo as "a building with one or more twisted facades connected to an orthogonal superstructure. The floors are basically repeated in vertical direction,

with interior columns and walls aligned". In tordo, unlike the twister, rotation axis is positioned on facade and those are different for both horizontal and vertical directions. As it is seen, basic systematic rules of twisters are not applicable for regeneration of a tordo.

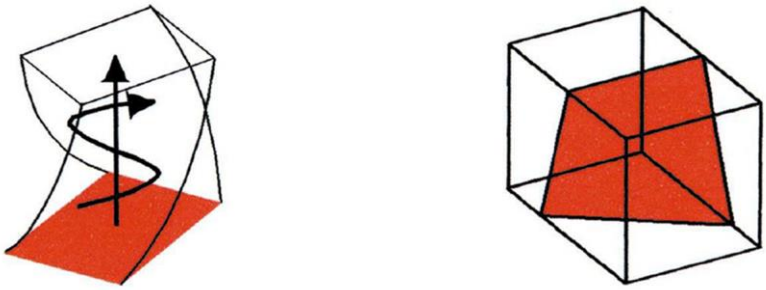

Figure 1.3. Twister (on left) and tordo (on right) (Vollers, 2005)

In Figure 1.4, Turning Torso (left) and Ocean Heights (right) are given as the current examples of twister and tordo respectively in accordance with the Vollers (2009).

Figure 1.4. Turning Torso (on left) (The Skyscraper Center, 2019h) and Ocean Heights (on right) (Wikipedia, 2019)

Turning Torso is widely accepted as the first twisting tall building, in other words history of twisting tall buildings started with it. 190 m high tower is completed in 2005 and located in Malmo, Sweden (CTBUH, 2016). According to Vollers (2009), it is categorized as basic twister due to rotating identical floors around a cylindrical core and repeating facades. Ocean Heights on the other hand is a more recent project which is completed in 2010. Tip height of the building is 310 m and it is located in Dubai. Three faces of the building twist from the base (The Skyscraper Center, 2019f) and rotates for 40° in total (CTBUH, 2016). Categorization of the building relies on the orthogonal superstructure and connection of mullions with parallel flat walls (Vollers, 2009).

Referring to the above given information, although the "tordo" can be accepted under the classification of twisted surfaces for tall buildings, this study mainly focuses on "twisters" and refers to twisters by saying twisting or twisted tall buildings.

For twisting buildings, numerous design results are possible by making alterations on floor geometry, twist angle between the floors, total rotation degree through the height or on the facade textures (CTBUH, 2016). Those also give rise to additional difficulties due to inherent complexity of twisting forms. However, their generation from the repetitive straight lines makes the twisters one of the easiest to comprehend design alternative for designers among the recently developed non-conventional shapes as well (Sev & Başarır, 2011).

In addition to these, CTBUH (2016) underlines the aerodynamic and in many cases energy-efficient features of twisting forms and declare them as some of the world's most iconic buildings. Addressing to the mentioned features, twisting forms are becoming more popular for form generation of tall buildings all over the world.

1.2. Argument

When compared to the early periods of tall buildings, a significant advancement and innovation process took place in material and construction technologies. Since the strength-to-weight ratio of structural elements increased, structural weight of the buildings decreased significantly. Consequently, much lighter and slender tall buildings became possible for today, however, it makes them much more vulnerable against wind loads (Günel & Ilgın, 2014).

Considering a tall building as a beam cantilevered from the ground, structural system of it must be resistant to excessive wind demands as it becomes higher. According to Irwin (2009), wind is the governing load for tall buildings and wind responses should be kept within the limits. Wind not only affects the structural integrity but also the serviceability of a tall building.

One of the main design concerns is to limit the maximum lateral top displacement of the structure which is caused due to sway motion of the structure (Taranath, 2010). Referring to Bennet (1995) and Taranath (1998), Günel and Ilgın (2014) state that, top displacement of a tall building should be limited to 1/500 of the building height. Correspondingly, Irwin (2009) says that more efficient and aerodynamically advantageous designs are required for high risers and this should be considered from the very outset.

If a tall building is subjected to wind flow, except the uplift forces over large roof areas, flow can be considered as two dimensional. Accordingly, corresponding forces and moments are significant for along-wind and across-wind (transverse wind) directions (Taranath, 2010) as depicted in Figure 1.5. More clearly, along-wind and across-wind demand refers to the drag and crosswind force, respectively.

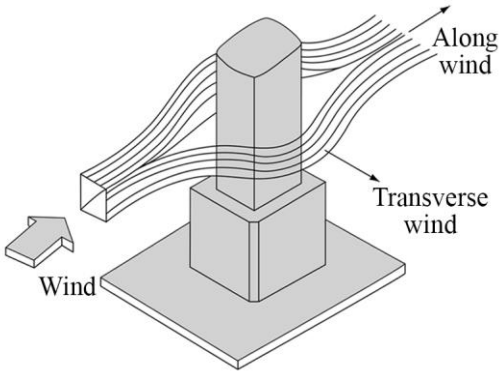

Figure 1.5. Wind flow directions for a tall building (Taranath, 2010)

Under the action of high-speed winds, tall buildings oscillate simultaneously in along-wind direction, across-wind direction and torsional directions. Previous studies showed that, because of the vortex shedding phenomenon (Figure 1.6) which is basically defined as the lateral impulse due to the periodical shedding of vortices from one side and then from the other side of the structure, across-wind response of a tall building can become more critical then along-wind response (Kurç, Kayışoğlu, Shojaee & Uzol, 2012). In fact, according to Moon (2015), the most critical structural design case occurs due to vortex shedding for tall buildings frequently.

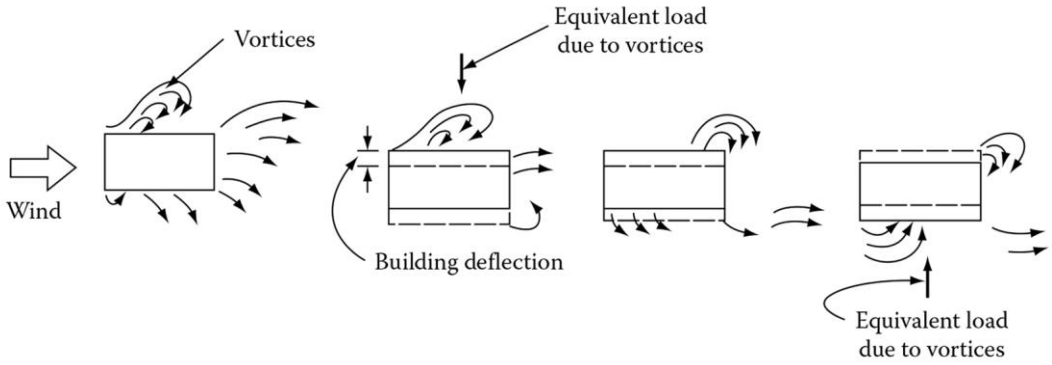

Figure 1.6. Vortex shedding phenomenon around a tall building (Taranath, 2010)

Regarding the wind induced responses of tall buildings, many researches have been carried out in order to improve the aerodynamic performance of the design. In general, architectural design approach (aerodynamic and structure based), structural design approach (structural systems) and mechanical design approach (auxiliary damping systems) are used for the subjected studies (Günel & Ilgın, 2014). In fact, auxiliary mechanical systems are only required when the architectural and structural performance is unsatisfactory against lateral loads, so those will not be mentioned in this study.

Aerodynamic modifications such as; setbacks, tapering, corner cut-outs and vertical-horizontal holes on building surface can be applied to tall buildings in order to mitigate the wind loads (Taghizadeh & Seyedinnoor, 2013). On the other hand, one of the most effective aerodynamic improvement can be achieved by designing an entirely aerodynamic building form such as the twisting form. It can significantly contribute to the mitigation of wind induced responses by disorganizing the alternating vortices around a tall building (Moon, 2015; Tanaka et.al., 2013).

Furthermore, it is worth to mention that, although wind loads are usually more critical than the earthquake loads, seismicity should not be underestimated for tall building design. Two different studies collected data from the real tall buildings which are located in non-seismic and seismic cities alternatively. According to Brownjohn and Pan (2001), long lasting motions resulting from the distant earthquakes – hundreds of kilometers distance - can create oscillations on tall buildings. Besides, according to Çelebi (2017), when the large magnitude earthquakes is the case, oscillations can become severe for tall buildings and this might cause to structural or non-structural damage due to prolonged shaking. Consequently, in addition to wind effects, earthquake effects should be taken into consideration for tall building design but not comprised within the scope of this study.

1.3. Aim and Objectives

Even the conventional prismatic tall buildings require a highly multidisciplinary coordination and planning during their design and construction processes. However, number of additional complexities are resulted from the twisting form itself comprising not only the architectural, aerodynamic and structural disciplines but also the curtain wall and MEP (mechanical, electrical and plumbing) related disciplines. Considering the difficulties arisen from the inherent complexity of twisting forms, this study investigates the aerodynamic and structural characteristics of these buildings, particularly those having structural members twisting and leaning with the floor plates. In other words, the main aim of this study is to analyze the aerodynamic and structural superiority or inferiority of twisting forms with respect to their prismatic counterparts through comparative tests and analyses. This way, the quest for preferability of this challenging form will be evaluated from the designers' and construction professionals' point of view.

The objectives of the study can be listed as;

- Providing background information about the emergence and progress of twisting tall buildings,
- Scrutinizing aerodynamic and structural features of twisting tall buildings,
- To find out possible challenges and potentials of twisting tall buildings via literature review,
- Investigating the aerodynamic features of twisting tall buildings with respect to their prismatic twins through comparative wind tunnel tests by using both high-frequency base balance (HFBB) method and synchronous pressure tests,
- To examine the structural response characteristics of twisting tall buildings with respect to their prismatic twins by means of structural analyses in accordance with the wind loads obtained from wind tunnel tests,
- Evaluation and comparison of results with the previous studies, this way, giving guidance for designers and investors.

1.4. Contribution

As summarized in the introduction and the literature review parts, current literature provides sufficient information related with the definition, history and structural system configurations of twisting tall buildings. Besides, several studies discuss the motivation behind design and construction of twisting tall buildings. However, majority of those studies are in a consideration from one aspect namely; aerodynamic, structural or financial way only. Among limited number of studies on this subject, Tanaka et. al. (2013) focused on both aerodynamic features and response analyses of unconventional forms but used only outrigger structural system whereas tube system is also a common lateral load-carrying mechanism for unconventional forms. More recently, Moon (2015) scrutinized the structural response of complex-shaped tall buildings, however code-based wind loading was used for the analyses which inherently ignores the complex formation of alternating vortices. In addition, Kim, Bandi, Yoshida and Tamura (2015) investigated the effect of helical shape and helical angle, yet hypothetic building forms have been taken into consideration. It is noteworthy to mention that; all these studies have used generic forms with square in plan except one rectangular case.

Not uncommon, but still as a relatively recent approach in realm of architecture and structure, the aerodynamic features of complex forms need further investigation. Thus, comprehensive and sophisticated wind loading studies complemented by structural response analyses are required for these emerging building forms. Regarding this objective, instead of a research that is based on generic forms and code-based wind loadings, this study intends to contribute to literature not only by analyzing the aerodynamic behavior of a real twisting tall building, but also its structural response characteristics under the action of wind. To provide a comprehensive comparison all analyses are conducted also for the its hypothetical prismatic counterpart. This way, this study aims to provide a comprehensive evaluation of twisting forms for designers, contractors and even for investors.

1.5. Disposition

The structure of this thesis comprises five chapters, first of which is the introduction part. It presents a background information and definitions about twisting tall buildings. Afterwards, argument, aim and objectives, contribution and lastly the disposition of the study take place respectively.

As the second chapter, the literature review firstly covers the history and then the structural system configurations of twisting tall buildings. Subsequently, aerodynamic features of twisting tall buildings are provided. Wind tunnel methodologies is also considered under the aerodynamics part. Finally, challenges and potentials of twisted tall buildings are discussed as the critical review of the given knowledge beforehand.

Material and methodology of the research are explained in the third chapter. Material section is introduced by the case study research, selection of the sample building and collection and evaluation of the data. Then, analytical and 3D modelling of twisting and prismatic forms and finally the wind tunnel of METU Center for Wind Energy (METUWIND) is overviewed. Regarding the methodology, wind tunnel tests and structural analyses are represented explicitly. As conducted, wind tunnel tests are approached in two phases which are the high-frequency base balance (HFBB) tests and synchronous pressure measurements on 3D models.

In the fourth chapter, results of the wind tunnel tests and structural analyses are given for both prismatic and twisting forms in a comparative manner. Discussion of the results are not limited to conducted tests, evaluation and comparison with the previous works of the literature are also covered.

The final chapter of the thesis is dedicated to conclusion part. Summary of the work is presented together with the interpretations of the conducted research. After the limitations of the study is mentioned, the thesis is concluded with the future study recommendations.

CHAPTER 2

LITERATURE REVIEW

Second chapter focuses on the literature review of twisting tall buildings in four sections. Firstly, history of twisting tall buildings is given. Then, structural system configurations are introduced through existing examples. Depending on their unique exterior geometry, knowledge about the aerodynamic features is given from the previous studies in literature by comprising the methodology behind their aerodynamic investigation. Afterwards, critical review of the previously given sections concluded the second chapter by discussing the potentials and challenges of those building types.

2.1. History of Twisting Tall Buildings

As mentioned earlier, history of twisting tall buildings started in year 2005 with the completion of Turning Torso (CTBUH, 2016). Their emergence is addressed to the dominance of pluralism (Aminmansour & Moon, 2010) in realm of high-risers. Besides, motivation behind such a trend is asserted by various statements from the designers' and investors' point of view. In general, those statements can be given as;

- Creating an iconic / landmark structure (CTBUH, 2016; Gensler, 2013),
- Aim for developing the different one to be part of competition (Alhatti, 2013),
- Having a competitive way of selling in the international financial contention (Bloomberg, 2014; DeSimone, Ramirez and Mohammad, 2015),
- Providing altering unique vista for each floor (SOM, 2013)
- Aerodynamic features (Moon, 2015; Kim et. al., 2015; Tanaka et. al, 2013)

After the emergence of Turning Torso, increase in number of twisting tall buildings continues in different parts of the world. Tallest 10 twisting buildings are illustrated in Figure 2.1. Listed buildings are either completed or under construction (UC) as of September 2019.

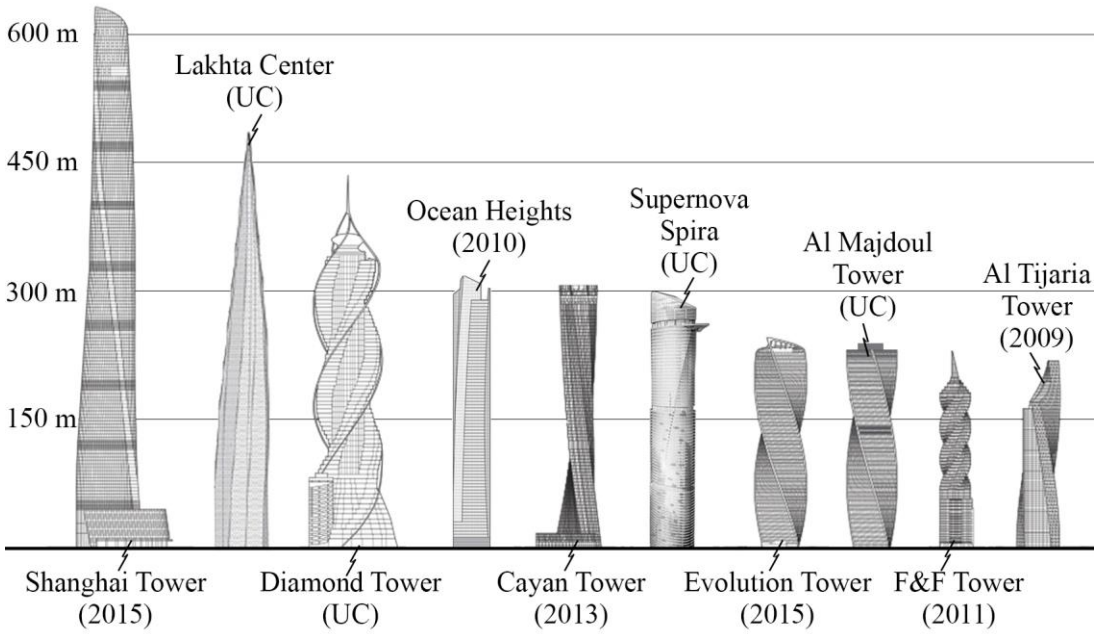

Figure 2.1. Tallest 10 twisting buildings in the world (Adapted from the Skyscraper Center, 2019b)

These symbolic structures are accepted in global scale. Thus, they spread over the world from Asia (Shanghai Tower and Supernova Spira) to Europe (Lakhta Center and Evolution Tower) and from Central America (F&F Tower) to Arabian Gulf (Diamond Center, Ocean Heights, Cayan Tower, Al Majdoul Tower and Al Tijaria Tower). Referring to the ranking (Figure 2.1), it is seen that all the tallest 10 twisting buildings are last decade's works. To note that, four of them are still under construction and this statistic can be evaluated as a sign for increasing number of twisting tall buildings in future cities. Stated information is gathered from The Skyscraper Center (2019b).

2.2. Structural System Configurations of Twisting Tall Buildings

Structural system classification of tall buildings is proposed by several references in literature. One of the relatively recent studies is Taranath (2010) but limited to reinforce concrete tall buildings. More recently, Günel and Ilgın (2014) proposed a comprehensive classification comprising reinforced concrete, steel and composite structures under nine categories which are listed accordingly;

- Rigid frame systems
- Flat plate/slab systems with columns and/or shear walls
- Core systems
- Shear wall systems
- Shear-Frame systems
    - Shear trussed frame (braced frame) systems
    - Shear walled frame systems
- Mega columns (Mega frame, space truss) systems
- Mega core systems
- Outriggered frame systems
- Tube systems
    - Framed-Tube systems
    - Trussed-Tube systems
    - Bundled-Tube systems

Due to unique characteristics of twisting tall buildings, structural systems are adapted almost project specifically. In general, a couple of design approaches are followed for the implementation of structural systems on twisting tall buildings. According to Taşkın (2019), those approaches are named as “non-adaptive system” and “adaptive system”. The former refers to orthogonal structural system with rotating floor plates whereas the letter is defined as the rotational twist of structural members while intertwining with the floorplates or the facade. In the light of above given information, those systems are represented through the existing examples.

2.2.1. Turning Torso

Known as the first twisting tall building, 190 m of Turning Torso has a mega core structural system composed of a circular reinforced concrete core. Thus, both gravity and lateral loads are carried by the central core (Santiago Calatrava Architects, 2019). Exterior diameter and shear wall thickness of the core change between 15.6 m to 11.4 m and 2.5 m to 0.4 m from the base to the top, respectively. Typical pentagon-like cast-in place reinforced concrete floor slabs (27 cm-thick) are cantilevered where the maximum distance from the core is about 15.2 m. This way, not only column free inner space but also typical architectural plan organization is achieved. Nine box units complete 90° rotation around the central core. Each unit contains 5 floors. An inclined steel spine system supports the units by diagonal and horizontal steel struts so that, wind induced lateral displacements are reduced (Günel & Ilgın, 2014). Typical floor plan (left) and 3D- projection of structural system (right) are illustrated in Figure 2.2.

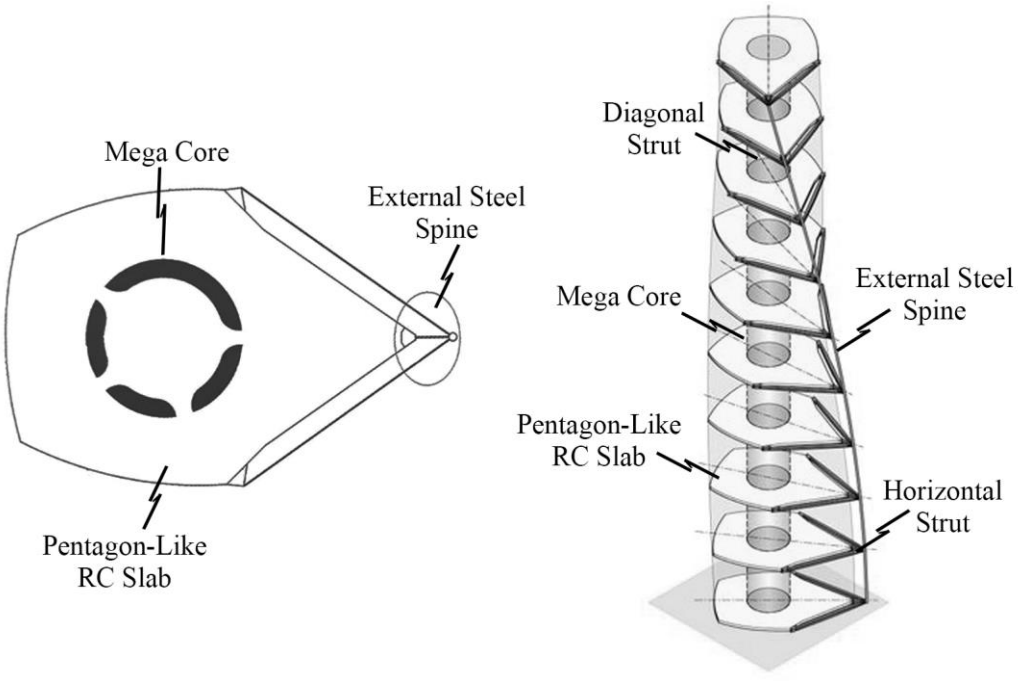

Figure 2.2. Turning Torso; typical floor plan (left) (Adapted from Günel & Ilgın, 2014) and 3D projection of structural system (right) (Adapted from Wikipedia, 2004)

2.2.2. New Songdo International City, Block D24 Buildings

Block D24 buildings are two residential towers located in Seoul with 50 and 45 stories high. Design goals of the designers were to minimize different unit types, to limit the maximum allowed floor height to 3.2 m and to avoid from external brace frame or diagrid like structural elements on the periphery of dwellings. Under these circumstances, circular reinforced concrete mega core structural system is used with radiating cantilevered partition walls and 240 mm thick flat plates. Five partition walls take place on each floor that alternate repetitively on the following floor. Since torsional forces are significant for twisting tall buildings, door openings on central core are placed on a switching layout in order to reduce the torsion resulting from the self-weight. Thus, thinner wall thickness is succeeded on the core (Clark & Scott, 2010). Repetitive two-story module (a), switching openings on the core (b) and structural system (c) of Tower 301 (50 floors) are depicted in Figure 2.3.

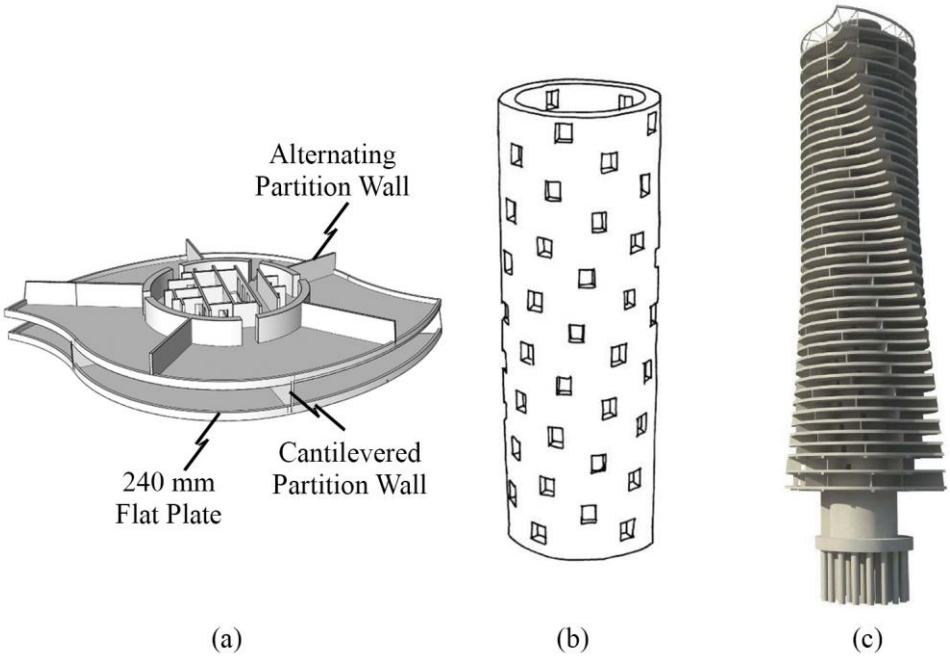

Figure 2.3. D24 Tower 301; repetitive two-story module (a), switching openings on the core (b) and structural system (c) (Clark & Scott, 2010)

2.2.3. F&F Tower

The conceptual design of F&F tower, formerly named as Revolution Tower, was simply arisen from the idea of twisting geometry with a prism. The structure with 236.4 meters-high holds 53 above ground floors (The Skyscraper Center, 2019e). “Tightest” twist is achieved by 5.94° rotation per floor which completes 315° in total. This way, four exterior balconies are generated on each floor (CTBUH, 2016). Shear walled frame system is used on the reinforced concrete structure which is formed by a rectangular central core and eight orthogonal columns. Eight circular columns and post-tensioned beams constitutes a circumference around the central axis of the structure. Rotating floor slabs are supported by post-tensioned concrete joists. Position of the joists are constant in order to simplify the construction. Top displacement is limited by 1/300 of the height for all lateral loads (Dutari, 2011). Site photo (on left) and the current view (on right) of F&F tower are represented in Figure 2.4.

Figure 2.4. F&F Tower; site photo (on left) (Arquitectobra, 2013) and current view (on right) (Skyscrapercity, 2017)

2.2.4. Absolute World Tower

The award-winning project was developed through an international competition which reflected the developers' desire to create an iconic design. Although unique layout of residential units caused a market related drawback initially, great public interest resulted by a sell out in few days. When it is the case, developers decided for a second tower. First tower has 176 m height and rotation of the floors fluctuates from 1° to 8°, whereas 158 m of second tower twists 4° per floor (Lagendijk, Pignetti & Vacilotto, 2012). Total rotations are 200° and 205° respectively. Both towers have shear walled frame structural system. Length of shear walls undulates in accordance with cantilevered twisting floor slabs. Exterior border of the cantilevered slabs formed the continuous balconies (Golasz-Szolomicka & Szolomicki, 2019). Floor plans of levels 24-40 (left panel) and 3D projection of structural system (right panel) for Absolute Word Tower 56 -first tower - are depicted in Figure 2.5.

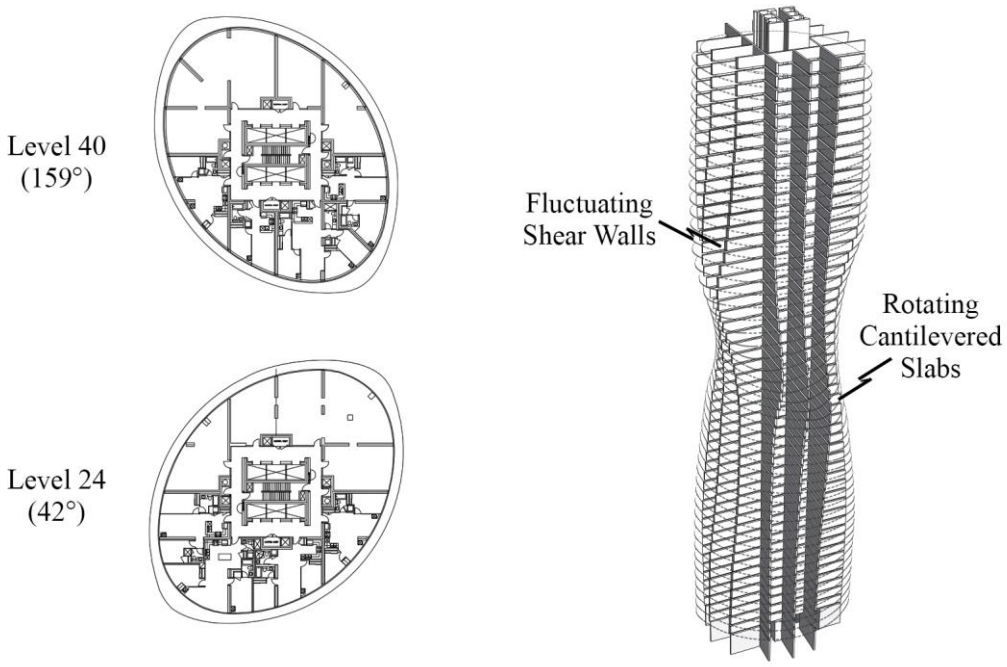

Figure 2.5. Absolute World Tower 56; floor plans of levels 24-40 (left panel) and 3D projection of structural system (right panel) (edited from Lagendijk et. al., 2012)

2.2.5. Mode Gakuen Spiral Towers

Plural name of Mode Gakuen Spiral Towers (Figure 2.6) springs from the three vocational schools that are hosted in this educational building. Triple function is expressed in a spiral manner both from the inside and outside. Three fan-shaped wings rise around an elliptical core radially by culminating at different levels, highest of which is 170 m. Size of the wings are reduced as they ascend and create a curvilinear silhouette. (Groesbeck, DeVries, Klemencic & McDonald, 2012). An orthogonal central core is used in a seismic-prone city of Nagoya (Parker & Wood, 2013). The core consists of 12 concrete-filled orthogonal steel columns and those are linked by braces in a mesh network creating an inner tube structure. A transparent vision is succeeded via minimal columns on the periphery. Viscosity dampers are also installed to reduce earthquake forces up to 20% with respect to non-installation of the system (International Association for Bridge and Structural Engineering [IABSE], 2019).

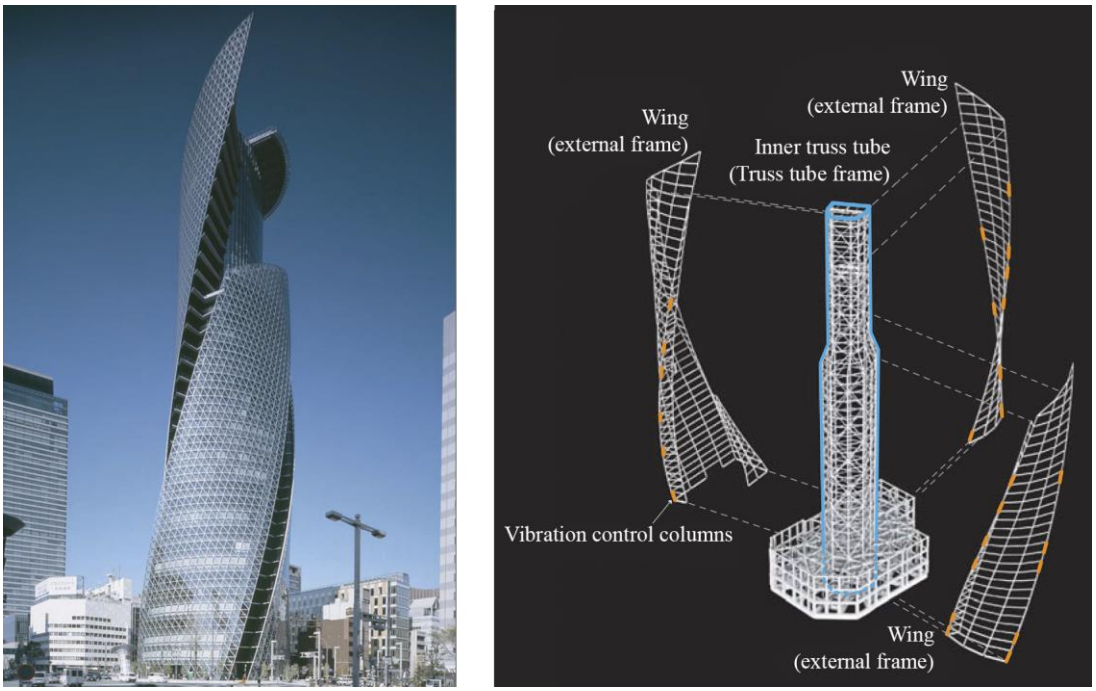

Figure 2.6. Mode Gakuen Spiral Towers; external view (on left) and 3D structural system (on right) (IABSE, 2019)

2.2.6. Shanghai Tower

The tallest twisting building in the world is located in Shanghai, where it is common to face with typhoon-level wind loads and active seismicity. Both exterior shape and the structural system of the tower was refined through a series of wind tunnel tests. (Xia, Poon & Mass, 2010). The tower with 632 meters-high has an outrigger framed structural system that comprises nine zones stacked on each other. Square shaped core and mega frame are connected with double story high steel outrigger trusses at six levels coinciding with mechanical floors. Although outriggers at bottom zones lowers the fundamental period of the structure, the others are mainly used for story drift control at top levels. The core is reinforced concrete, but embedded steel plates are used for the connection of outriggers. Besides, top and bottom chords of the outriggers cross through the core. (Zhu, Poon, Zhou & Fu, 2012). Typical floor plan (on left) and components of lateral load carrying system (on right) are demonstrated in Figure 2.7.

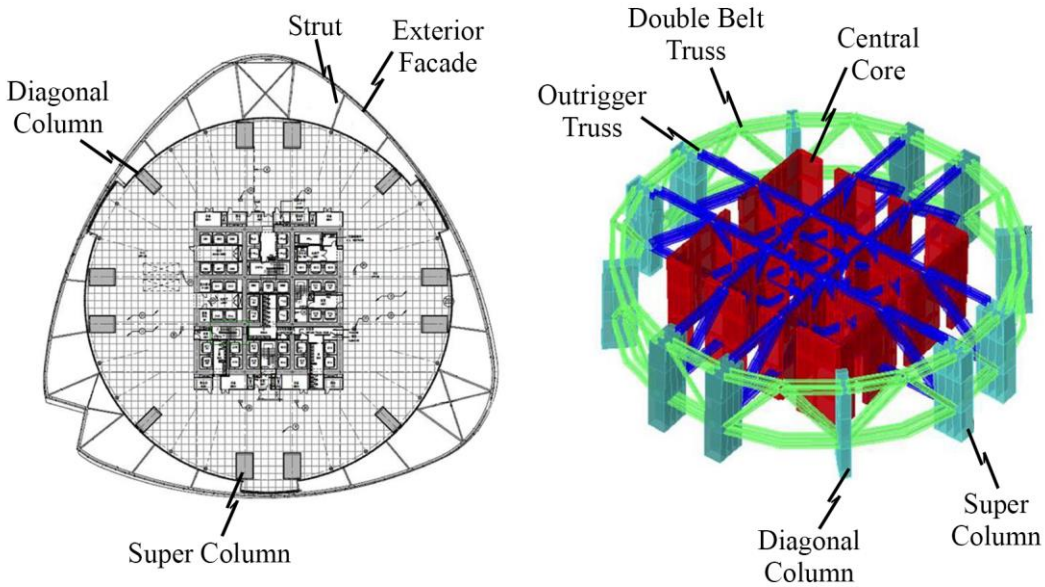

Figure 2.7. Shanghai Tower; typical floor plan (on left) and components of lateral structural system (on right) (Zhu et. al., 2012)

Four pairs of super columns on orthonormal axis, four diagonal columns and double belt trusses constitutes the mega frame. Composite super columns are made of steel sections encased by concrete. The gravity and lateral loads are resisted by the above given structural system named as inner cylindrical tower. Due to seismically active location, this simplified structural system is implemented by the structural engineers (Xia et. al., 2010). The maximum story drift is h/500 for expected wind loads and h/623 for earthquake loads (Zhu et. al., 2012). Twisting shape of the tower is given by an exterior transparent cladding system which tapers from bottom to top. This cam-shaped exterior facade is drawn by a series of hoop rings. Hoop rings are tied to inner cylindrical tower by suspending struts. The space between two shells creates atriums height of which changes from 12 to 15 floors (Gensler, 2013). Figure 2.7 shows the typical zone section (on left) and exterior view (on right). Results of the wind tunnel tests showed that, 24% of lateral loads are reduced due to twisting form of the building. Thus, 58 million dollars of cost saving is achieved ultimately.

Figure 2.8. Typical zone section (left) (Gensler, 2013) and exterior view (right) (The Skyscraper Center, 2019g)

2.2.7. Al Bidda Tower

Unique silhouette of 227 m tower in Doha skyline is achieved by continuous twist of the rotor shaped floors. Each floor rotates around 1.5° which completes 60° rotation in total. Floor plan areas are getting wider from 14th floor while ascending and descending concurrently (Arabian Construction Company, 2009). The building has an adaptive structural system composed of reinforced concrete circular core and nine twisting perimeter columns. There are not any internal columns. Due to twisting geometry of the columns, steel diagrid system is integrated as and additional lateral load resisting system (Wood, 2011). The assembly of bracings is postponed for 56 days after concrete pouring. Prediction of expected creep is about 45% through this period. This way, it is intended to reduce the increased loading on diagrid system. In addition, use of unique glazing panels became essential due to building geometry (Wood, 2011). Second floor plan (left) and site photo (right) are given in Figure 2.9.

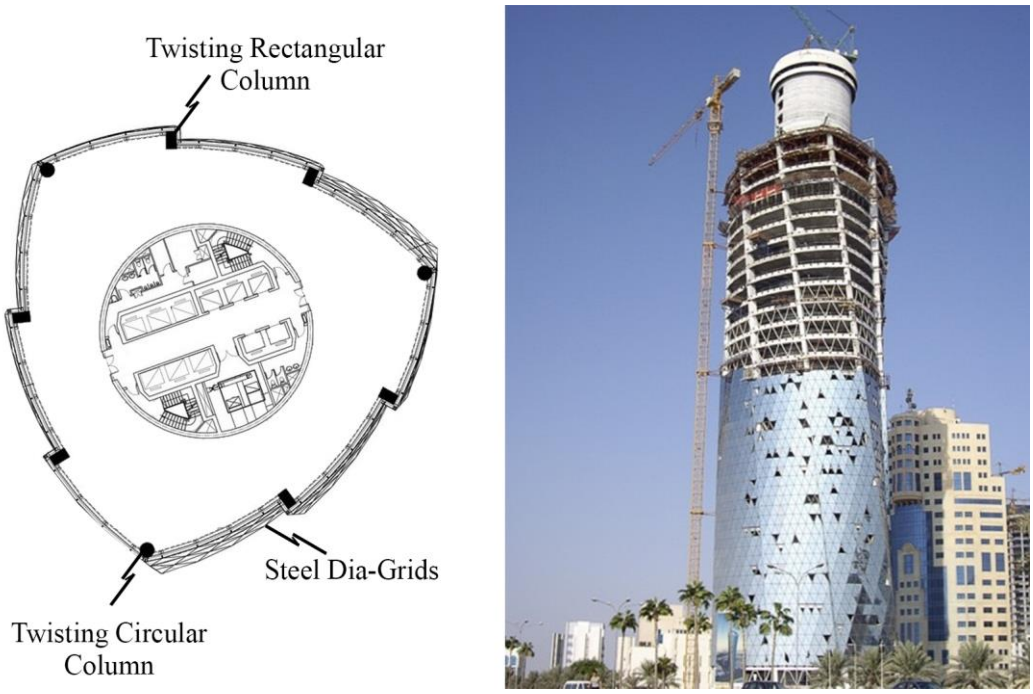

Figure 2.9. Al Bidda Tower; second floor plan (on left) (Architectural, 2011) and site photo (on right) (Safetravels196, 2018)

2.2.8. Lakhta Center

Lakhta Center is the second tallest twisting building in the world with its 462 m height and 87 floors above ground. Pentagram-like floor plans twist around a central circular core by completing 89° twist in total. In addition to twisting, the area (due to tapering) and the layout of the floors also vary, which results in unique floors. Composite columns (15 for the bottom, 10 for the upper levels) draw the border of curved facade. Under the wind loads, lateral load resisting capacity of the reinforced concrete core is insufficient. Therefore, outrigger trusses take place at 4 levels of every 14 floors (RMJM, 2019b). Because of the rotational motion, core-outrigger connections change for each point which became a challenge in construction process. Furthermore, not only rotational motion but also shifting connection of the outriggers ended up with a constant torsion on the core (AskariNejad, 2014). Floor plans (left) and components of structural system (right) are depicted in Figure 2.10.

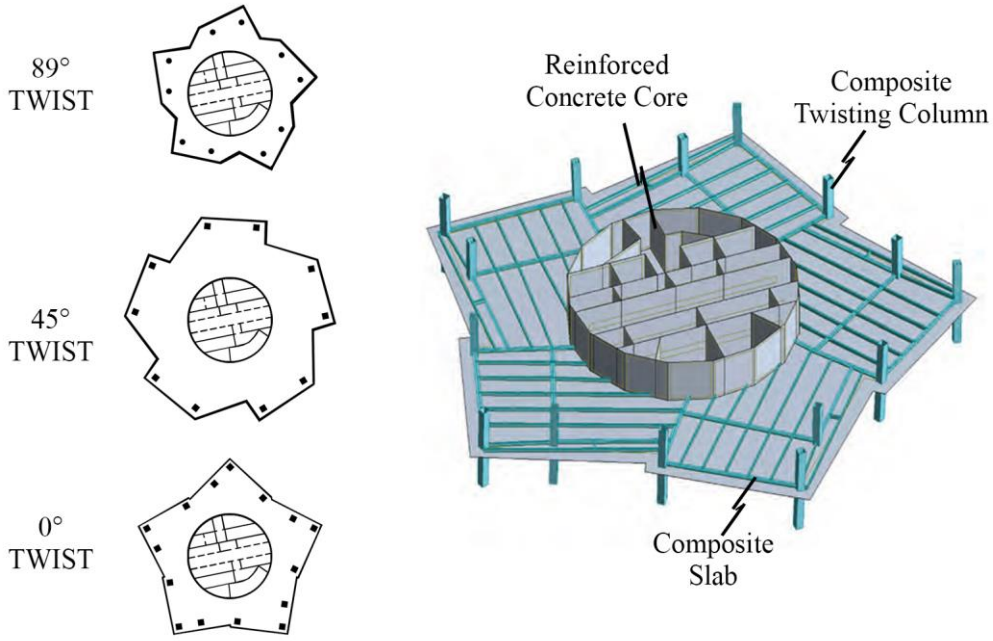

Figure 2.10. Lakhta Center; floor plans of 0° - 45° - 89° rotation (left) (RMJM, 2019a) and components of the structural system (right) (AskariNejad, 2014)

2.3. Aerodynamics of Twisting Tall Buildings and Measurement Techniques

Before discussing the aerodynamic characteristics of twisting tall buildings, it is worth to mention about the methodologies that are widely used for predicting wind induced loads and dynamic responses of tall buildings. Primarily, either wind tunnel tests or computational fluid dynamics (CFD) techniques are utilized in today's engineering. Although traditional use of wind tunnel is usually preferred to check the final geometry of a building, its use recently expanded to the design phase of the building for aerodynamic shape optimization (Irwin, 2009). Referring to the design of Burj Khalifa (828m, Dubai), Baker (2017) states that, a lot of the design were done in the wind tunnel. Wind tunnel tests are applied in three different ways (Cermak, 2003);

- High-frequency base balance (H-FBB) tests
- Synchronous multi-pressure scanning system (SM-PPS)
- Aeroelastic model tests

It is possible to come across with alternative names or abbreviations of the above given techniques. For instance, first one is named as high frequency force balance (HFFB) and the second one refers to high frequency pressure integration (HFPI) (Irwin, 2009). For the sake of simplicity, those techniques are named as high-frequency base balance (HFBB) and synchronous pressure measurement respectively in this study.

In HFBB technique, a stiff measurement system acquire data from the base of rigid model where there is no need for the replication of building dynamic properties. Mean and fluctuating shear forces are obtained together with the base moments of the structure (Holmes, 2015). Data is measured as time series by revealing information on mean, root mean square and peak wind loads. Overall wind load statistics and aerodynamic admittance can be predicted from a single HFBB test. This way, appropriate structural system is resolved at the early design stages. When compared, application of HFBB is the least time consuming and the most cost-efficient one

among three methods. On the other hand, negative aerodynamic damping cannot be determined through static HFBB tests, in this case an aeroelastic model test become necessary (Cermak, 2003).

Synchronous pressure measurement is a more recently developed technique than HFBB. Momentary pressure distributions of exterior surfaces are gathered by pressure taps and transmitted to electronic sensitive pressure scanning system which is alternatively known as pressure transducer (Holmes, 2015). Major advantage of this system is that, not only fundamental mode – as in the case of HFBB – but also higher modes and higher wind speeds can be analyzed (Irwin, 2009). In addition to overall statistical force and moment data, vertical distribution of pressure is also obtained by this method. Thus, it is possible to measure positive and negative pressures for cladding systems. However, accuracy of synchronous pressure measurement depends on the density of pressure taps on exterior surfaces. Results of this technique might be uncertain for very slender tall building where the placement of sufficient pressure taps is not practical or for the buildings with very complex forms (Cermak, 2003).

The last wind tunnel technique is using aeroelastic models which reflects the stiffness properties of the real structure. Metal spine with tapering cross-section might be embedded in the core of scaled model. This technique may allow to predict the full response characteristics of structure comprising higher mode shapes and aerodynamic damping. Despite having extensive benefits, it is the most complicated and expensive wind tunnel measuring technique. Accordingly, final stages of the design are relatively more convenient to use aeroelastic modeling tests (Irwin, 2009).

Depending on the cost effectiveness and practicality of use, computational fluid dynamics (CFD) is accepted another powerful tool for the aerodynamic design of tall buildings. Behavior of wind is simulated via software-based technology. It can be

either directly used for the design of tall buildings (Mohotti, Mendis & Ngo, 2014) or for the verification of wind tunnel tests (Yılmaztürk & Sezer-Uzol, 2011).

Aerodynamic forms such as tilted, twisting or free forms contribute to disruption of wind flow around the bluff body of a building. Accordingly, these building forms might be considered as advantageous in terms of wind induced structural responses (Alaghmandan et. al., 2014). An earlier study, Ali and Moon (2007) explained this situation by saying; "aerodynamic forms in general reduce the along-wind response as well as across-wind vibration of the buildings caused by vortex-shedding by "confusing" the wind". Within this context, although various studies have been reported related to the aerodynamic modifications of tall buildings, limited number of studies have been conducted regarding both the aerodynamic features and wind-based performance of those aerodynamic forms.

Tanaka et. al. (2013) investigated the aerodynamic and structural response characteristics of tall building models with aerodynamic modifications or entire aerodynamic forms; including but not limited to corner cut, setbacks, helical forms, etc. A series of HFBB tests were conducted to 1/1000 scaled models of 400 m high generic buildings. Then, structural analyses were performed. However, all the buildings investigated in Tanaka et. al. (2013) have outrigger frame structural system. Figure 2.11 represents maximum mean moment coefficients taken from Tanaka et. al. (2013) by limiting to prismatic and helical forms. Those coefficients refer to maximum values of mean along-wind $\left|\overline{C_{MD}}\right|_{\max}$ and mean across-wind $\left|\overline{C_{ML}}\right|_{\max}$ overturning moments for all angle of attacks. According to comparison, helical square models are subjected to less moment with respect to square model especially on across-wind direction. Although, 180° twisting rectangular model is subjected to larger moment compared to square model on along-wind direction, its moments are smaller for both directions in comparison to prismatic rectangular model.

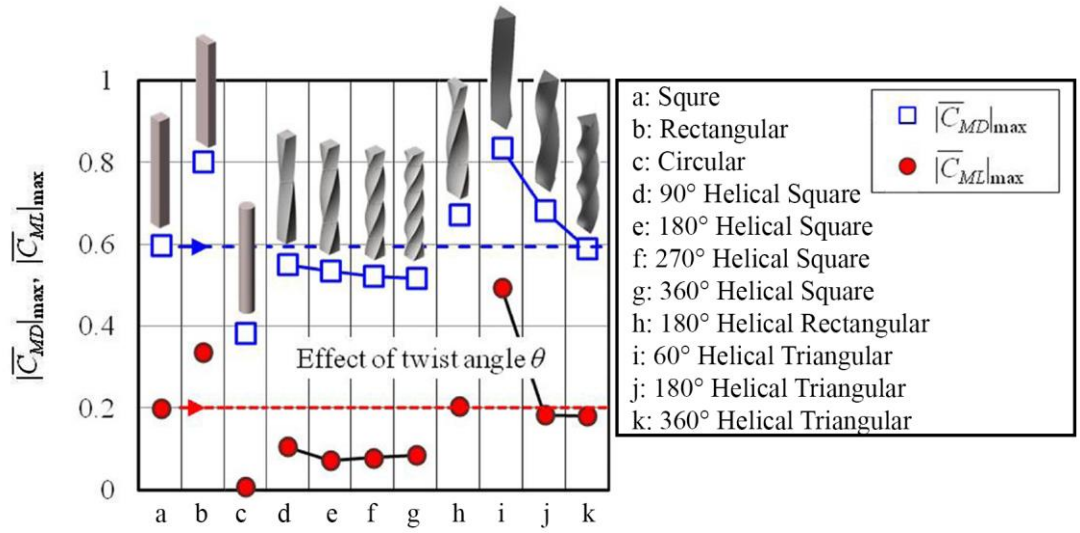

Figure 2.11. Maximum mean overturning moments (Tanaka et. al., 2013)

In addition, dynamic responses of buildings investigated in Tanaka et. al. (2013) are given in Figure 2.12. As depicted below, smaller shear force, displacement, torsion and acceleration is obtained for both twisting forms compared to prismatic one.

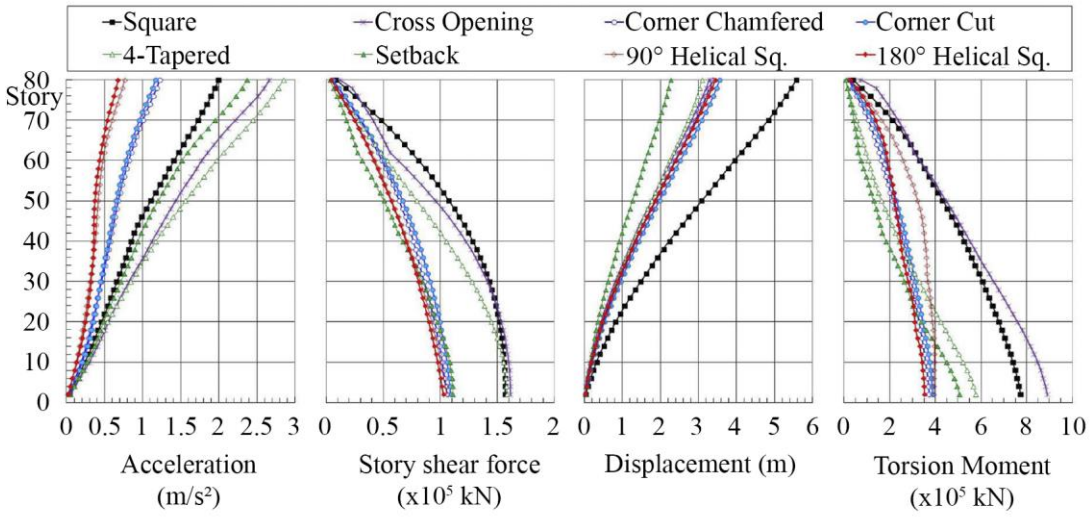

Figure 2.12. Comparison of aerodynamic responses for 500-year return period (Tanaka et. al., 2013)

More recently, performance based structural responses of complex shaped tall buildings is studied by Moon (2015). Investigation focused on generic models with twisted, tilted, tapered and free forms having alternative lateral structural systems including braced tube, diagrid and outriggers. Design wind loads are based on the SEI/ASCE code. The floor plan dimensions of the models are 36 m square, and they are 60, 80, 90 or 100 floor heights respectively. In addition, different rotational degree per floor is used for twisting models. Maximum lateral displacements of various models observed by Moon (2015) are shown in Figure 2.13.

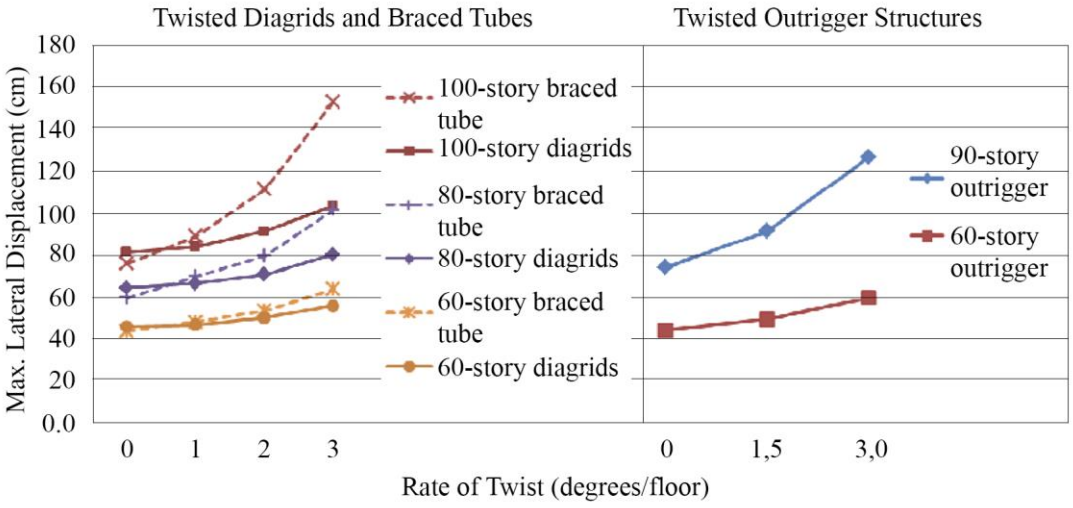

Figure 2.13. Comparison of maximum lateral displacement for diagrids, braced tubes and outrigger structures (Adapted from Moon, 2015)

Although Moon (2015) noted the superior aerodynamic behavior of twisting tall buildings, significant lateral stiffness reduction is emphasized resulting from the twisting motion of structure. In fact, this stiffness reduction become larger as the height and the rate of twist increases. Moreover, deformability of braced tubes and outriggers are bigger with respect to diagrid models investigated by Moon (2015).

Another research related to dynamic response characteristics of twisting tall buildings is conducted by Kim et. al. (2015). Effects of side numbers and twisting form is scrutinized through synchronous pressure measurement tests. 6 prismatic tall building models and their 180° twisting identical counterparts whose plan cross-section changes from triangle to dodecagon are tested. Circular model was the additional one. Height to total volume ratio was equal for the all configurations. According to the results, correlation between the overturning moment, torsion and dynamic responses to twisting form is reduced with the increasing side numbers. A similar situation is observed for the largest fluctuating coefficients and peak accelerations which are represented in Figure 2.14. Those refer to largest values at all wind angles.

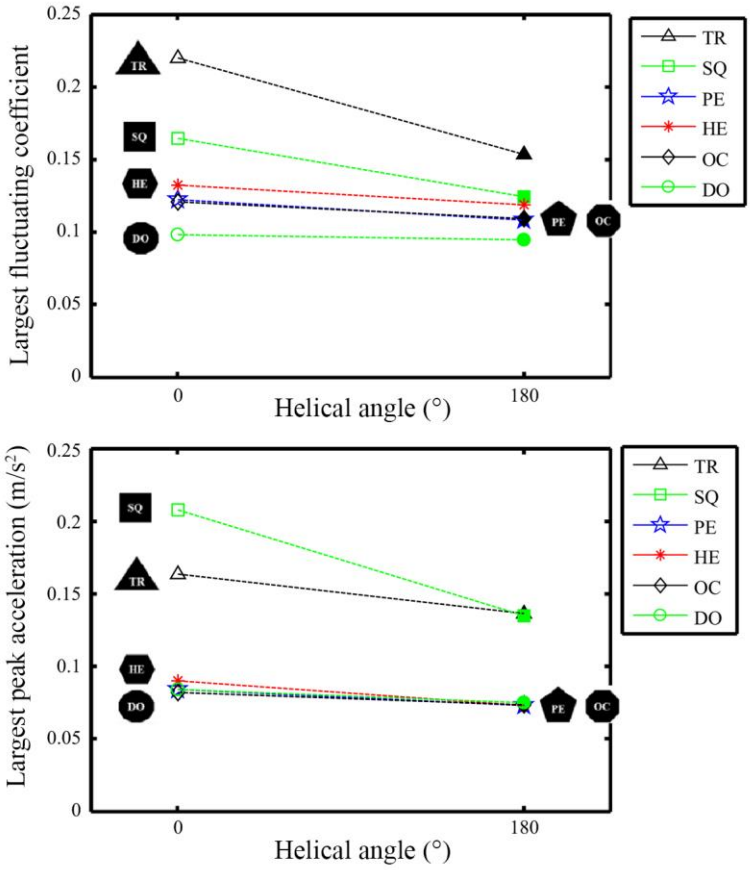

Figure 2.14. Effects of twisting form on fluctuating force (on top) and peak acceleration (on bottom) (Kim et. al., 2015)

2.4. Discussion About Potentials and Challenges of Twisting Tall Buildings

Design and construction of twisting tall buildings comprise both potentials and additional complexities with respect to prismatic forms. These complexities are mainly related with architectural plan organization, MEP shaft optimization, curtain wall design and construction, increased torsion, decreased lateral stiffness levels, etc. Both potentials and challenges are discussed herein below.

Regarding the design considerations, even architectural plan of conventional prismatic tall buildings is compelling. One of the design criteria is to achieve maximum net floor area to gross floor area ratio. The ratio is accepted as the key parameter on construction costs and sales prices (Watts, Kalita & Maclean, 2007). However, simple repetition of floors for twisters may not be possible in any case, so it turns into a demanding design phase. In fact, it depends on the structural system. When rotating floor plates are supported by constant vertical columns, configuration of architectural and structural members varies at each floor (Scott, Farnsworth, Jackson & Clark, 2007) where different architectural plan organization is needed for each floor. F&F Tower and Absolute World Towers can be shown in this category. Furthermore, rotation of floor plates around a straight core leads to adversity due to differential positioning of usable areas to constant elevators and MEP shafts. This situation might necessitate circulation corridors which inevitably reduces net leasable area. The New Songdo International City, Block D24 buildings (Clark & Scott, 2010) and Cayan Tower (Baker, Brown, Young & Zachrison, 2010) have such circulation corridor rings.

Another challenge is related to curtain wall systems. Although curtain walls are not structural elements, their role is significant on creating external facade and transferring wind loads to the structural system (Fu, 2018). Yet, regarding the complex geometry of twisting tall buildings, use of unique glazing units which necessitates expensive custom manufacturing might become inevitable as in the case of Al Bidda Tower.

As discussed through the case studies, torsion is a major challenge for twisting tall buildings. Additional procedures are followed to come up with a structural solution. It is possible to find out various ways in accordance with the source of the problem. Those can be in the form of alternating door openings on the core wall as in the case of Block D24 towers or using hat truss as in the example of Grove at Grand Bay of Miami (93.8 m) (DeSimone et. al., 2015). Moreover, additional precautions might become necessary for the construction processes due to rotational movement of the floors as in the case of Lakhta Center (AskariNejad, 2014). Indeed, the whole construction processes might be extended due to such rotational movement as in the case of Al Bidda Tower (Wood, 2011).

Despite the challenges exemplified above, all twisting buildings are indicated as iconic structures and landmarks in their surrounding environments with their sculptural postures. Not only vantage point based swinging skin from the outside but also altering unique vista for the inhabitants attract great public interest. This way, easy sell outs are succeeded even with higher sale prices (Lagendijk et. al., 2012).

While there is the evidence of lateral stiffness reduction due to twisting motion, this should be considered along with the superior aerodynamic features of those buildings. Regarding the Cayan Tower, Baker et. al (2010) declared that; “when compared to a similar building taken as a straight extrusion with height (no twist), it is estimated that the twisting form of the Infinity Tower reduced the structure’s across-wind excitation by some 25% or more”. Consequently, there is a tradeoff between reduced wind loads and the stiffness of twisting forms. However, the superiority or inferiority of twisting structures is studied in literature from one perspective only. Thus, the wind load demands and corresponding dynamic responses of those structures should be studied in a holistic way.

CHAPTER 3

MATERIAL AND METHODOLOGY OF THE RESEARCH

This chapter is devoted to the material and methodology. As the material of the research, first part of the chapter represents the essential information about the case study building, its analytical and scaled 3D test models. Besides, physical properties of the wind tunnel in the METUWIND - located in the Middle East Technical University (METU) – is introduced in this part. In the second part, wind tunnel tests which comprise both HFBB tests and synchronous pressure measurements are covered in detail. Finally, structural analyses are given explicitly within the context of methodology part.

3.1. Research Material

Prior to the methodology of the research, this section clarifies the selected case study building and its regenerated counterpart in conjunction with their both the analytical and 3D modelling processes. Data collection and evaluation are also explained within the scope of this section.

3.1.1. Case Study Research

A comparative case study research was conducted by making use of an existing twisting tall building; Cayan Tower – also known as Infinity Tower - (Dubai, 306m) and its regenerated prismatic counterpart. The prismatic twin is regenerated by removing the progressive rotation of the floors whereas the floor plan area, structural system, size of structural members, story height and the total height is kept the same to the original building.

3.1.2. Selection of the Sample Building

Regarding the tall buildings, contribution of twisting form at reducing dynamic wind effects for the structure is revealed through some studies (e.g., Tanaka et. al., 2013). However, comprehensive and precise wind loading studies complemented by structural response analyses are required for this relatively recent building forms by encapsulating the comparison with their prismatic twins. As briefly stated in the first chapter, the main objective of this research is to analyze the aerodynamic and structural response characteristics of "twisters", particularly those having adaptive structural systems. Mentioned earlier; adaptive structural system can be defined as the helical placement of structural members through height and usually around a central axis. Cayan Tower has an innovative adaptive structural system that will be discussed in the following part. Due to gravity effect, twisting structures show and inherent tendency to additional motion arising from the gravity loads on the structure (Baker, et. al., 2010). Being an outstanding example of this type, Cayan Tower (Figure 3.1) is selected as the sample building for this study.

Figure 3.1. Cayan Tower and its surroundings from Dubai Marina (The Skyscraper Center, 2019c)

3.1.3. Collection and Evaluation of the Data

At the time of its completion in 2013, Cayan Tower was the tallest twisting building in the world with its 306.4 m architectural height (CTBUH, 2016). Serving as a residential building, it is located in Dubai City; at the edge of Dubai Marina and Arabian Gulf. Formerly named as Infinity Tower, it takes full advantage of waterfront vista and surrounding environment not only by its location but also with the twisting facades (Skidmore, Owings & Merrill LLP [SOM], 2013).

As of September 2019, following the Shanghai Tower, it is the second completed tallest and still the highest residential twister in the world (The Skyscraper Center, 2019d). The structural system of the tower is framed tube and the structural material is high strength, cast-in-place reinforced concrete (Baker et. al., 2010). Both architectural and structural designs belong to SOM Architecture.

The tower has a chevron-like form and approximately 32m by 40 m dimensions in plan section. It completes a total 90° of twisting from the ground level to the top floor (Efstathiou & Baker, 2014). Identical floors ascend and turn around the circular central core by 1.2° of clockwise rotation (The Skyscraper Center, 2019c). The number of floors above ground is declared as 73 by both SOM and CTBUH. Nevertheless, due to double floor height of mechanical floor – located on 29^{th} floor level – (Gane & Haymaker, 2007), the number of floors above ground is accepted as 74 in this study. Even though the existence of floors with different floor-to-floor heights in podium part, all the floors are considered as having equal height of 3.8m. Moreover, the height of crown-like structure located at the very top is accepted as 6 floors height (Figure 3.2). Thus the 306.4-meter structure is accepted as 80 floors height. In analytical and 3-dimensional modelling of the tower, top 11.4 m of the crown part is ignored but the three-story height volume which located within the crown (on the top of floor 74) is taken into account.

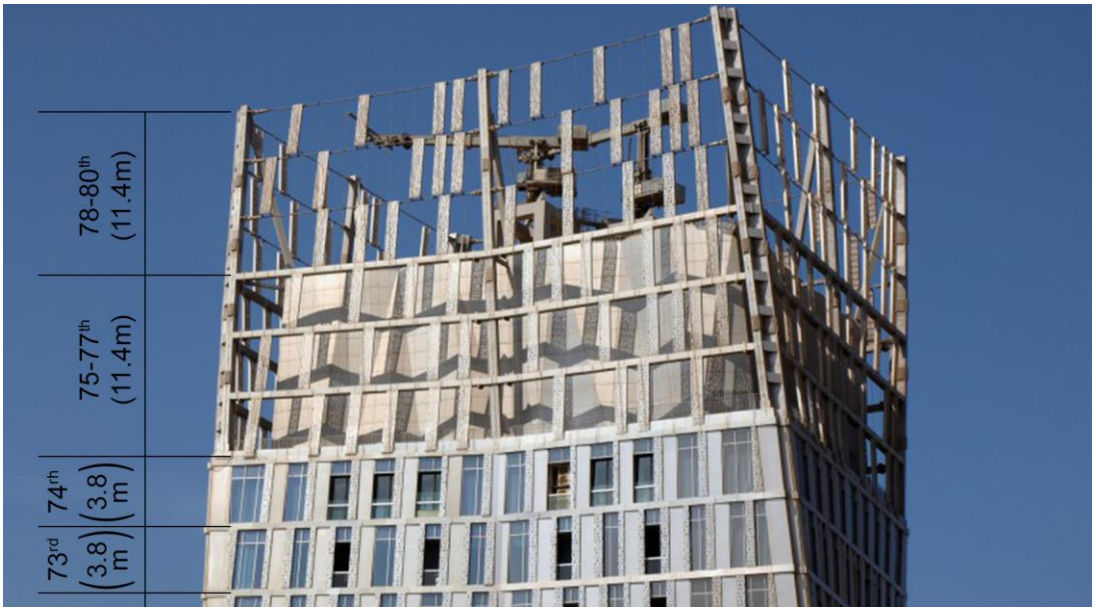

Figure 3.2. Top part of the Cayan Tower (The Skyscraper Center, 2019c)

Lateral loads acting on tower are mainly carried by its perimeter composed of closely spaced perimeter columns and deep spandrel beams because of its tube structural system. More efficiently, 75% of lateral loads are carried by the perimeter tube and the remaining 25% is taken by the circular central core (Rath, 2014).

Expression of the structural system to the exterior form is one of the main architectural design principles of the project (The Skyscraper Center, 2019c). In case of tilted and helical placement of the perimeter columns, secondary twist motion was expected under gravity loads (Shapiro, 2013). Therefore, an innovative stepped perimeter frame design was developed. Through ascending of the floors, stepped perimeter columns lean forward or back perpendicular to relevant location while making small shifts at the same time along the spandrel beams. This way, position of structural members retained constant in typical interior layout (Baker et. al., 2010). Figure 3.3 represents the stepped perimeter columns (above) and their positioning through spandrel beams (below) respectively.

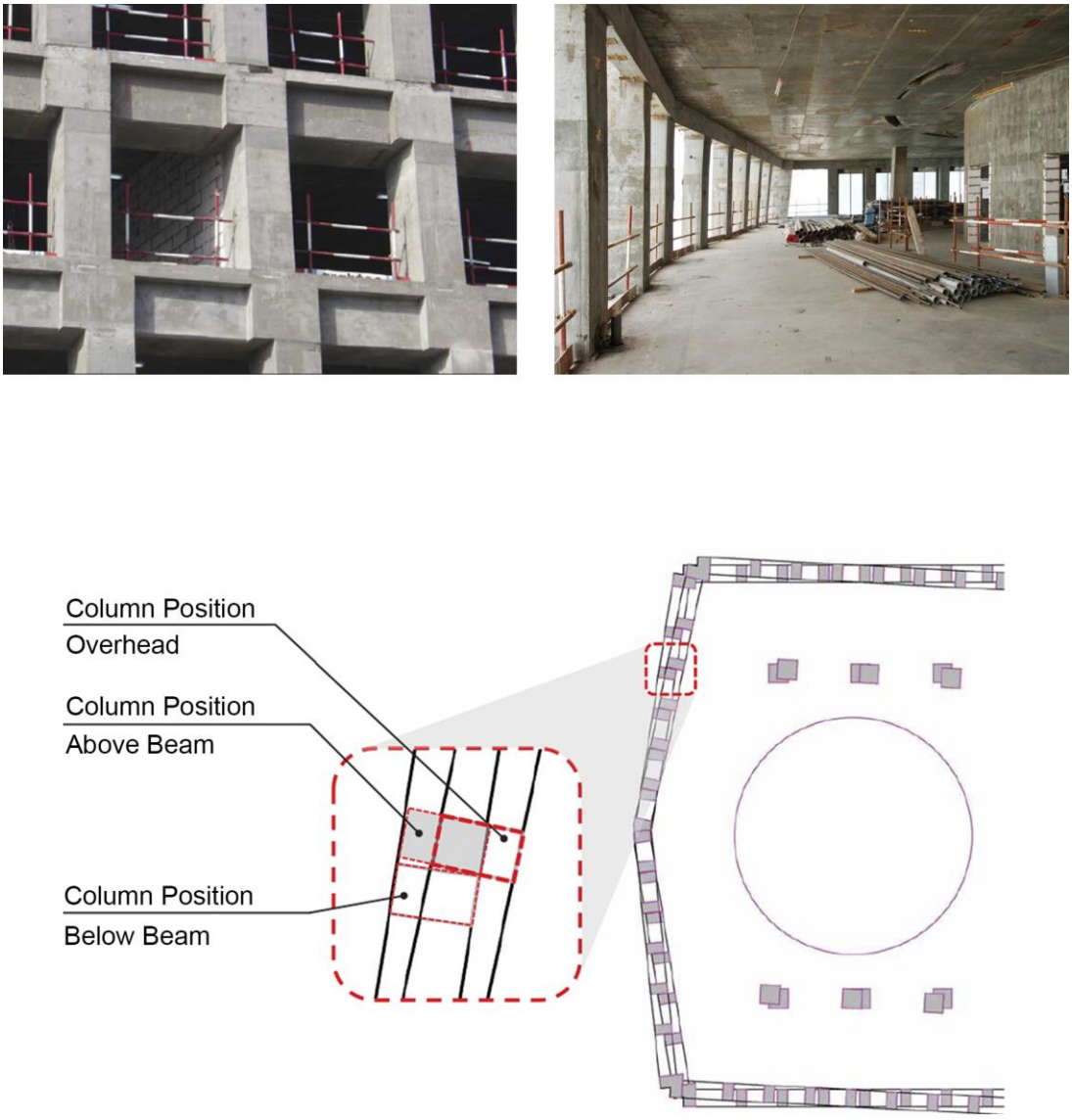

Figure 3.3. Stepped and leaning perimeter columns (above) and perimeter column positioning to beams (below) (Efstathiou & Baker, 2014)

In addition to these, secondary (additional) twist motion was eliminated by that innovative perimeter frame design (Efstathiou & Baker, 2014). Figure 3.4 shows the simplified lateral displacement alternatively for inclined (left) and stepped (right) perimeter columns resulting from the self-weight of the structure.

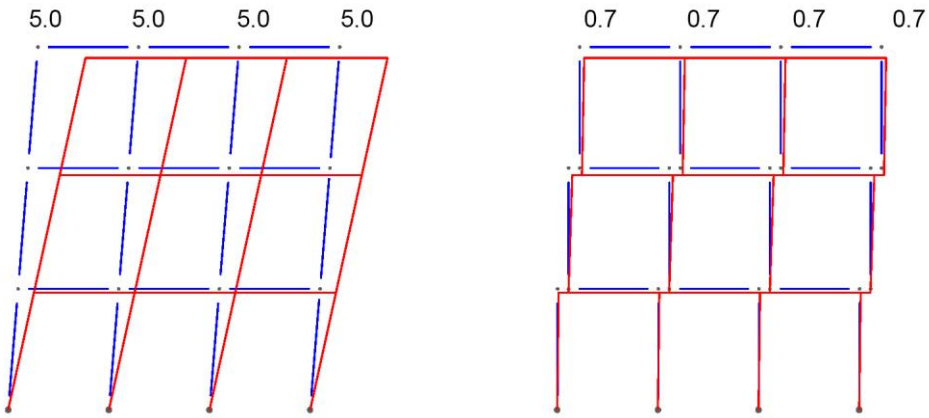

Figure 3.4. Simplified lateral displacement for inclined (left) and stepped (right) perimeter columns due to self-weight (Edited from Efstathiou & Baker, 2014)

Following a different rule from the perimeter frame, the four L-shaped corner columns and the six interior columns twist permanently through the ascending of the structure (Baker et. al., 2010). The corner columns are working as a part of perimeter tube whereas interior columns are mainly to reduce the span. Structural system members of Cayan Tower is illustrated in Figure 3.5.

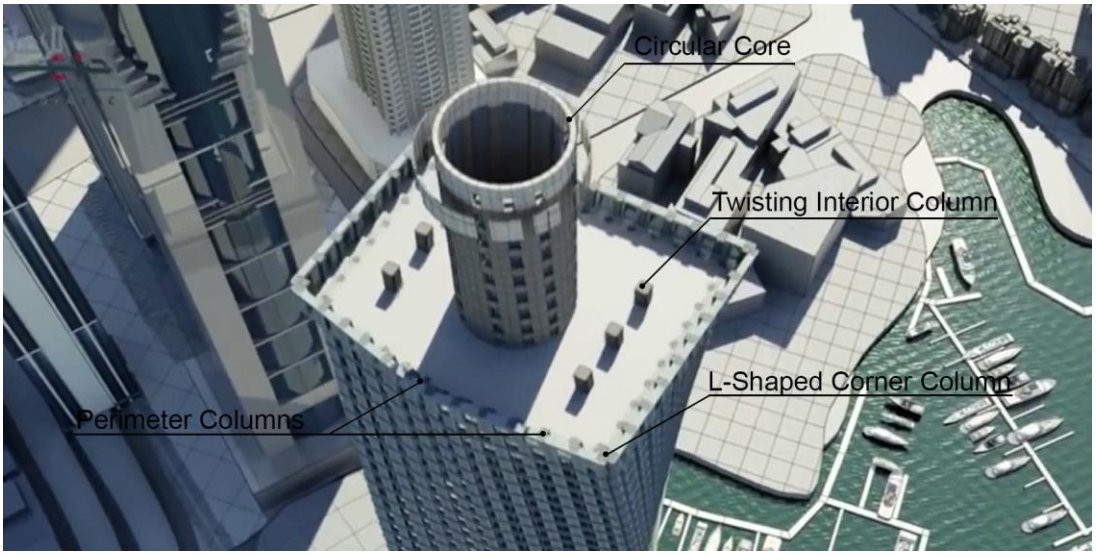

Figure 3.5. Illustrated structural system of Cayan Tower (Bunyan Program – Dubai TV, 2014)

3.1.4. Analytical Modelling of Twisting and Prismatic Forms

Due to fast and accurate production advantages, 3D printing technology is preferred for the physical modelling of this case study. First, commercial software AutoCAD (version 2017) have been used for preparing analytical models. In real building, screens were used (see Figure 3.2) as a passive solar protection element on the facade (Baker et. al., 2010). However, twisting form is modelled similar with the real building except the surface texture. Then, identical prismatic model is regenerated by removing the progressive rotation of twisting form as explained in the Section 3.1.1. An aluminum connection tool is specifically designed and produced for this research. Details of the connection tool will be given in the following part (Section 3.1.5). In order to fix the models with the metal tube of the connection tool, a circular hole -with a certain dimension - which is centering the circular core is left under the models. Figure 3.6 depicts the twisting (on left) and prismatic (on right) analytical (AutoCAD) models. Models are exported to STL as the common data format before the print out process.

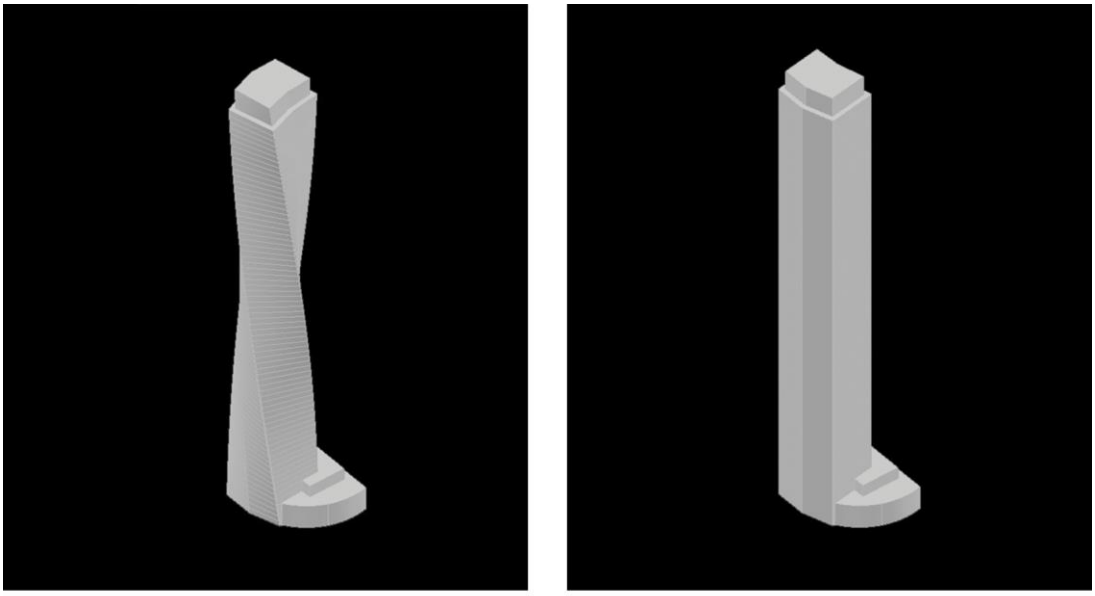

Figure 3.6. Twisting (left) and prismatic (right) analytical (AutoCAD) models

3.1.5. Wind Tunnel of METUWIND, Balance System and 3D Test Models

Both HFBB and synchronous pressure measurement tests have been conducted in the METUWIND C3 tunnel located in the Middle East Technical University (METU). It is an acrylic, medium scale suction type wind tunnel with 1m x 1m cross section and 8 m length. 45 kW electric motor can create 25 m/s maximum velocity in the test section. Flow conditioning is achieved by the honeycombs and screens at the inlet of the tunnel. This way, turbulence intensity is kept smaller than one percent (uniform air flow) (METUWIND, 2019). METUWIND C3 tunnel is shown in Figure 3.7.

Figure 3.7. METUWIND C3 Tunnel (METUWIND, 2019)

According to Holmes (2015), blockage effects should be taken into consideration. Depending on the blockage ratio, the boundaries of wind tunnel constraints the flow around the models. The blockage ratio is defined as the ratio of maximum model cross-sectional area to the cross-section of wind tunnel (Holmes, 2015). When the blockage area exceeds five percent, wind speed around the model increases remarkably and creates pressure on the model (Holmes, 2015). Under such circumstances, correction factors become necessary for the calculations of measurements. In order to avoid the blockage effects, 1/750 scale is used depending on the 306.4 m of real building height. Blockage ratios are shown in Appendix A for all angle of attacks

A connection tool that is custom-designed for the wind tunnel tests of this study is manufactured so that, it can be used for both HFBB tests and synchronous pressure measurement tests. It is composed of two parts which are the headpiece and bottom part. Aluminum is selected for minimizing the weight and additional holes are formed at the bottom part for reducing the weight further. Final weight of the connection tool is around 3 kg. Bottom part of the unit can be fixed to the load cell (HFBB sensor) via bolts, whereas headpiece can be rotated around central axis with 15 degrees steps above the bottom part.

Dummy load cell with exactly the same dimensions - to the original load cell - is used on pressure measurement tests in order to complete the mechanism. Headpiece and the hollow tube are welded and works altogether. Two symmetrical holes on the faces of hollow tube are used for the passage of pressure tubes on the pressure measurement tests. A steel ball system is used between the bottom part and the headpiece for providing stepwise axial rotation (each 15 degrees) capability. Figure 3.8 depicts the headpiece and bottom parts separately (on left) and connection of the tool with a model (on right).

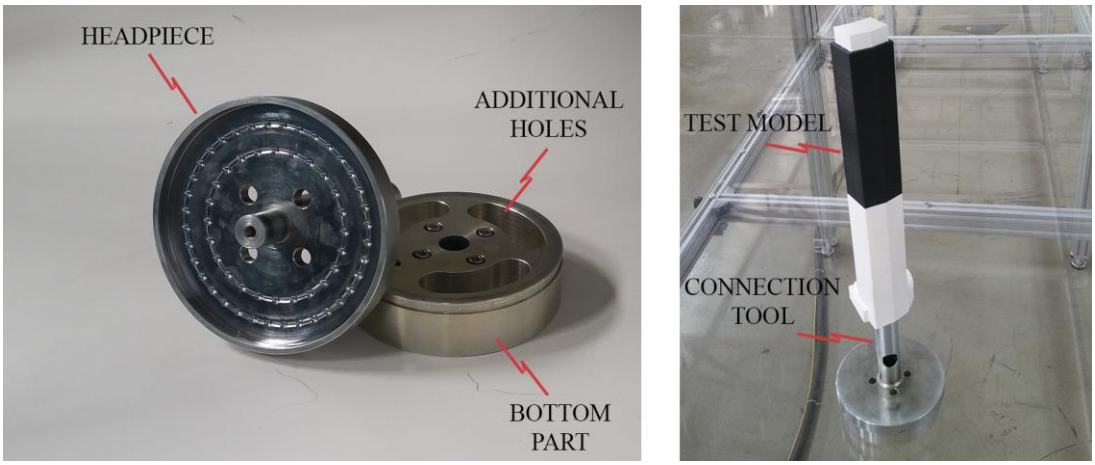

Figure 3.8. Parts of the connection tool (on left) and its connection with a model (on right)

In HFBB method, wind induced base responses are measured by a sensitive measurement system (load cell) located under the stiff support unit (Kurç et. al., 2012). In this study, ATI branded ultra-sensitive SI-32-2.5 type load cell have been used for HFBB tests. It is capable of measuring shear forces (F_x, F_y, F_z) and bending moments (M_x, M_y, M_z) simultaneously in six directions up to 10.000 Hz of sampling rate. Aeroelastic properties is not required for the models, in fact, stiff (Holmes, 2015) but lightweight (Gamble, 2003) models are required for HFBB technique. Correspondingly, polylactic acid (PLA) filament is used as the printing material. 1/750 scaled test models are printed by High Definition (HD) sensitive 3D printers. Use of 3D printers is provided by METU Design Factory which is an interdisciplinary center located in METU, providing space and infrastructure for students and researchers. 3D printing settings are indicated in Table 3.1. In order to achieve the equivalent conditions, same settings are used both for the HFBB test models and synchronous pressure measurement test models, except the surface openings and internal spacing for pressure tubes on the letter one.

Table 3.1. *3D printing settings*

Printing Device	Mass Portal Pharaoh HD 10
Material	PLA
Filament Diameter	1.75 mm
Layer Height	0.2 mm
Infill Percantage	20%
Internal Fill Pattern	Honeycomb
Support Infill Percentage	30%
Extruder Temperature	200°C
Bed Temperature	60°C

Note that, honeycomb internal fill pattern (Table 3.1) have been used to minimize the weight of the 3D models without sacrificing rigidity. Section of honeycomb pattern and the circular hole – centering the core - at the bottom of twisting model (podium level) is given as in Figure 3.9.

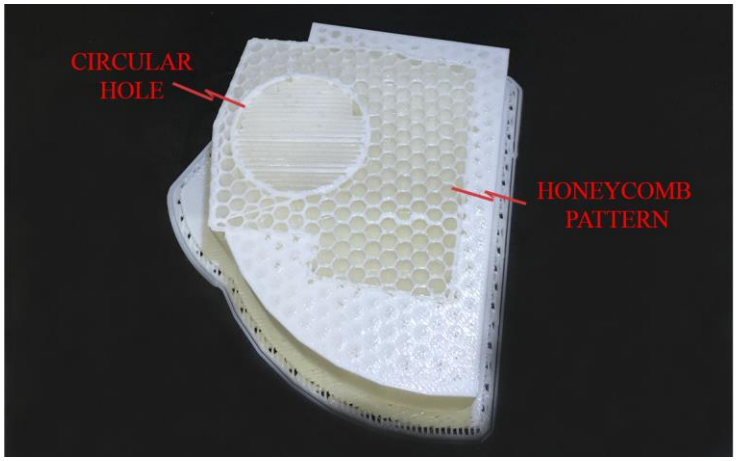

Figure 3.9. Internal section of twisting model (podium level)

Due to the maximum build area of 3D printers (30 x 30 x 30 cm cube), models are printed in two parts and the very top part which represents the three-story height volume is printed as the third one. Those three parts are glued together subsequently. To accelerate the printing process, two identical 3D printers and filaments have been used except the colors of available filaments. Twisting (left panel) and prismatic (right panel) models of HFBB tests are depicted in Figure 3.10.

Figure 3.10. Twisting (left panel) and prismatic (right panel) models of HFBB tests

Unlike the HFBB test models, openings with 1 mm diameter are left on the surfaces of pressure measurement test models for the placement of pressure tubes. Two pieces of openings are positioned at five different levels on each facade, the number of which is 10 per facade and 40 in total for all facades. In addition, five openings are left at the top of the model for taking measurements from the roof level. Passage for pressure tubes from model surfaces to pressure transducer is provided by the internal space which is the section remaining from the 5 mm wall thickness of the whole model plan section. It is accepted as the optimum thickness for ensuring the rigidity of the model.

1 mm nominal diameter of polyurethane pressure tubes which is branded TE Connectivity and coded as 27-02-0040P is used for the transmission of pressured surface air to the pressure transducer. All pressure tubes are indexed with different numbers for matching with the respective channel of pressure scanner. Lengths of the polyurethane tubes (from model surface to pressure transducer) are fixed to 1500 mm to avoid different inner tube resistance levels. 1/750 scaled twisting (left panel) and prismatic (right panel) models with integrated pressure tube orifices of pressure measurement tests are depicted in Figure 3.11.

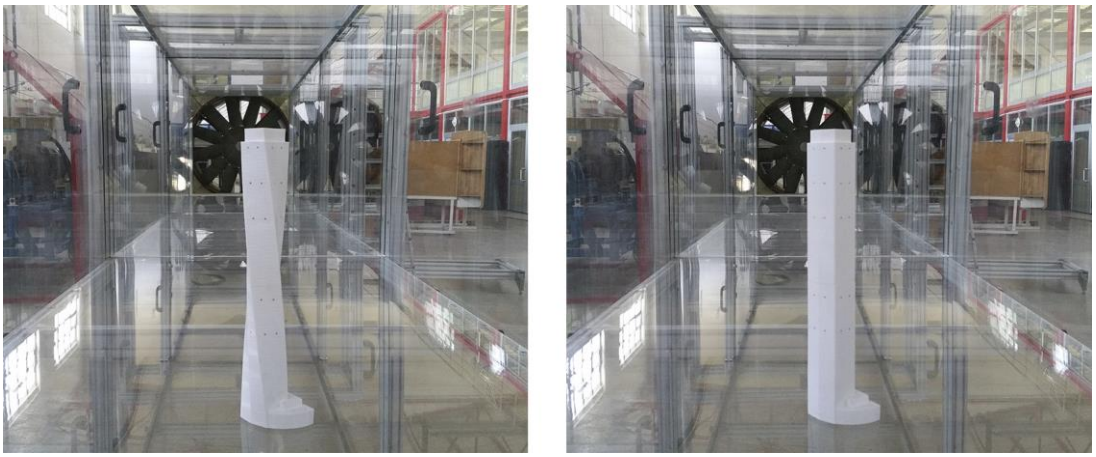

Figure 3.11. Twisting (left) and prismatic (right) models with integrated pressure tube orifices of pressure measurement tests

3.2. Research Methodology

Details of HFBB tests and synchronous pressure measurement tests are given in this part. The section and the chapter are concluded with the explication of the structural analyses within the context of research methodology.

3.2.1. Wind Tunnel Tests

Even though the progressive use of computational fluid dynamics (CFD) method through the recent years, wind tunnel tests are still accepted as the most effective and accurate instrument for the measurement of aerodynamic loads on civil engineering field (Duthinh & Simiu, 2011; Hernandez et. al, 2013). Similarly, Cermak (2003) and Taranath (2010) render the benefits of wind tunnel tests by focusing on accurate measurement of wind induced motions, estimation of load distribution on structure and analyzing the effects on surrounding domain.

In addition, various building codes such as ASCE/SEI 7-16 (2017), Eurocode 1 (2005) and Dubai Wind Code (2013) point out requisiteness of wind tunnel testing for the design of buildings having irregular architectural form, complex structural system or extraordinary height. Simulation of atmospheric boundary layer (ABL) in test section is critical for the account of real building oscillations (Kurç et. al., 2012; Liu, Zheng, Wu, Flay & Zhang, 2019). On the other hand, alternative studies (e.g. Prohasky, Castro, Watkins & Burry, 2016; Yong & Dol, 2015) show that uniform air flow wind tunnels can be used as a cost-efficient credible tool at conceptual base. In fact, rather than calculating the wind loads with ultimate accuracy, the main aim of this study is to perceive the difference between the aerodynamic features of prismatic and twisting forms. HFBB and synchronous pressure measurement tests are conducted in this study. In accordance with the objectives of the study, comparative wind tunnel tests were carried out under equivalent test conditions for both test methods.

3.2.1.1. High-Frequency Base Balance Tests

A series of HFBB tests were conducted for both twisting and prismatic models in METUWIND C3 tunnel (Figure 3.12) with the inside tunnel wind velocity of 6.85m/s. Velocity is determined empirically in accordance with the instrument capacity.

Figure 3.12. HFBB test (left) and connection tool/load cell placement (right)

Measurements were performed for each 15° angle in order to understand the effect of wind direction (Figure 3.13). 1.000 Hz of sampling rate is used for gathering data through 2 minutes of duration for each angle.

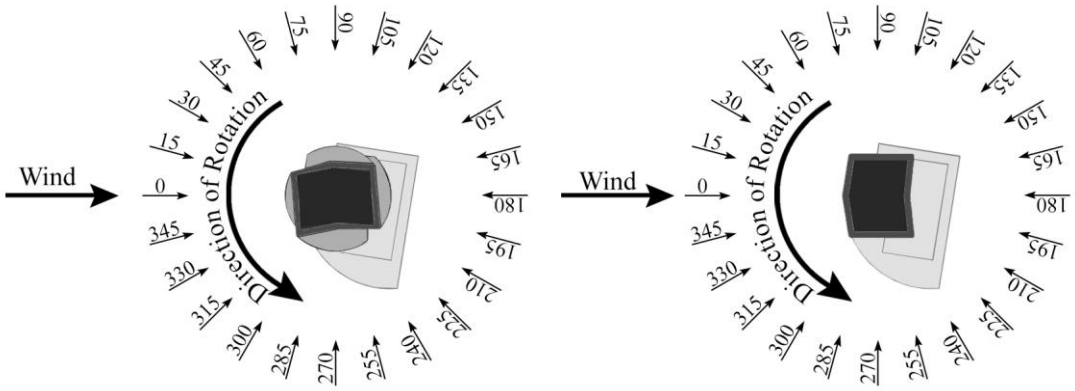

Figure 3.13. Wind flow direction on twisting (left) and prismatic (right) models (top views)

3.2.1.2. Synchronous Pressure Measurement Tests

A series of pressure tests were conducted in order to compare the pressure distribution on building facades. Equivalent conditions are ensured to HFBB tests (Figure 3.14).

Figure 3.14. Synchronous pressure test (left) and pressure tube/scanner connection (right)

As the maximum sampling rate of the pressure transducer, 25 Hz of sampling rate have been used for one minute of duration for each angle of attack. Number of taps - 45 in total - is determined in accordance with the scale of models.

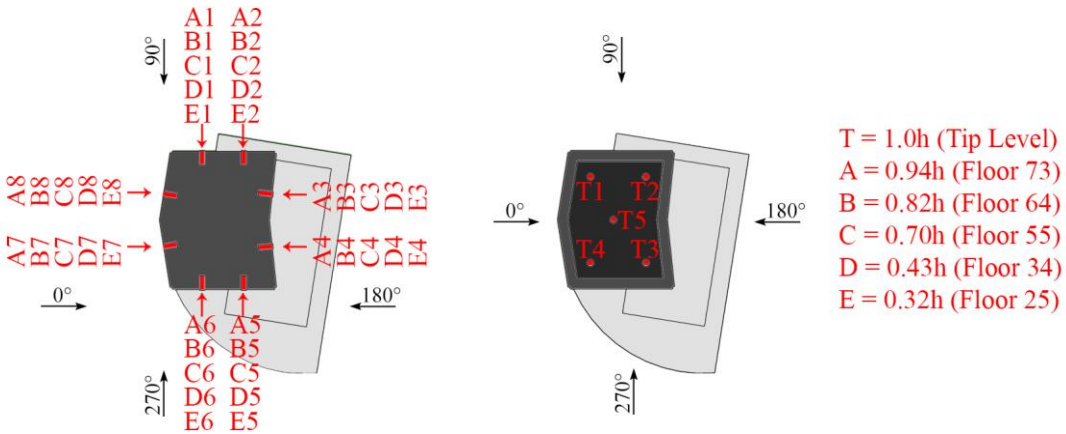

Figure 3.15. Layout of the pressure tubes on tower (left) and top (right) levels of prismatic model

The layout of the pressure tubes is shown for prismatic and twisting models in Figure 3.15 and Figure 3.16 respectively along with the wind directions.

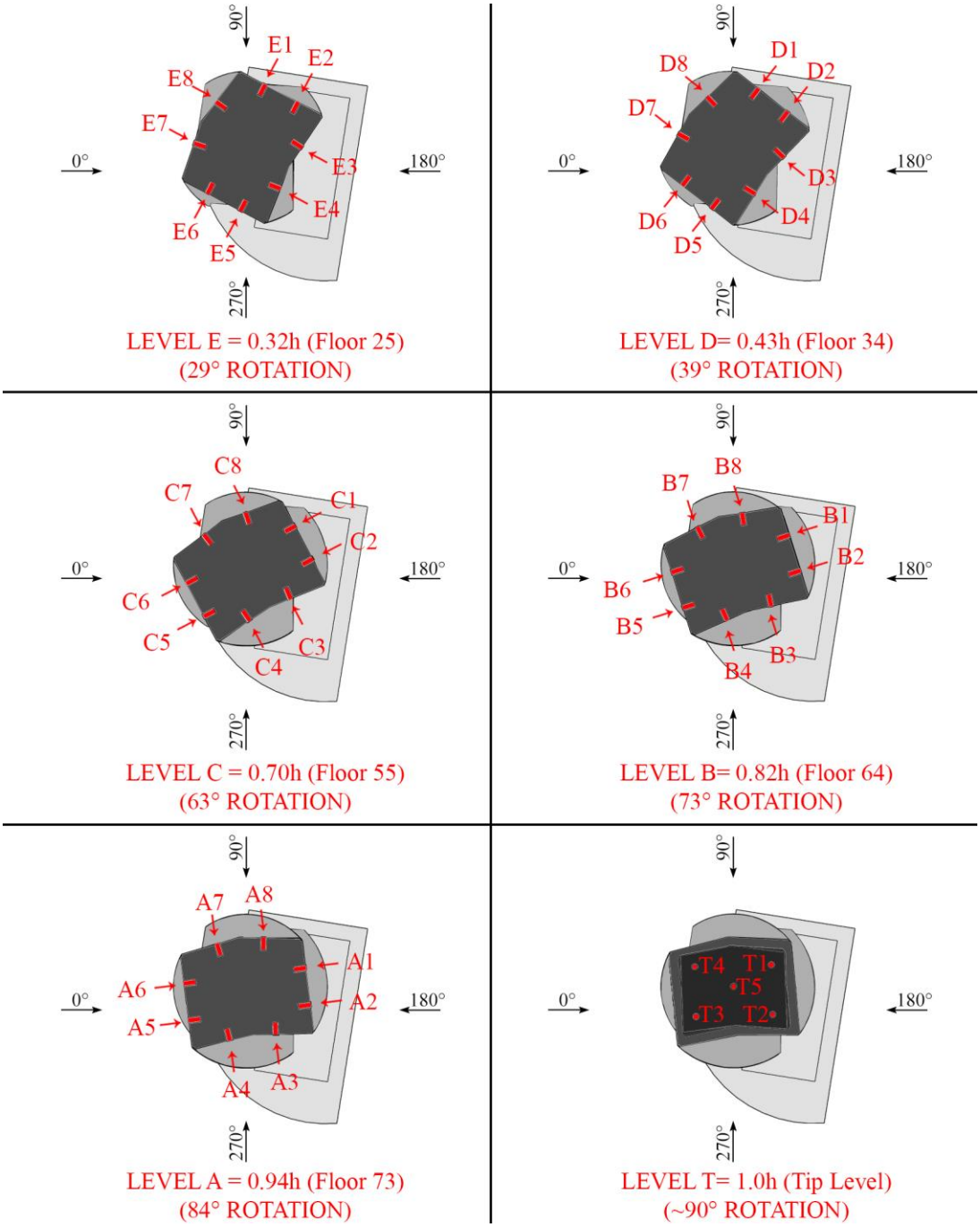

Figure 3.16. Layout of the pressure tubes on tower (A-B-C-D-E) and top (T) level of twisting model

3.2.2. Structural Analyses

Comparative structural analyses were carried out in accordance with the wind loads obtained from HFBB tests for twisting and prismatic forms. This way, base shear forces, story displacements, torsional moments and the distribution of loads on structural members are examined. Due to its compatibility with tall buildings and code-based capabilities, the commercial software, ETABS (ver. 17.0) have been preferred for the analyses. Prior to the wind load analyses, modal analyses were performed in order to verify the analytical models. Details of modal analyses are given in the fourth chapter.

3.2.2.1. Structural Analysis Models

The structural analysis model of twisting form was constructed in accordance with the real building properties. Stepped perimeter columns, six interior twisting columns and spandrel beams are defined as frame elements. Typical spacing of axes is 3 m. Section of typical perimeter column is assigned as 80 x 120 cm and typical spandrel beam is defined as 100 x 110 cm. Head column has a section of 100 x 120 cm. Dimensions of six twisting interior columns are 140 x 140 cm. Unlike the rest of the columns, the four L-shaped corner columns are modelled as shell elements (100 cm shell thickness) in two pieces in accordance with Efstathiou & Baker (2014).

Regarding the difficulties of analyzing the 100 cm thick reinforced concrete circular core as a whole; it is divided into equal pieces of shell elements. 30 cm thick inner shear walls of core are modelled separately. Auto rectangular mesh is applied to the circular core. Flat plate slabs are modelled as shell elements with a thickness of 23 cm. Semi-rigid diaphragm is assigned to the slabs. All above given size of structural members are retrieved from Baker et. al. (2010) and Efstathiou & Baker (2014). Typical floor structural system of twisting model is depicted in Figure 3.17.

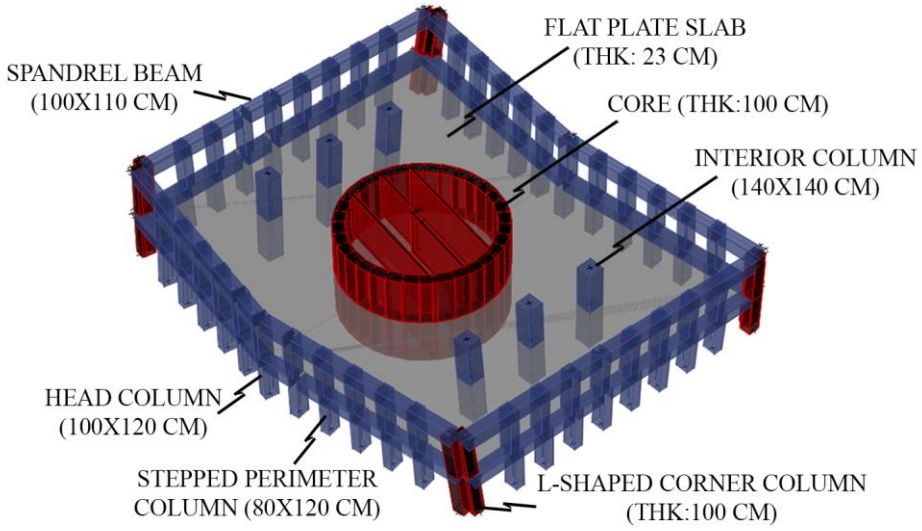

Figure 3.17. Typical floor structural system of twisting model (constructed in accordance with Baker et. al., 2010 and Efstathiou & Baker, 2014)

Clockwise rotation of the floors (approximately 1.2° per floor) and the stepped perimeter column concept is reflected by modelling the spandrel beams as two parts. Division point is identified so that, upper node of stepped perimeter column and consecutive parts of the spandrel beam is connected at this exact node, thus leaning forward or leaning back of related perimeter column is modelled accordingly. Modelling detail is depicted in wireframe mode in Figure 3.18.

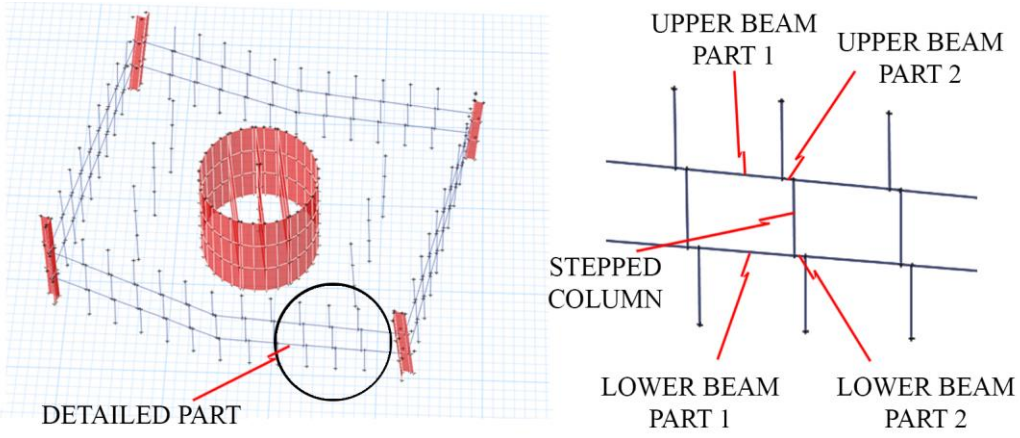

Figure 3.18. Modelling detail of stepped perimeter column (twisting model)

Efstathiou and Baker (2014) state that, two different concrete classes is used on the sample building by dividing the height. 90 days minimum concrete compressive cylinder strength of the concrete at first 50 floors is 70 MPa, whereas 50 MPa of minimum compressive cylinder strength concrete (28 days) is used from floor 51 to top level. Mathematical analysis model is prepared accordingly by assigning C70/85 and C50/60 concrete classes for the related levels respectively. Furthermore, Efstathiou and Baker (2014) declare the average concrete modulus of elasticity for the first 50 floors and the rest as 49.000 MPa and 45.000 MPa, respectively. These concrete material properties are assigned to the analysis model.

Regarding the size of structural members, story height, total height, material properties and modelling methodology, the prismatic model is reconstructed identically with the twisting model except the progressive rotation of the floors. In other words, prismatic structural analysis model can be designated as the conventional twin of the twisting model. It should be noted that, stepped perimeter column concept is not a concern for the prismatic model inherently. Wireframe and extruded view of twisting (left panel) and prismatic (right panel) ETABS models are depicted in Figure 3.19.

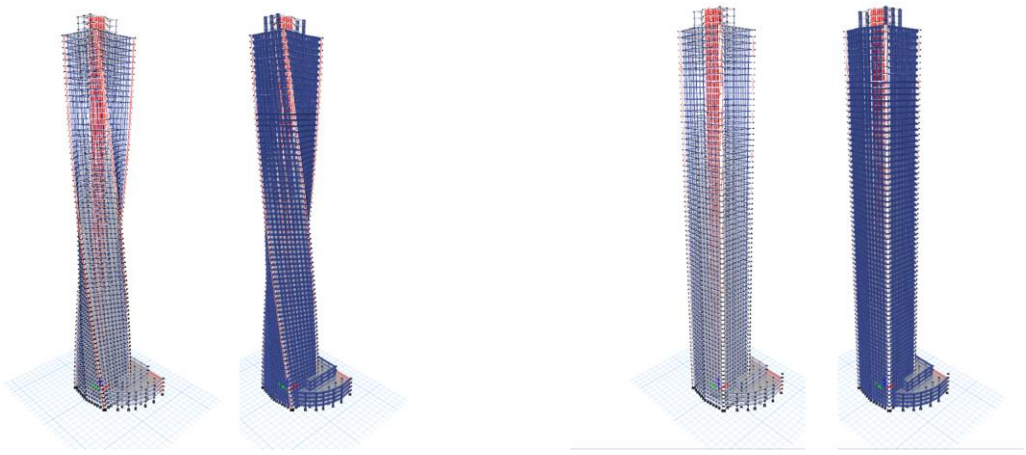

Figure 3.19. Wireframe and extruded view of twisting (left) and prismatic (right) ETABS models.

3.2.2.2. Gravity and Lateral Loading on the Structural Analysis Models

Vertical (gravity) loads are assigned under three categories which are dead load, super dead load and live load. Simply, dead load is the self-weight of the structure itself. On the other hand, super dead load is the load resulting from the weight of non-structural materials including floor coverings, partition walls, facade members etc. Super dead and live loads are applied as uniformly distributed loads. 2 kN/m² live load is assigned, whereas 3.5 kN/m² super dead load is implemented based on the common practice of structural engineering. Above defined loads are given for all the floors except the triple floor height mechanical volume located on the top of floor 74. Live load and super dead loads are assigned as 2 kN/m² and 0.5 kN/m² for this part due to different intended use.

Linear static and modal analyses have been performed in this study. Cracked section properties of concrete members are modelled in accordance with the ACI 318-14 (2014) code. Regarding the lateral loads, wind load is the key parameter for this research. Here, the loads in question are obtained from the HFBB tests. As stated by Cermak (2003), HFBB tests provide data for determining the base shear forces around main X and Y axes and base moments around X, Y and Z axes of real scale building. Aforementioned data is gathered as time series. Note that, aerodynamic forces along and moments around vertical axis have relatively little importance for building aerodynamics (Taranath, 2010), so they are not taken into consideration.

Effects of wind is scrutinized by taking measurements at each 15° angle; thus calculations are made in this context. According to the results, maximum subjected wind loads are found at different yaw angles for twisting and prismatic forms. These maximum loads are assigned on principle axis (X and Y) of the related mathematical model.

CHAPTER 4

RESULTS AND DISCUSSION

Chapter 4 is dedicated to results and discussions of the study. HFBB and synchronous pressure measurement test results are given together with their calculation steps. Afterwards, the results of comparative structural analyses with HFBB loads are presented explicitly. Finally, all deductions are discussed in the light of previous studies from the literature.

4.1. Results of Wind Tunnel Tests

This section focuses on the processing of wind tunnel test measurements of both HFBB and synchronous pressure techniques and corresponding results. These are used to compare the aerodynamic loads on twisting and prismatic forms. Then, structural analyses are performed by making use of wind loads obtained from HFBB tests to scrutinize the trade-off between demands and capacities of twisting and prismatic forms.

4.1.1. HFBB Post Processing

In HFBB method, maximum shear forces and moments M_y, M_x (bending), and M_z (torsion) acting on the real structure can be calculated by using shear force and moment signals measured from the base of scaled rigid model. By assuming the fundamental mode shape of a tall building as linear, calculations are based on linear first mode shape assumption (Tschanz & Davenport, 1983). Thus, acting forces on the structure for translational modes can be calculated in proportion to measured bending moment (Kayışoğlu, 2011; Zhao, Xu, Sun & Lan, 2014).

Primarily, mean, standard deviation and power spectral density values of time dependent HFBB data is found for each 15° angle of attacks. Aforesaid values are computed via MATLAB (R13) scripts that are particularly developed for this study. Then, base bending moments of twisting form and its prismatic counterpart are calculated. Maximum base bending values – those used as the design moments – of twisting and prismatic building have been calculated from HFBB test data by using Equation (4.1).

$$\hat{M}_{\theta} = \bar{M}_{\theta} + \sqrt{\hat{M}_{B\theta}{}^{2} + \hat{M}_{R\theta}{}^{2}} \qquad (4.1)$$

In Equation (4.1), $\hat{M}_{\theta}$ represents the maximum base bending moment of actual building whereas $\bar{M}_{\theta}$ is the corresponding mean moment. Besides, $\hat{M}_{B\theta}$ and $\hat{M}_{R\theta}$ represents background and resonant components, respectively. These values are calculated for both primary axes (X and Y) of the structure and subscript θ refers to yaw angle for all premises. Primary axes of the twisting (left) and prismatic (right) models are depicted in Figure 4.1.

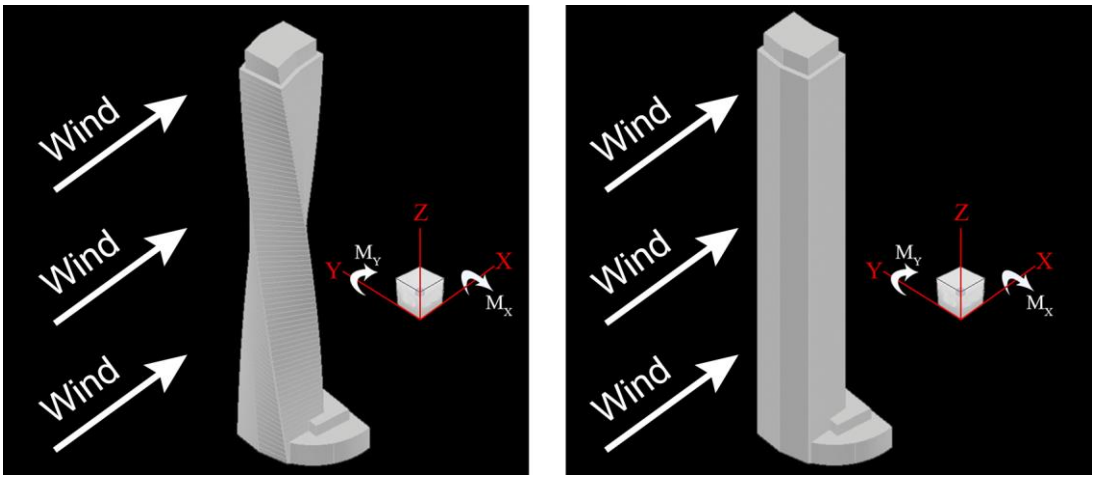

Figure 4.1. Primary axes of twisting (left) and prismatic (right) models

Along wind mean moment ($\bar{M}_{\theta}$) is determined through the Equation (4.2) given below;

$$\bar{M}_{\theta} = \int_0^H 1/2 \rho C_D V_m{}^2(z) B z dz \tag{4.2}$$

Given by the Equation (4.2), ρ represents the density of air, $B(z)$ is the width of the building perpendicular to wind flow at height (z), and $C_{D\theta}$ means drag force coefficient that is stated as the nondimensional resistance of an object against wind stream in fluid dynamics. $V_m(z)$ in Equation (4.3) is mean wind velocity for the reference height z and found as follows;

$$V_m(z) = C_e(z).C_t.V_b \tag{4.3}$$

Parameters of Equation (4.3) are given below;

$C_e(z)$: Surface roughness effect

C_t: Surface topography effect

V_b: Basic wind velocity

In HFBB technique, statistical random properties of the wind - inside the tunnel - is the main interest rather than its speed. Instead of determining the complexity of nature, averaged values and similarities are used and it is called random vibration approach (Holmes, 2015). Accordingly, once normalized power spectrum is obtained using wind tunnel velocity, the properties of real building including the design wind speed is used for the rest of the calculations (Kayışoğlu, 2011).

Mean wind speed at a specific location or height is usually computed via logarithmic law or power law (Holmes, 2015). Since the sample building is located in Dubai, basic wind velocity V_b is taken as 30 m/s (return period of 50 years) in accordance with the Dubai Wind Code (2013).

Coefficient of surface roughness is found by the Equation (4.4) depending on the condition specified below, which is related with the terrain categories. In addition, Equation (4.5) represents the formulation of surface topography coefficient.

$$\text{For } z \geq z_{min}\text{: } C_e(z) = k_r \ln\left(\frac{z}{z_0}\right) \text{ and } k_r = 0.23.(z_0)^{0.07} \tag{4.4}$$

where z_0 is defined as the length (m) of the surface friction. For different terrain categories, z_0 and z_{min} values are given by the Table 4.1 directly taken from Dubai Wind Code (2013) which is originally adopted from the Euro Code.

Table 4.1. *Surface friction lengths (z_0) and minimum friction heights (z_{min}) (Dubai Wind Code, 2013)*

Terrain No	Terrain Type	z_0 (m)	z_{min} (m)
0	Coastal areas exposed to open sea	0.003	1
I	Lake shores and flat open areas with no obstacles	0.01	1
II	Areas with low vegitaton and isolated obstacles where the average obstacle separation is more than 20 times the average obstacle height.	0.05	2
III	Villages and suburbs, where the average obstacle seperation is less than 20 times the average obstacle height.	0.3	5
IV	City centers and similar areas, where more than %15 of the terrain is covered with structures taller than 15 m.	1	10

$$C_t = 1 + 0.001\Delta \tag{4.5}$$

In Equation (4.4), z_0 is defined as the surface friction and Δ is the difference between the reference z height and the sea level in Equation (4.5). Since location of the sample building is located in Dubai Marina, Δ is accepted to be 0, and C_t is found as 1. z_0 is directly taken from the code as 0.003.

The mean wind velocity is calculated with reference to actual location of the sample building and the formulations described above. The resulting height-dependent wind speed profile is shown in Figure 4.2. As clearly seen from the profile, mean wind speed at the top of the building height (306.4 m) is slightly larger than 52 m/s.

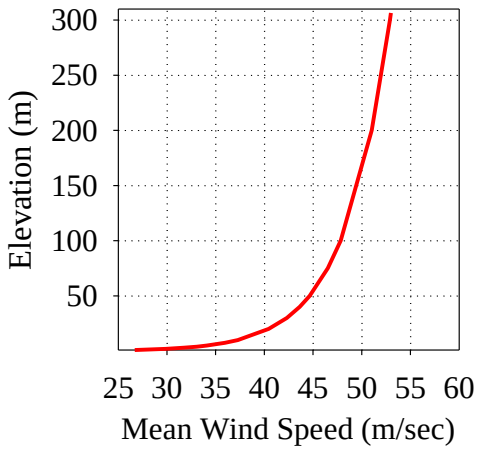

Figure 4.2. Height dependent wind speed profile for the sample building location in accordance with Dubai Wind Code (2013)

$\hat{M}_{B\theta}$ and $\hat{M}_{R\theta}$ occur as a result of dynamic response of the structure under the wind load effects. They are determined via following Equations (4.6) and (4.7).

$$\hat{\mathrm{M}}_{\mathrm{B}\theta} = g_{B\theta} \times \sigma_{MB_\theta} \tag{4.6}$$

In Equation (4.6), $g_{B\theta}$ is the background peak factor and σ_{MB_θ} is the standard deviation of the measured base bending moment.

$$\hat{\mathrm{M}}_{R\theta} = g_{R\theta} \sqrt{\frac{\Pi}{4\zeta_1} f_1 S_M(f_1)} \tag{4.7}$$

In Equation (4.7), $S_M(f)$ is power spectral density of the measured moment whereas, f_1 and ζ_1 are the natural frequency and structural damping ratios for the first mode, respectively. $g_{R\theta}$ is resonant peak factor and computed by Equation (4.8).

$$g_{R\theta} = \sqrt{2\ln(f_1 T)} + 0.5772 / \sqrt{2\ln(f_1 T)} \tag{4.8}$$

T in the Equation (4.8) is observation time.

In this chapter, all above given calculation steps, essential parameters and pre-accounted coefficients are retrieved from Zhou et. al (2003), Kayışoğlu (2011), Kurç et.al., (2012), Dubai Wind Code (2013) and ASCE 7-16 (2017).

Furthermore, time series data of HFBB tests and their FFT graphs are available at the end of the report in Appendix B for 0°, 30°, 90°, 135°, 180° and 270° yaw angles. To clarify, twisting and prismatic forms are subjected to their maximum wind loads at 30° and 135° angle of attacks respectively. Those are also mentioned in the following related sections of structural analyses part.

The variables that are used on the calculations of twisting and prismatic buildings are listed accordingly;

- Natural frequency of actual twisting building in X direction, f_{tx} = 0.124 Hz (Modal analysis of the building)
- Natural frequency of actual twisting building in Y direction, f_{ty} = 0.138 Hz (Modal analysis of the building)
- Natural frequency of actual prismatic building in X direction, f_{px} = 0.134 Hz (Modal analysis of the building)
- Natural frequency of actual prismatic building in Y direction, f_{py} = 0.156 Hz (Modal analysis of the building)
- Background peak factor, $g_{B\theta}$ = 3 (Zhou et. al., 2003)
- Structural damping ratio, ζ = 0.02 (ASCE 7-16, 2017)
- Observation time, T = 3600 sec. (ASCE 7-16, 2017)
- Density of air, ρ = 1.25 kg/m³ (Dubai Wind Code, 2013)
- Drag coefficient of prismatic building at 0° angle, C_D = 1.3 (Zhou et. al., 2003)

The drag coefficient (C_D) of prismatic building at 0° wind angle is assumed to be 1.3 (Zhou et. al., 2003) in this study. Since the building width perpendicular to wind flow and corresponding mean moment measured in HFBB tests change with the angle of attack, drag coefficient for other angles of attack ($C_{D\theta}$) are found by using C_D = 1.3 as the function of measured base bending moments. Figure 4.3 illustrates the sections of twisting (on left) and prismatic (on right) models in elevation for 0°, 45° and 90° angle of attacks. Regarding the perpendicular building width in height (z) ($B(z)$) in Equation (4.2), constant B values are easily measured from the prismatic building elevations. On the other hand, referring to the Figure 4.3, width of the twisting building varies constantly through the building height.

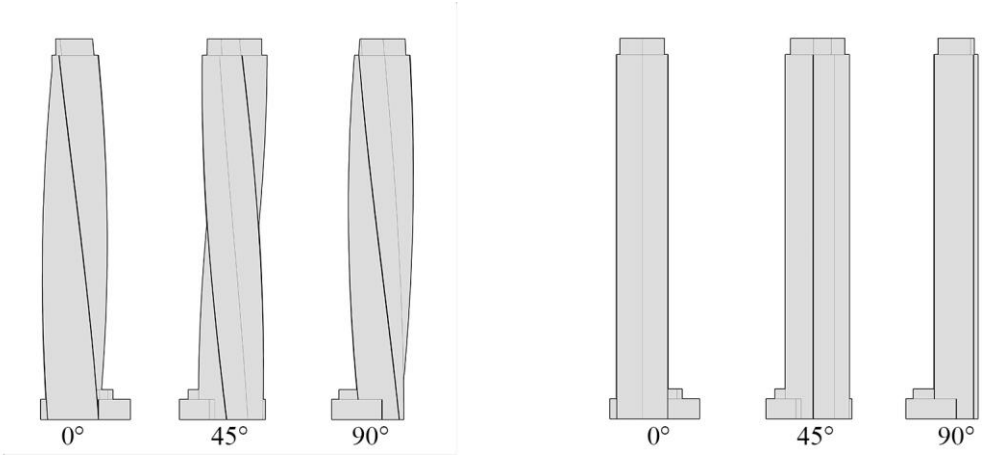

Figure 4.3. Sections of twisting (left) and prismatic (right) models for 0°, 45° and 90° yaw angles

However, by assuming the resulting error is fairly small, average B values are computed and implemented in Equation (4.2) for the twisting building. Figure 4.4 compares the drag coefficients for each angle of attack for twisting and prismatic models. Results show that drag coefficients calculated for twisting form are smaller than those of prismatic form for right angles 0°, 90°, 180° and 270°. Besides, the dispersion in $C_{D\theta}$ of twisting form is much smaller than that of prismatic form.

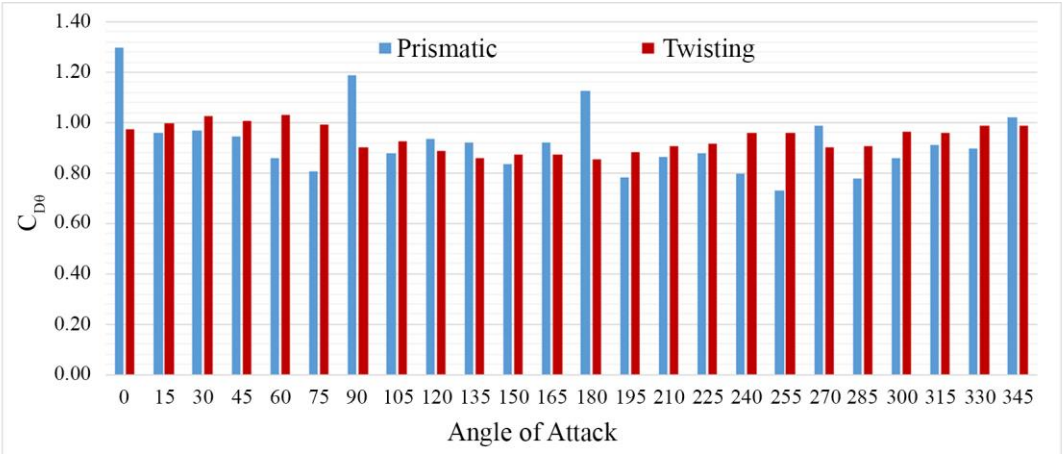

Figure 4.4. Drag coefficients for various angles of attack on building form

4.1.2. HFBB Moment Results

For both building forms and each angle of attack, mean base moments of twisting and prismatic buildings have been calculated for each principal axis of the actual buildings. Figure 4.5 compares $\bar{M}_X$ (left panel) and $\bar{M}_Y$ (right panel) of these forms. The results showed that, compared to the prismatic model, $\bar{M}_Y$ of twisting model is about 20% less for 0° and 180°. The difference between drag coefficients (Figure 4.4) of twisting and prismatic form as well as the effect of changing width perpendicular to the flow through the height (Figure 4.3) are main reasons for this difference. Considering the $\bar{M}_X$ results, wider facades of twisting building is exposed to wind direction for 90° and 270° yaw angles, thus it is estimated as the reason for larger moments of twisting form at these angles of attack. As the acute angle between wind direction and X axis of the model (maximum 90°) increases, $\bar{M}_X$ of prismatic model gets smaller than that of twisting model. This result highlights the impact of rectangular plan of the tower when compared to the square plans investigated by other studies in literature (Moon, 20015; Tanaka et. al., 2013).

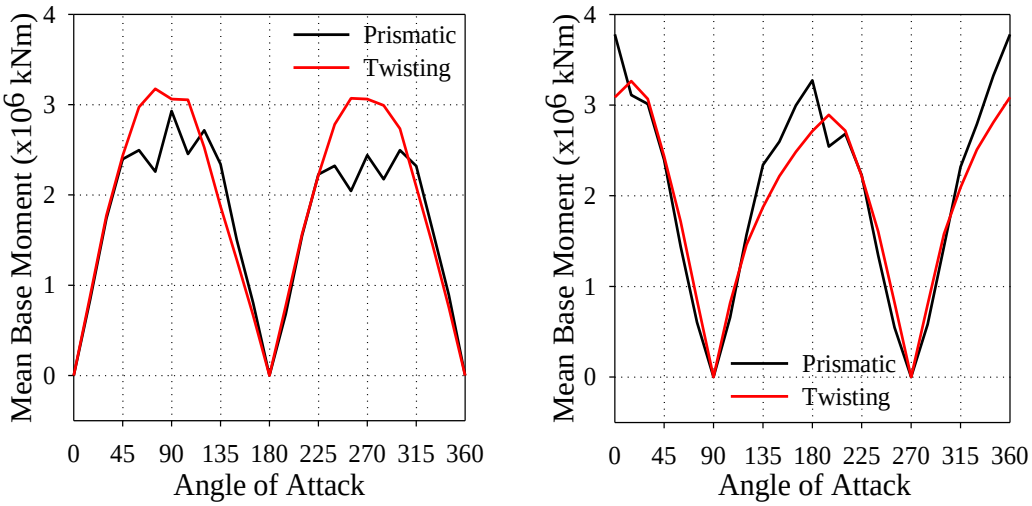

Figure 4.5. $\bar{M}_X$ (left panel) and $\bar{M}_Y$ (right panel) of twisting and prismatic buildings for different angle of attack

Background and resonant moments in X and Y direction ($\hat{M}_{BX}$, $\hat{M}_{BY}$ and $\hat{M}_{RX}$, $\hat{M}_{RY}$ respectively) of twisting and prismatic forms are shown in Figure 4.6 and Figure 4.7. Figure 4.6 showed that, background moment component of twisting form is smaller on both directions but especially for Y direction which is differentiated about 25%.

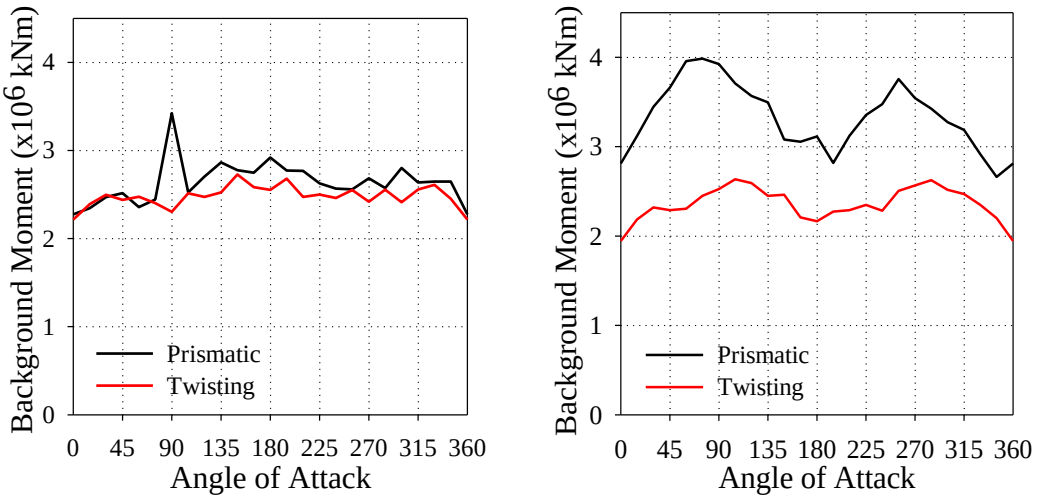

Figure 4.6. Background moments $\hat{M}_{BX}$ (left) and $\hat{M}_{BY}$ (right) of twisting and prismatic buildings

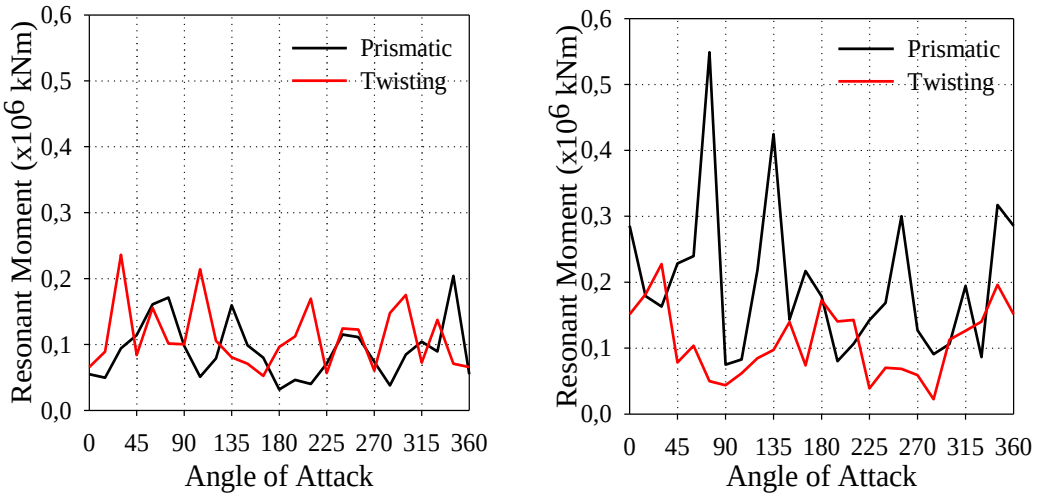

Figure 4.7. Resonant moments $\hat{M}_{RX}$ (on left) and $\hat{M}_{RY}$ (on right) of twisting and prismatic

The results of the resonant moments (Figure 4.7) highlighted that, twisting form shows relatively constant resonant moments for both directions, compared to resonant moment of prismatic form which changes on a larger scale with respect to direction and angle of attack. Inherent distinction between those two forms is the main reason for this difference. It is estimated that, due to sharp edged form of prismatic building, vortex shedding characteristics are different for each angle of attack, whereas twisting form have a smoother response depending on the shape. However, such an estimation requires verification by investigating the wake flow field but not included in this study.

With the known values of $\bar{M}_{\theta}$, $\hat{M}_{B\theta}$ and $\hat{M}_{R\theta}$, maximum base moments in principle axes of the structure are calculated in accordance with the Equation (4.1). In Figure 4.8, maximum base moment in X (on left) and Y (on right) axes are shown for different yaw angles. Regarding the maximum base moments in Y axis, moment of twisting form compared to the prismatic one can be summarized as; 20% reduction on 0°, 35% reduction on 90°, 25% reduction on 180° and finally reduction 25% on 270° is obtained in along wind direction

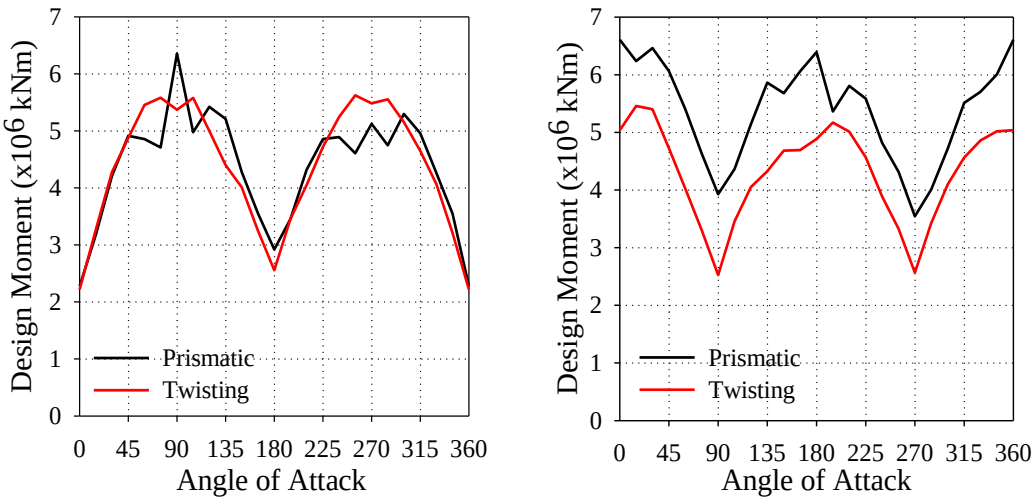

Figure 4.8. Maximum base moments $\hat{M}_X$ (left) and $\hat{M}_Y$ (right) of twisting and prismatic models

On the other hand, obtained design moments around X axis is rather close for both twisting and prismatic forms. Due to height dependent alteration on the width section of different forms, a slight difference is observed for some angles. Finally, twisting and prismatic twin structures are compared in terms of resultant moments that is calculated by using the Equation (4.9) and the comparison is given in Figure 4.9

$$\hat{M} = \sqrt{\hat{M}_X{}^2 + \hat{M}_Y{}^2} \tag{4.9}$$

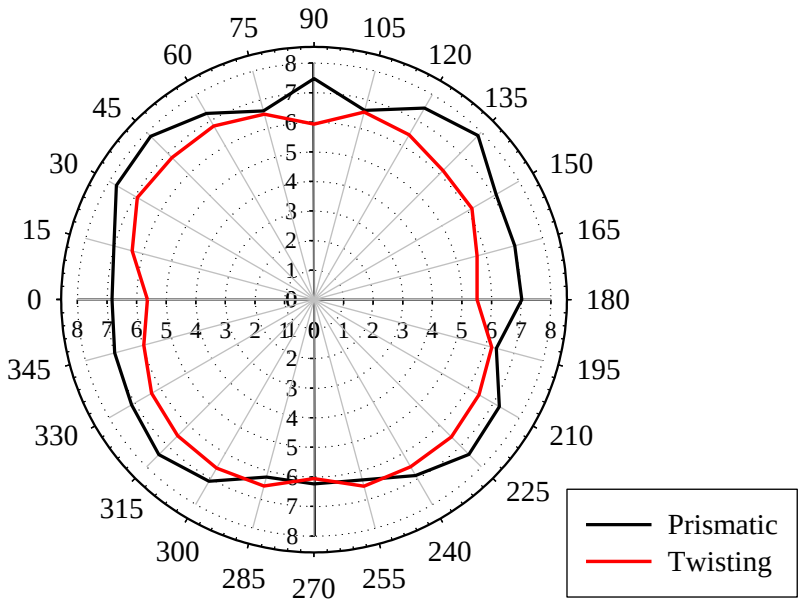

Figure 4.9. Resultant moments for twisting and prismatic forms in accordance with angle of attack

Compared to the prismatic form, resultant moment of twisting form is 10% less in average. In addition, maximum reduction is observed as 22% for 135° angle of attack. The tower plan is not simply a rectangle, front and back sides have chevron like form as well (Figure 3.13), so it is not symmetrical. Consequently, dynamic response of each angle has its own characteristics. The results showed that twisting building is superior compared to its prismatic counterpart in terms of aerodynamic form.

4.1.3. Synchronous Surface Pressure Measurement Results

In synchronous surface pressure measurement tests, facade pressures and overall wind loading data can be obtained by taking several pressure measurements simultaneously from the outer surface of a tall building model (Aly, 2013). As stated previously, equivalent conditions and inside tunnel wind velocity (6.85 m/s) are provided with the HFBB tests which are conducted for each 15° angle. Results are compared for twisting and prismatic forms in terms of local pressures - or suctions - on pressure taps and surface pressure distribution with angle of attack.

Instead of real dimensional pressure values, use of nondimensional pressure coefficient (C_P) is a common practice in aerodynamic engineering (Anderson, 2011). It is not only applied for measurement scaling (e.g., wind tunnel testing) but also for understanding the mean pressure dispersion of surfaces. Pressure coefficients have been computed from wind tunnel test data by using Equation (4.10).

$$C_P = (p_x - p_r) / q \tag{4.10}$$

p_x represents the pressure measured from the related probe, p_r means the static reference pressure in tunnel and q is the dynamic pressure. Static pressure (p_r) is measured with pitot tube which is located before the tested model on undisturbed wind flow area. Dynamic pressure q is defined by the Equation (4.11).

$$q = \frac{1}{2} \rho V_r^2 \tag{4.11}$$

Where ρ and V are the air density and free flow velocity respectively. Above given formulations are retrieved from ASCE (1999). Local pressure coefficients obtained from the probe points are demonstrated from Figure 4.10 to Figure 4.17 for 0°, 90°, 180° and 270° angle of attacks.

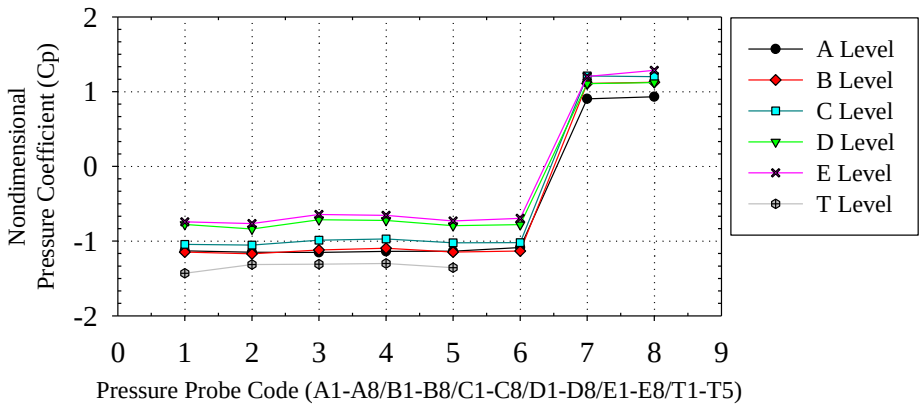

Figure 4.10. Pressure coefficients on pressure probes of prismatic building at 0° angle of attack

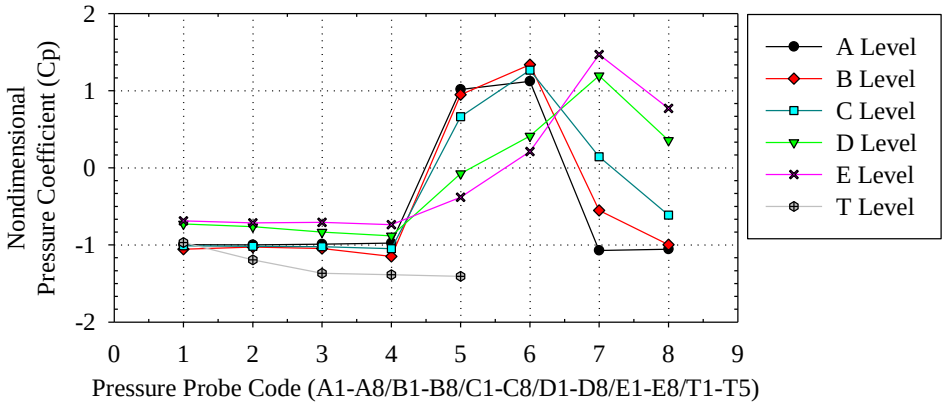

Figure 4.11. Pressure coefficients on pressure probes of twisting building at 0° angle of attack

Layout of the probes and wind directions are already given by the Figure 3.15 and Figure 3.16. Regarding the Figures 4.10 to 4.17, pressure coefficients above the 0 line show positive pressure, whereas, the rest with negative sign refer to suctional pressure. When Figure 4.10 is examined (0° angle of attack), there are two different situations for facade probes 1 to 6 and 7-8 respectively for the prismatic model. Located on the windward direction, positive pressure is observed for 7-8 probe series at all tower levels (A-B-C-D-E). On the other hand, there is suction not only at the crosswind probes (1-2 and 5-6 series) but also at the backside probe (3-4) series. As expected, separated flow streamlines reattach at the backside and creates suction.

Besides, it is important to clarify that, since the average values are taken into consideration for the calculations, alternating shading of vortices (vortex shedding) results in suction on crosswind directions.

In addition to above given discussions, the pressure coefficients gradually decrease from level A to level E in proportion to height only with the exception of A7 and A8 probes. Although they are located at the very top level of the tower, their pressure coefficients are smaller with respect to B7 - B8, C7 - C8, D7 - D8 and E7 - E8. It is estimated due to rapture of flow around peak levels of the structure. Yet, it requires detailed wake flow field studies for a clearer statement.

Regarding the Figure 4.11, facade pressure coefficients of probes show similarities with the related probes of prismatic model in terms of positive/negative sign and degree. However, it is dependent on the rotational motion of the building. Facing surface of the probes changes even if they are indexed with the same name. For instance, although there is suction on D5 and E5, positive pressure is observed at D6 and E6 because of their proximity to wind flow direction. In this context, facing surface of 5 to 8 probe series deviate depending on the height (A-B-C-D). Correspondingly, this led to an intermediate degree of pressure coefficients in the respective probes.

When the results of the Figure 4.12 to Figure 4.17 are compared in the following pages, it can be deducted that the surface pressure coefficients display similar features with the results in Figure 4.10 and Figure 4.11 depending on the probe, height and angle of attack. It is valid for both forms. Furthermore, roof probes (T level) of prismatic form have a close pressure coefficient degree for all yaw angles. Besides, couple of probes on the wind flow direction are exposed to bigger pressure coefficients which can be clearly seen in Figure 4.12. Fluctuation of pressure coefficients is even smoother regarding the twisting form.

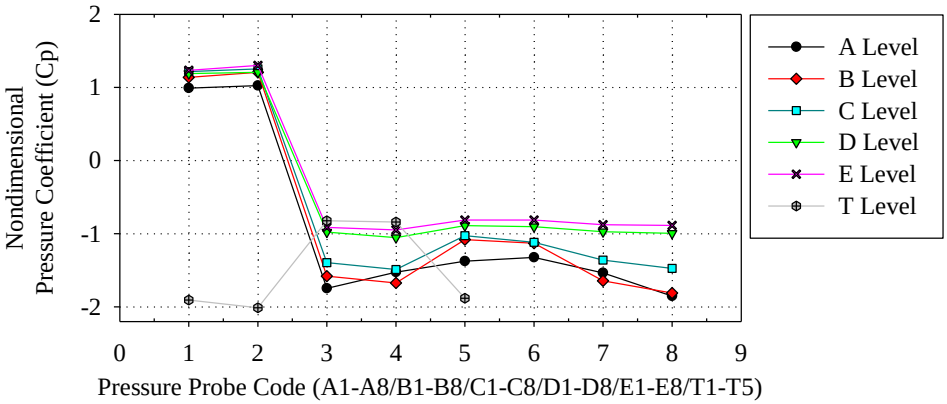

Figure 4.12. Pressure coefficients on pressure probes of prismatic building at 90° angle of attack

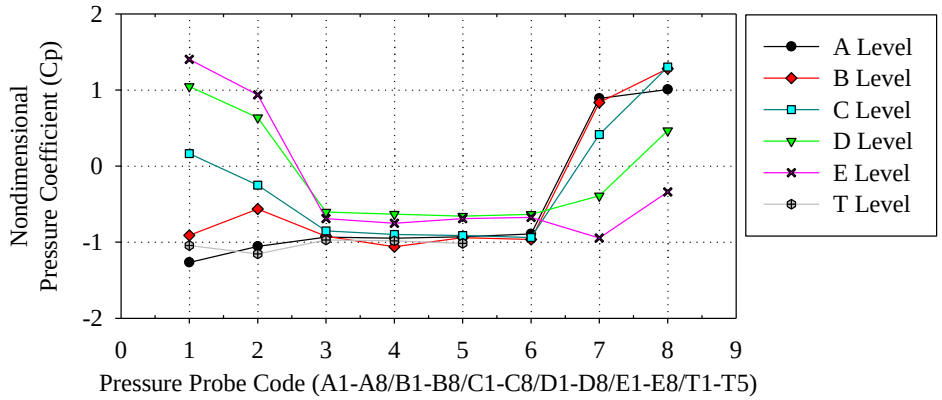

Figure 4.13. Pressure coefficients on pressure probes of twisting building at 90° angle of attack

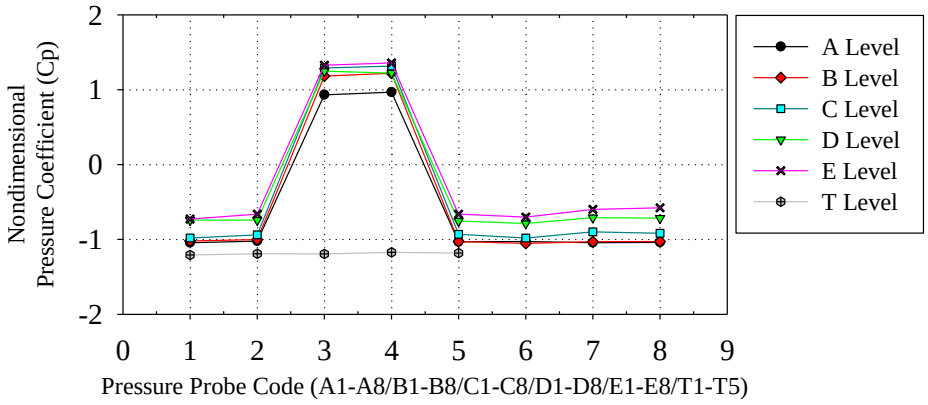

Figure 4.14. Pressure coefficients on pressure probes of prismatic building at 180° angle of attack

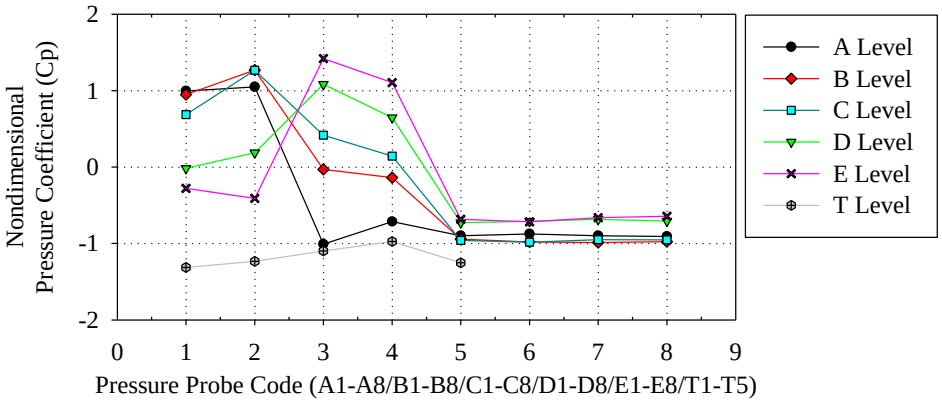

Figure 4.15. Pressure coefficients on pressure probes of twisting building at 180° angle of attack

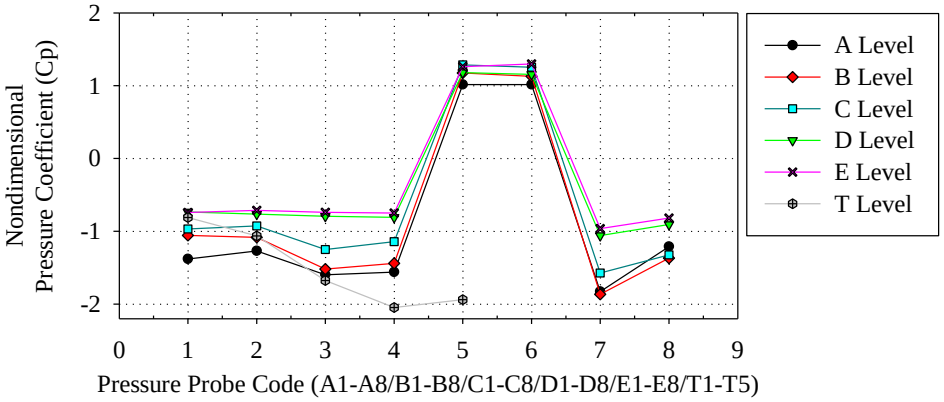

Figure 4.16. Pressure coefficients on pressure probes of prismatic building at 270° angle of attack

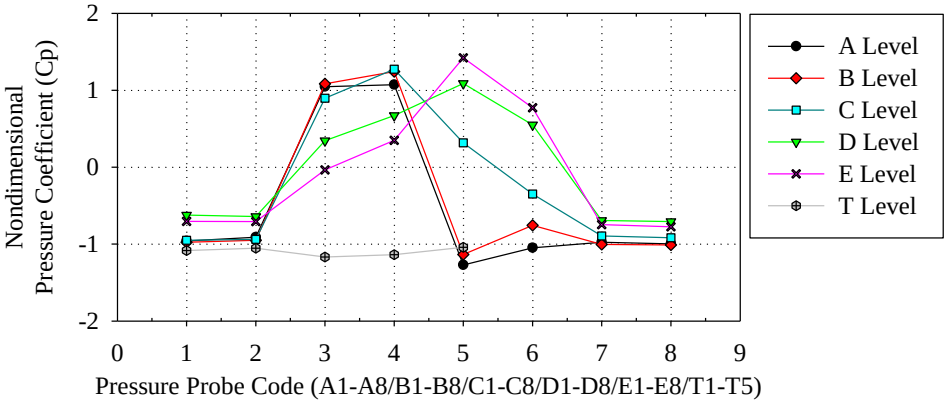

Figure 4.17. Pressure coefficients on pressure probes of twisting building at 270° angle of attack

Within the scope of this research, facade pressure distribution was also investigated by using 3-dimensional interpolation method. This part of the study was carried out by using the pressure coefficients via commercial software Tecplot 360 (version 2018). Figure 4.18 to Figure 4.25 represent surface pressure distributions of prismatic and twisting buildings in accordance with the angle attack for 0°, 90°, 180° and 270°. It is noteworthy that, as the measurements have been taken from relatively few numbers of taps (45 in total) depending on the 1/750 scale, facade pressure distributions have been obtained approximately by 3-dimensional interpolation.

According to the results, surface pressure is distributed smoothly over the prismatic model. It shows a fluent characteristic while changing through the facades. On the other hand, deviation is more explicit and pressure distribution changes on a shorter distance over the surfaces of twisting model. This situation is particularly observed around the twisting edges.

Considering the results limited to Figure 4.18 to 4.25, the aerodynamic superiority of one to another cannot be clearly explained due to inherent difference between the geometries and the complexity arising from the nature of the twisting form. Moreover, Cermak (2003) stated that pressure test results for structures with complex geometry may be uncertain and technical details are available from the relevant reference.

However, in the light of above given discussions related to HFBB and synchronous measurement tests results, it can be stated that, although twisting model is subjected to lesser base bending moments, larger and localized surface pressure can be observed on it. Accordingly, it might bring additional complexities for cladding design of twisting form.

Furthermore, deductions show the role of both wind tunnel techniques - HFBB and synchronous pressure measurement tests – individually and the significance of complementary study through alternative techniques.

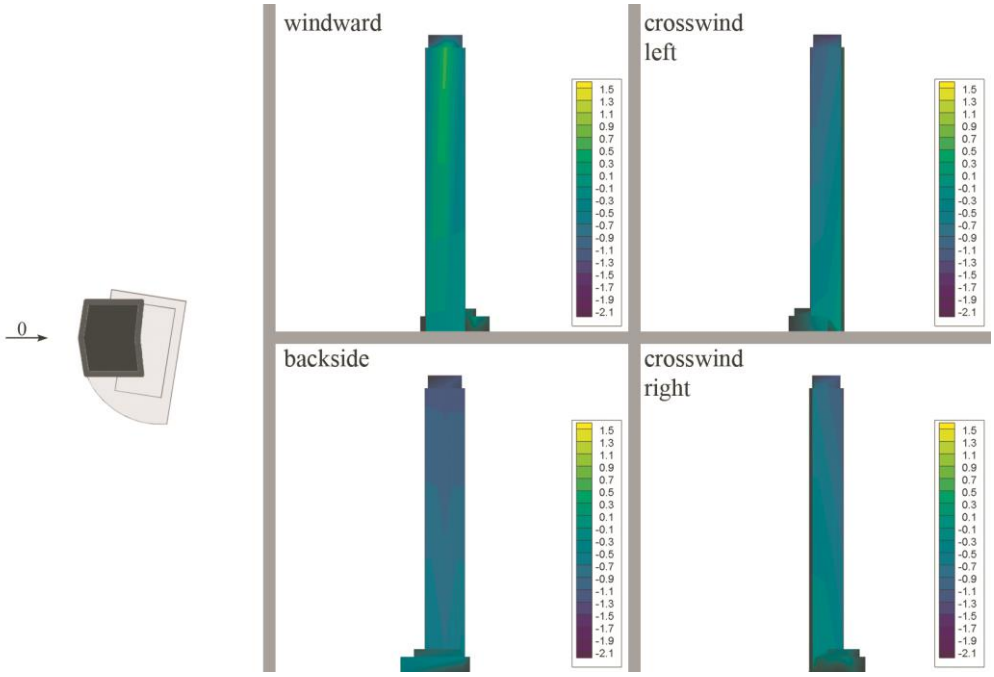

Figure 4.18. Wind direction and surface pressure distributions on windward, crosswind and back facades of prismatic building at 0° angle of attack

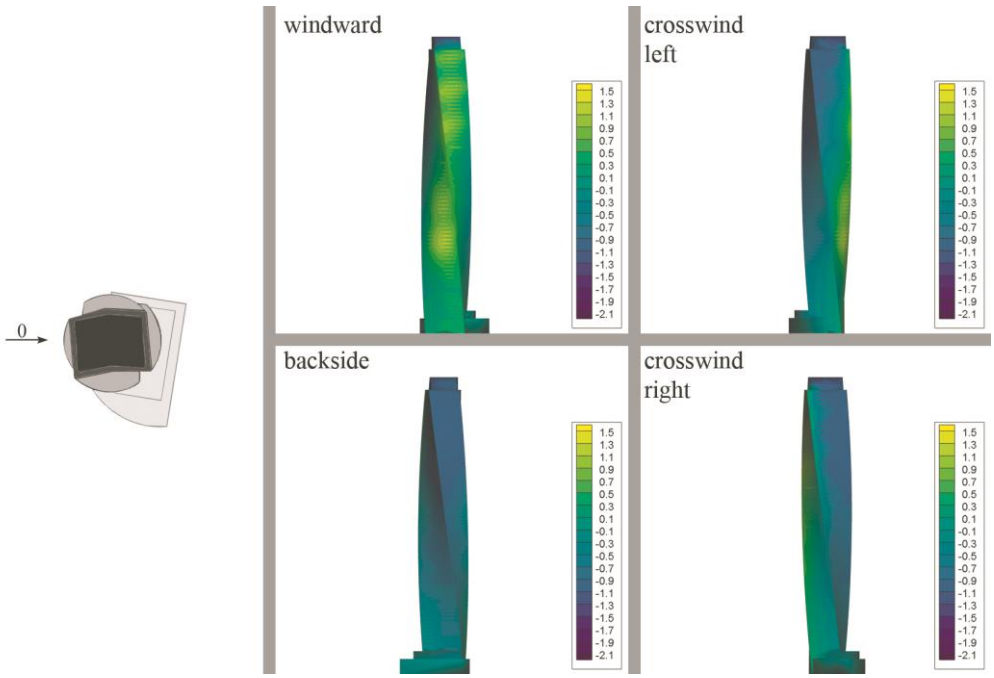

Figure 4.19. Wind direction and surface pressure distributions on windward, crosswind and back facades of twisting building at 0° angle of attack

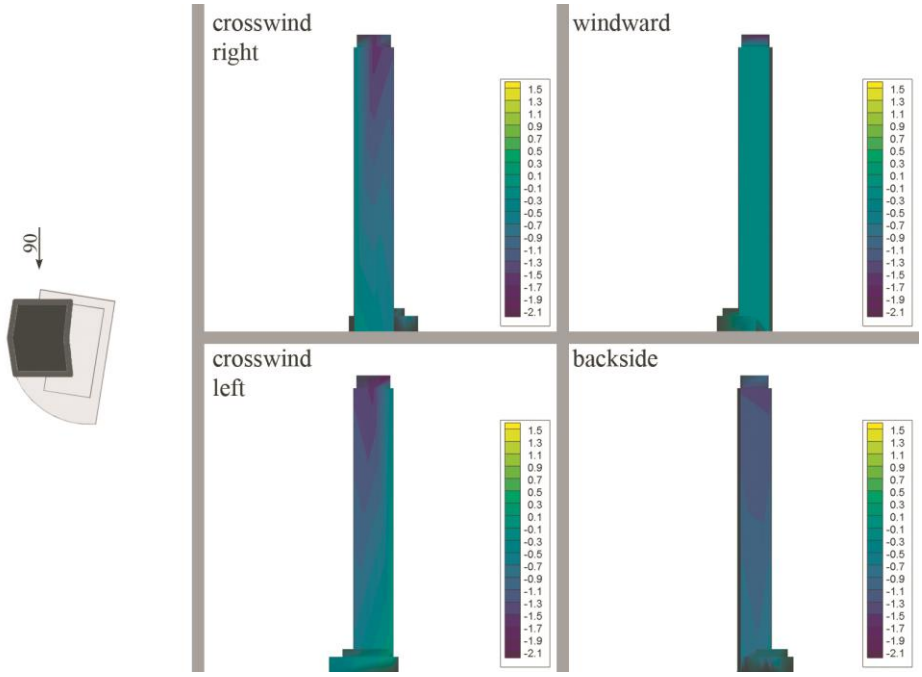

Figure 4.20. Wind direction and surface pressure distributions on windward, crosswind and back facades of prismatic building at 90° angle of attack

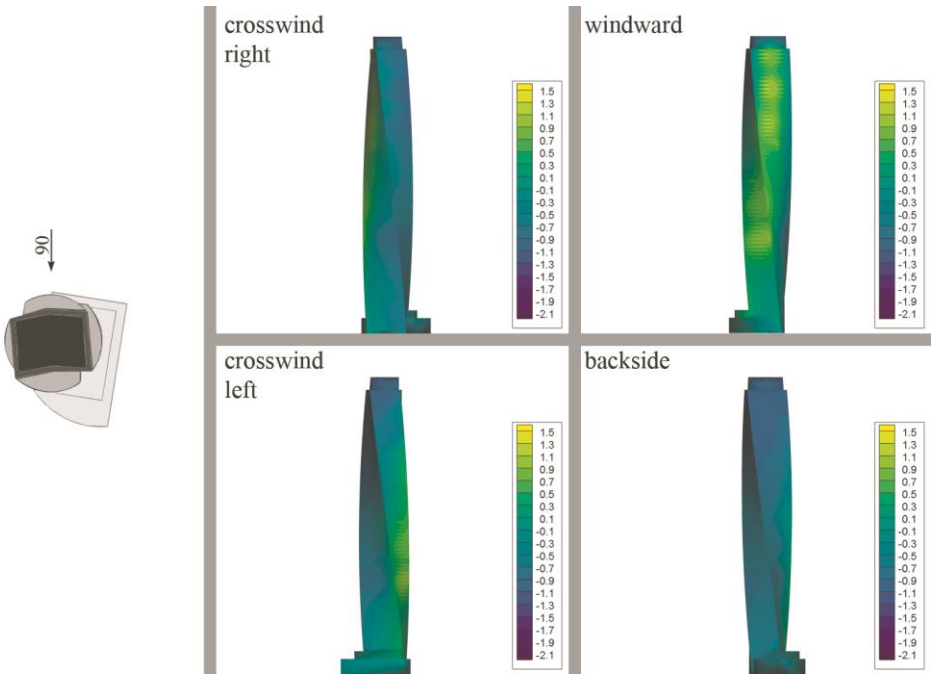

Figure 4.21. Wind direction and surface pressure distributions on windward, crosswind and back facades of twisting building at 90° angle of attack

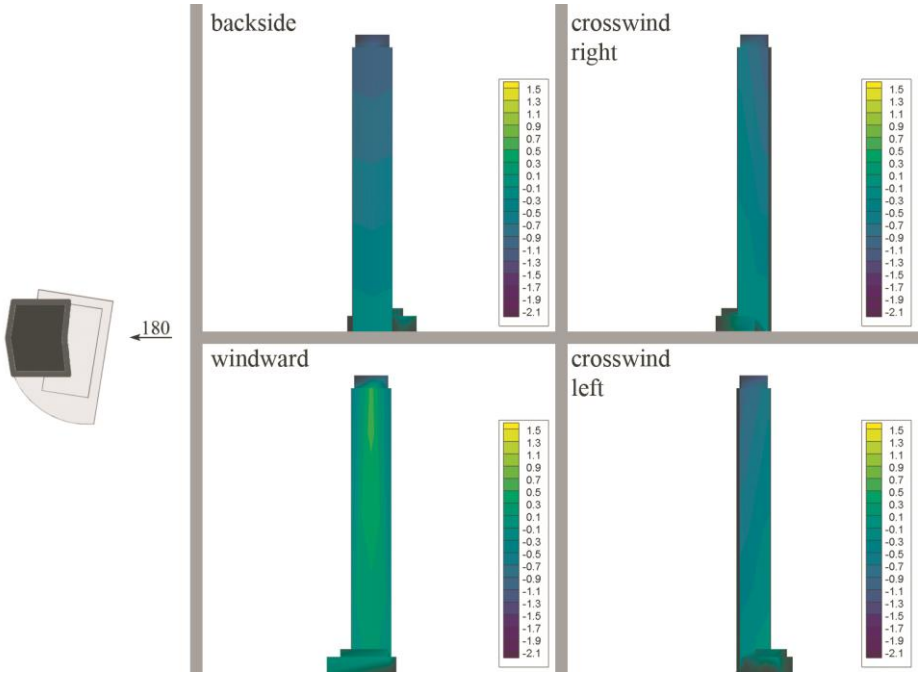

Figure 4.22. Wind direction and surface pressure distributions on windward, crosswind and back facades of prismatic building at 180° angle of attack

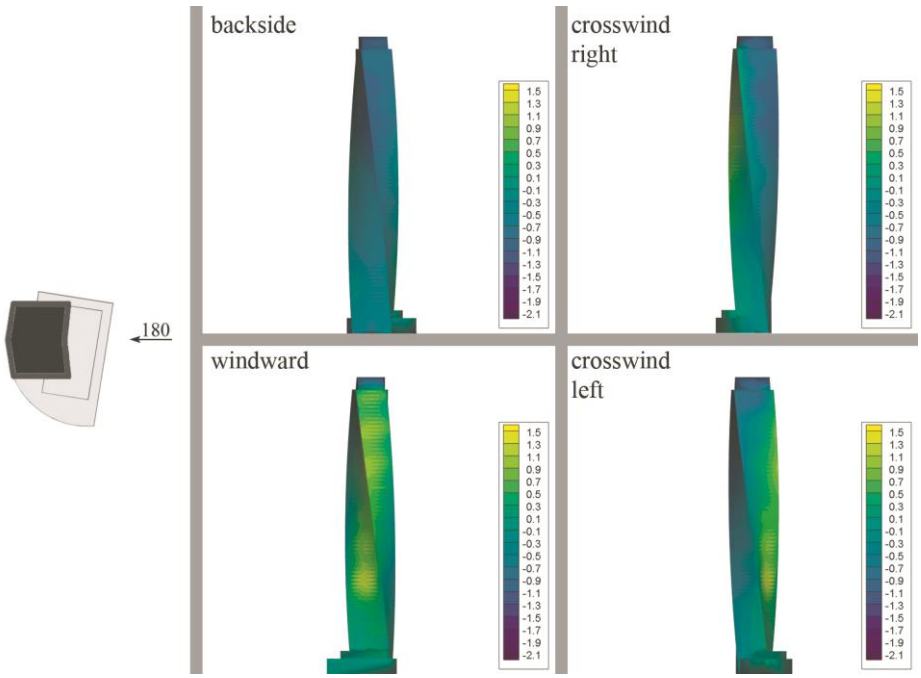

Figure 4.23. Wind direction and surface pressure distributions on windward, crosswind and back facades of twisting building at 180° angle of attack

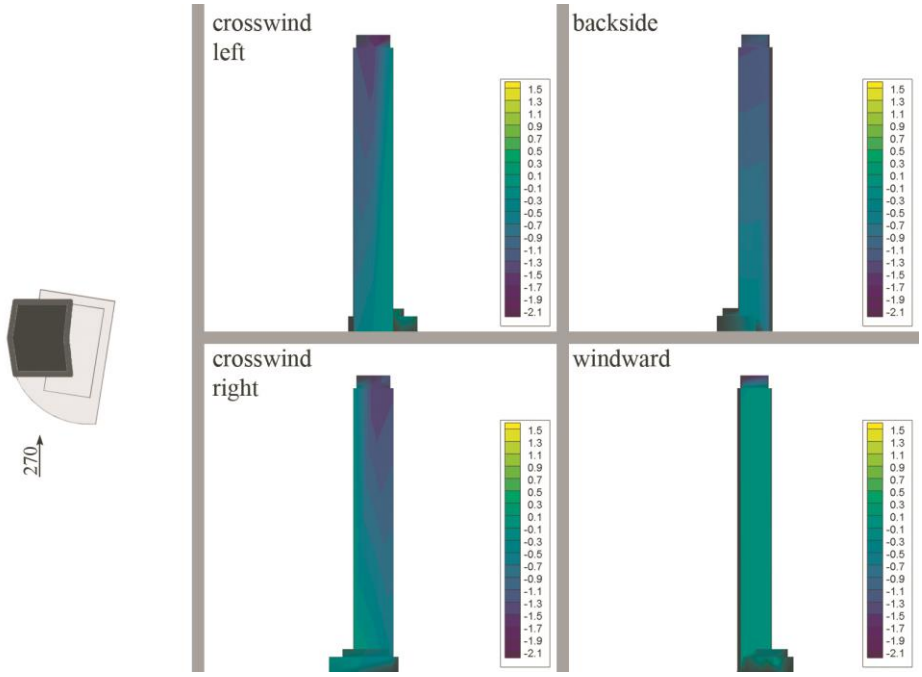

Figure 4.24. Wind direction and surface pressure distributions on windward, crosswind and back facades of prismatic building at 270° angle of attack

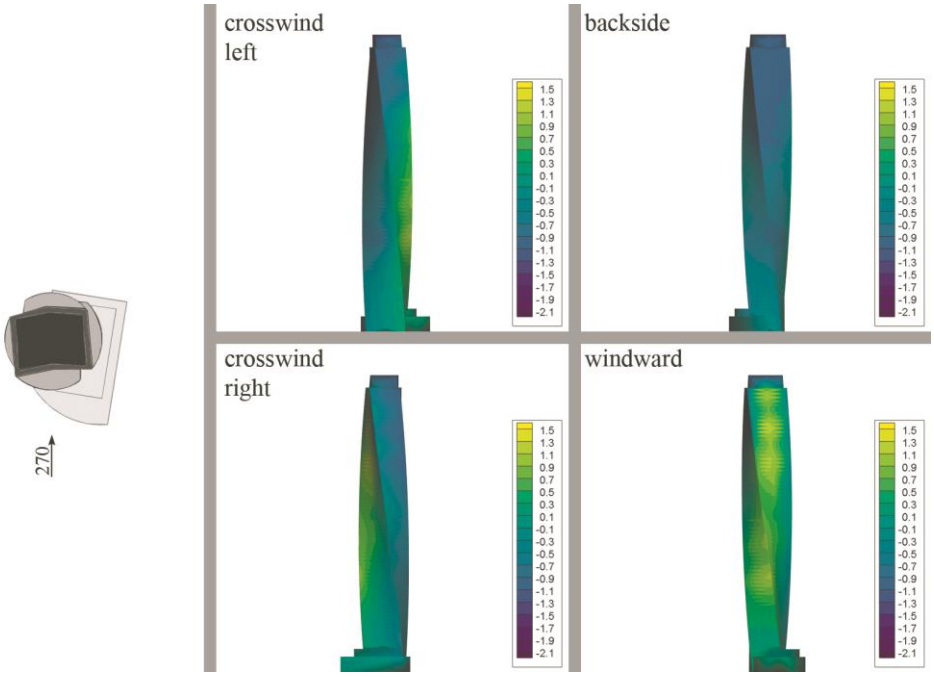

Figure 4.25. Wind direction and surface pressure distributions on windward, crosswind and back facades of twisting building at 270° angle of attack

4.1.4. Comparison with CFD Analyses

This section is dedicated to comparison of experimental and numerical investigations to show the consistency between the results of HFBB tests and CFD analyses. CFD analyses of twisting and prismatic buildings have been performed within the scientific research project, BAP-08-11-2016-064 (Ay, Sezer-Uzol, Bilgen, & Orbay, 2018). Analysis were carried out by using the facility at the High-Performance Computing Laboratory of METUWIND. Besides, preliminary results for small scale models are presented by Orbay, Bilgen, Sezer-Uzol, Ay & Ostovan (2017).

Wind tunnel conditions are replicated in CFD simulations. The commercial software, Pointwise was used to generate computational grid around the models and the models are exported to CFD++ for analysis processes. Flow streamlines around twisting (left) and prismatic (right) forms is given in Figure 4.26 for 0° angle of attack. Contour lines represent the pressure distribution. Air flow around the twisting building model has a more complex structure with respect to the prismatic one and 3-dimensional effect of twisting form can be clearly observed when the flow streamlines are examined.

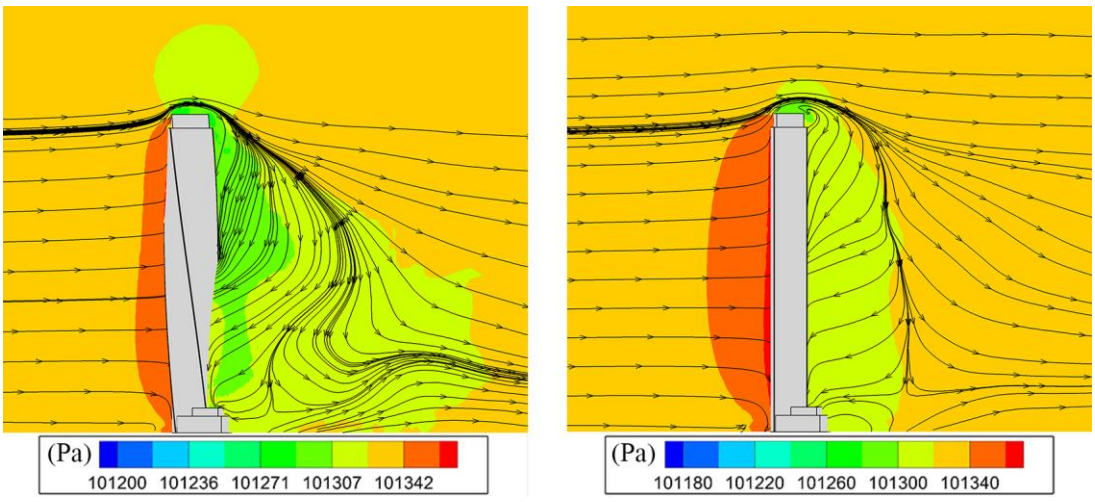

Figure 4.26. Flow streamlines around twisting (left) and prismatic (right) models for 0° angle of attack (Ay et. al., 2018)

Similar characteristics is drawn by 3-dimensional flow streamlines of 15° yaw angle as depicted in Figure 4.27. Streamlines are obtained from the 10th second of time dependent analyses. Vortices reach to further distances behind the twisting form when compared to the prismatic model.

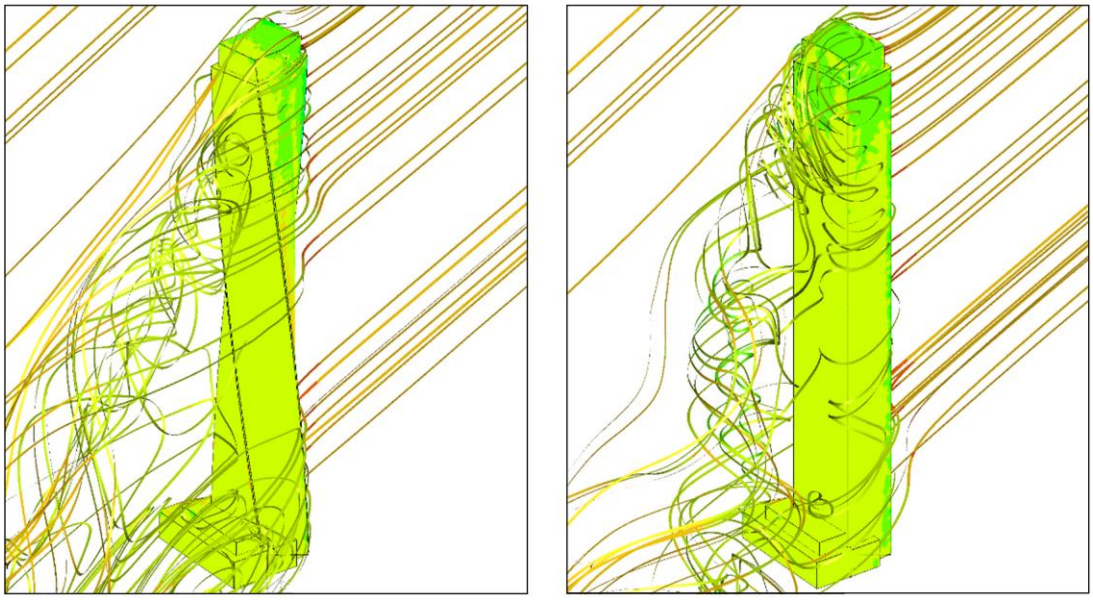

Figure 4.27. 3-dimensional flow streamlines around twisting (left) and prismatic (right) models for 15° angle of attack (Ay et. al., 2018)

Shear forces and mean moments of 1/750 scaled twisting and prismatic models are compared in Figure 4.28 and Figure 4.29 respectively for 15°, 75°, 105°, 255°, 285° and 345° yaw angles. Comparisons are given upon the results of HFBB tests and CFD analyses. The results are quite compatible substantially only with the exceptions. Regarding the prismatic model, a degree of variance is obtained for the shear force F_Y (75° and 255°) and moment M_X (255°) at specific angles of attack. In consequences, outcomes of HFBB tests and CFD analyses are accepted as consistent. Detailed comparative results are available from the final report of scientific research project BAP-08-11-2016-064 (Ay et. al., 2018).

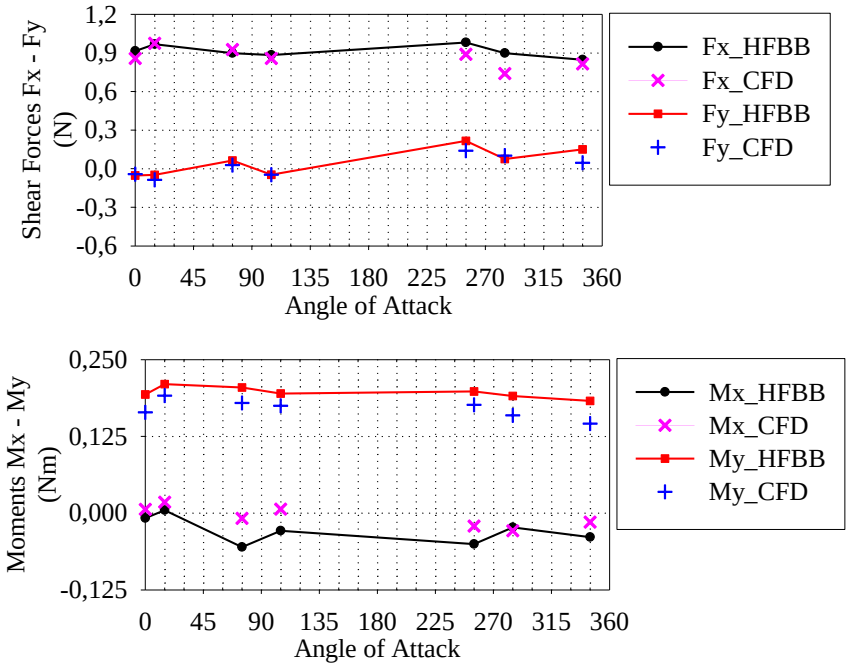

Figure 4.28. Shear forces (F_x and F_y) (top) and mean moments (M_x and M_y) (bottom) of twisting building; HFBB tests vs. CFD analysis (Ay et. al., 2018)

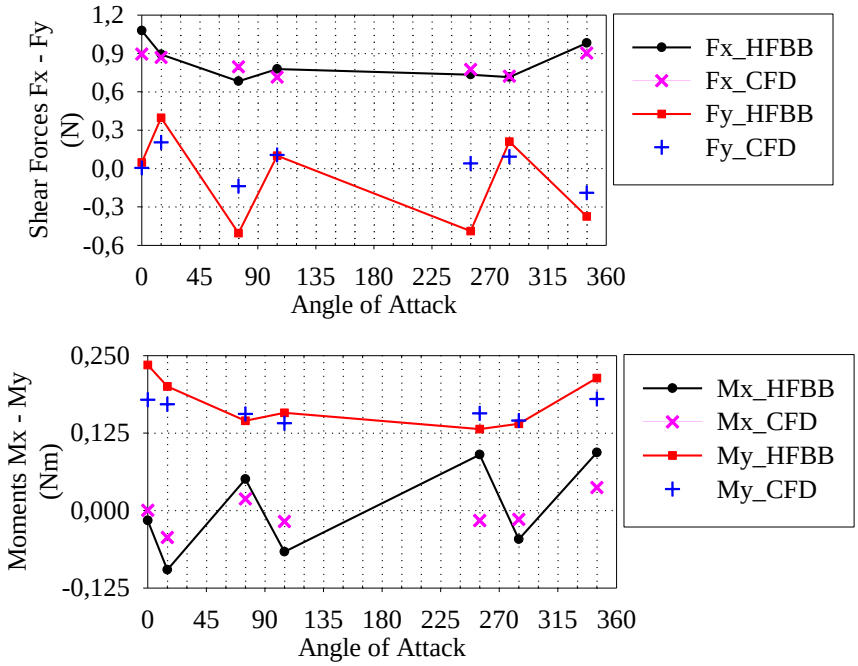

Figure 4.29. Shear forces (F_x and F_y) (top) and mean moments (M_x and M_y) (bottom) of prismatic building; HFBB tests vs. CFD analysis (Ay et. al., 2018)

4.2. Results of Structural Analyses

Determination of wind loads through HFBB tests are explained in Section 4.1.1. Comparative results of the analyses are discussed in two phases including the overall structure and structural members particularly for twisting and prismatic structures.

4.2.1. Modal Analyses of Twisting and Prismatic Forms

As mentioned earlier, reliability of twisting structural model is verified by comparing the results of modal analysis with the results of Baker et. al. (2010). It is seen that, obtained period values almost coincide with the values declared by the structural designer (Baker et. al., 2010). In this regard, the model is considered to be accurate enough for the analyses. Since prismatic analysis model is prepared in the same format, it was accepted that the structural analysis results to be obtained from this model is also reliable. Modal direction factors and mass participation ratios for twisting and prismatic models are given in Table 4.2 and Table 4.3 respectively.

Table 4.2. *Modal direction factors and mass participation ratios of twisting model (ETABS Model)*

Mode	Period (sec)	UX	UY	RZ	Sum UX	Sum UY	Sum RZ
1	8.1	0.933	0.067	0	0.580	0.036	0.000
2	7.23	0.07	0.93	0	0.622	0.612	0.005
3	1.92	0.348	0.586	0.066	0.665	0.730	0.053
4	1.87	0.016	0.051	0.933	0.667	0.740	0.614

Table 4.3. *Modal direction factors and mass participation ratios of prismatic model (ETABS Model)*

Mode	Period (sec)	UX	UY	RZ	Sum UX	Sum UY	Sum RZ
1	7.48	1	0	0	0.618	0.000	0.001
2	6.4	0	1	0	0.618	0.627	0.005
3	1.83	0.997	0.001	0.002	0.780	0.627	0.006
4	1.81	0.002	0.004	0.994	0.780	0.628	0.612

First four mode shapes of twisting and prismatic models are drawn in Figure 4.30 and Figure 4.31 respectively. Mode shapes are depicted at 2000 scale factor for all views.

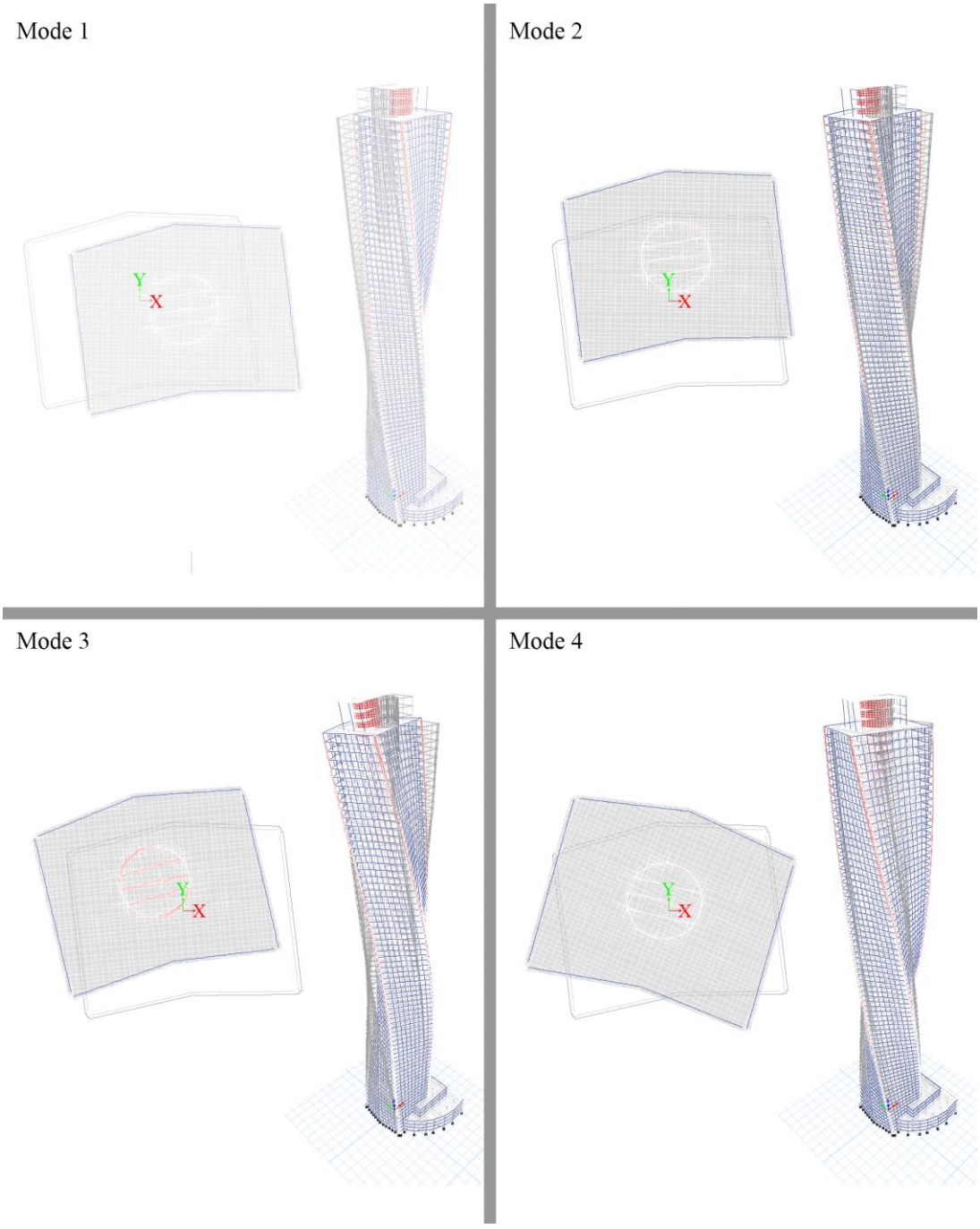

Figure 4.30. Mode shapes (1-2-3-4) of twisting model

Note that, Cayan Tower has a podium level consisting of 6 floors in total. Regarding the effects on modal periods, structural analysis models are prepared accordingly.

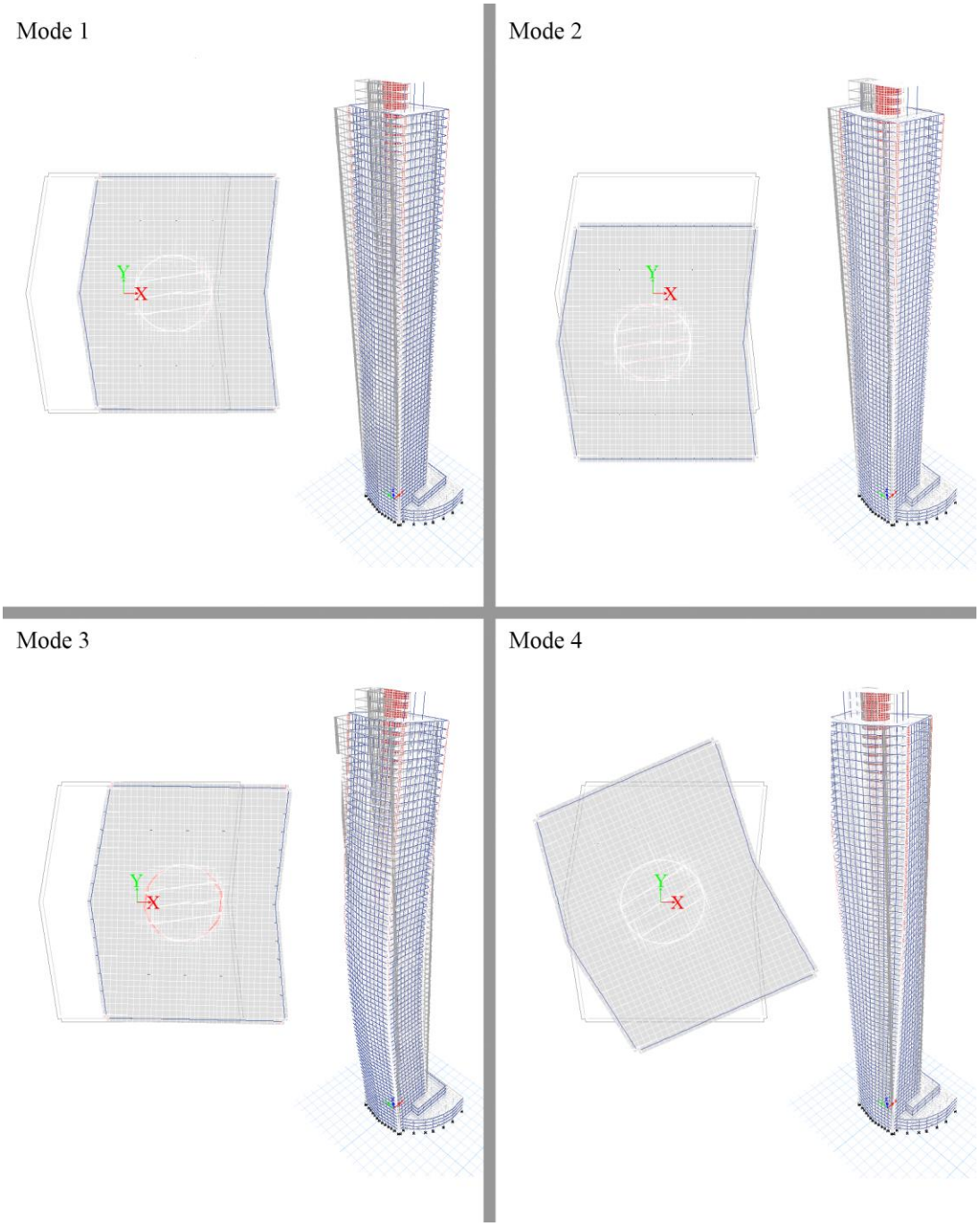

Figure 4.31. Mode shapes (1-2-3-4) of prismatic model

4.2.2. Base Moment and Top Deflection

Wind loads are obtained from the HFBB tests and assigned to building facades in a distributed formation through the height. Figure 4.32 illustrates shear force along X (left panel) and Y (right panel) axes of twisting and prismatic forms which are subjected to their maximum wind loads (30° and 135°angle of attack for twisting and prismatic form, respectively). As drawn below, a relatively constant 10% of lesser shear force was obtained through the height, along X axis for twisting form. Besides, along Y axis, twisting form is subjected to six percent to 23% (average 18%) less shear force with respect to its prismatic twin. It is worth mentioning that maximum difference is observed at base level.

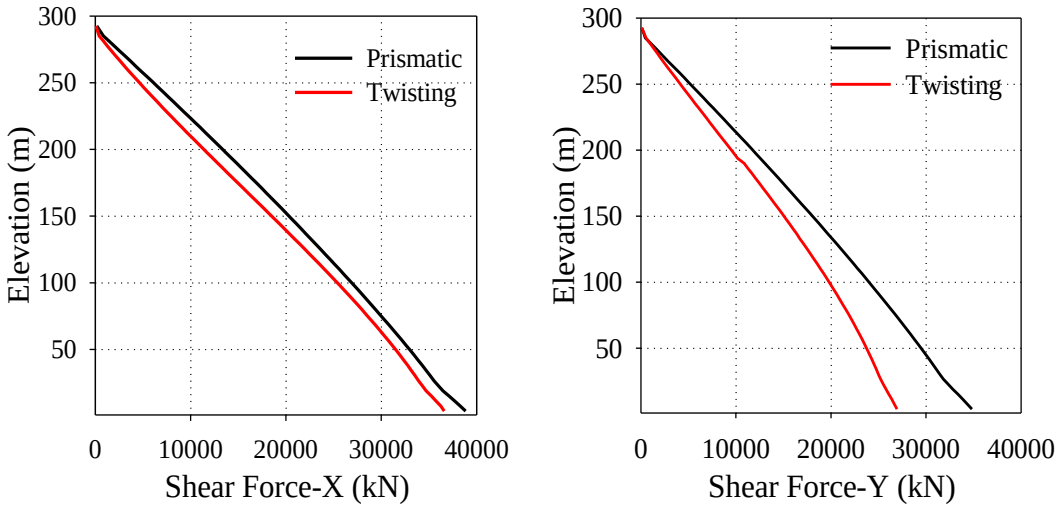

Figure 4.32. Comparison of shear forces along X (left panel) and Y (right panel) axes of twisting and prismatic forms

As well as the base moments and base shears; top displacement value is critical for the structural design of a tall building (serviceability design). In accordance with the wind loading shown above, Figure 4.33 compares story displacements in principle axes of twisting and prismatic buildings.

Although story displacements in X axis of twisting and prismatic forms are relatively close to each other up to a level of 133 m (floor 34), twisting structure displays less story displacement after this level with respect to its prismatic twin. On the other hand, difference between story displacements in Y axis is distinct from bottom to top in favor of twisting form. In addition, top displacement of twisting building is found as h/773 in X axis and h/1466 in Y axis. Those are h/651 in X axis and h/1007 in Y axis for prismatic building. As drawn, top displacement of both forms is quite smaller according to h/500 limit design criteria (serviceability). Note that, obtained displacement values are calculated with reference to center point of the core.

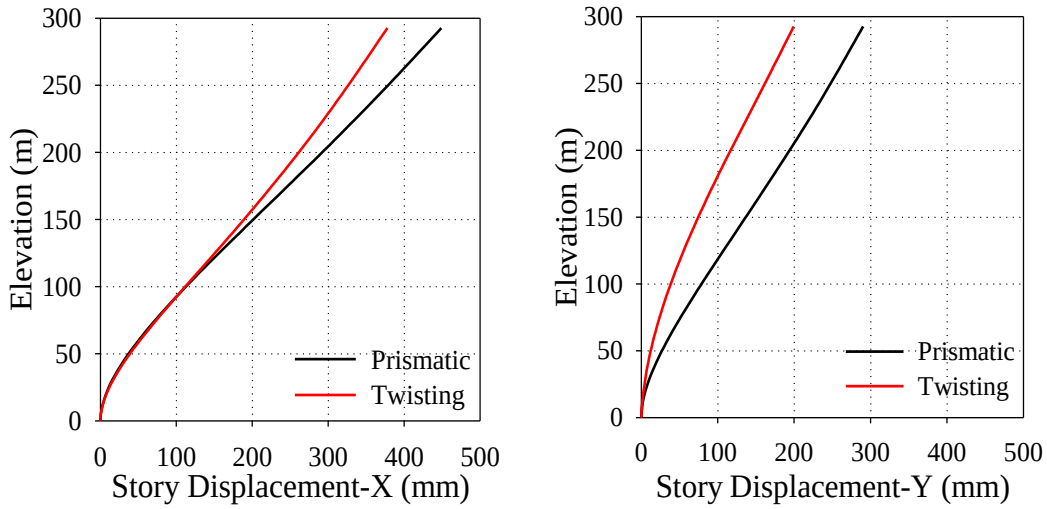

Figure 4.33. Story displacement in X (left) and Y (right) axes of twisting and prismatic forms

Finally, exposed torsion levels of equivalent twisting and prismatic forms are depicted in Figure 4.34. As shown below, different characteristics are drawn through the podium levels and tower levels for both forms. When compared, despite the lesser story displacements and shear forces, almost 3 times larger torsion is observed for the twisting form. Such a considerable divergence is obtained only under the wind loads and effects of gravity loads is argued in the next section.

Considering the obtained outcomes; even in different rates, results of this study are similar in terms of shear forces and story displacements with the results of Tanaka et. al. (2013). The main reasons for this rate difference can be easily understood. The tower plan is in square form for 90° rotation, but rectangular form has 180° rotation and outrigger structural system was investigated by the aforesaid study.

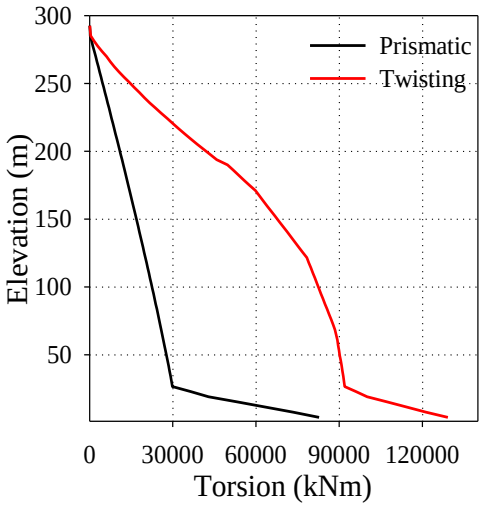

Figure 4.34. Torsion of twisting and prismatic models through the height

Besides, torsional response of this research varies from the findings Tanaka et. al. (2013) which is also presumed due to difference between the lateral load carrying systems of outrigger and tube structures. On the other hand, it is consistent with the findings of Moon (2015).

4.2.3. Load Distribution and Member Responses

In tube structures, significant portion of the lateral loads are carried by the perimeter tube (Günel & Ilgın, 2014) whereas, core is primarily responsible for carrying torsion (Clark & Scott, 2010). In order to compare the torsional demand on cores of twisting and prismatic forms, section cut is applied on ETABS models.

The comparison of core demands is shown in Figure 4.35. In the legend, the word "Total" refers to combination of overall static loads comprising dead load, super dead load, live load and the wind loads.

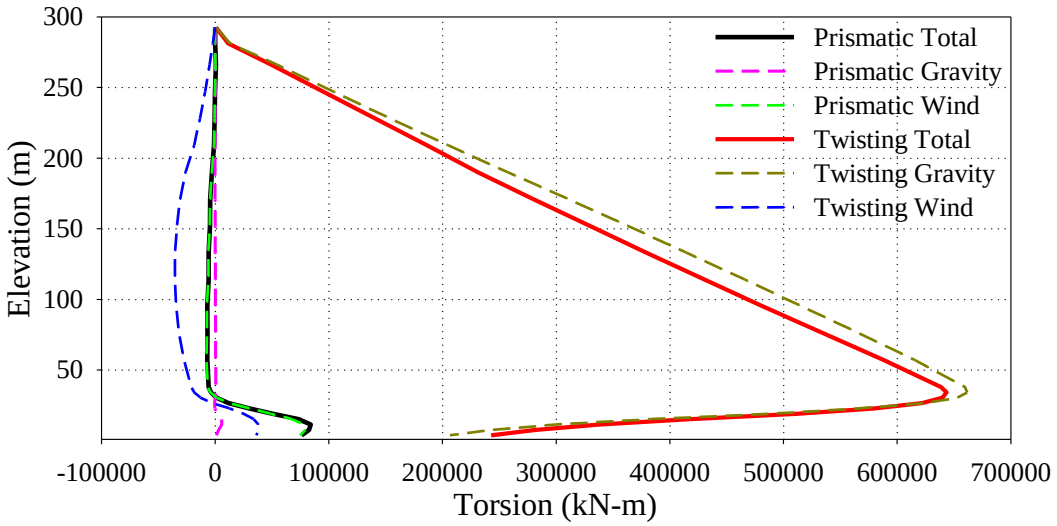

Figure 4.35. Core torsion levels of twisting and prismatic structures

Results unambiguously indicate that, wind-based torsion on the core (green dashed line) almost coincides with the total torsion (gravity + wind load) on the core (black solid line) of prismatic form. In twisting form, a significant part of the torsion occurs due to gravity loads (dark yellow dashed line). This observation is consistent with the results reported in Baker et. al. (2010).

In this particular angle in which the base moment is maximum, wind results in a negative torsion on the core (blue dashed line) of twisting form. Thus, the total torsion on the core (red continuous line) of twisting form is slightly smaller than the torsion due to gravity loads. Large perimeter shear walls located only in one side of the podium levels result in a dramatic change in torsion on core walls.

Structural member wise distribution of overturning moments is investigated under the combination of gravity and wind loads. Figure 4.36 illustrates the results for twisting (on top) and prismatic (on bottom) forms. As drawn below, significant portion of overturning moments is taken by the perimeter columns for both forms as typical behavior of tube structures. It is consistent with the expression of Rath (2014) regarding the real building.

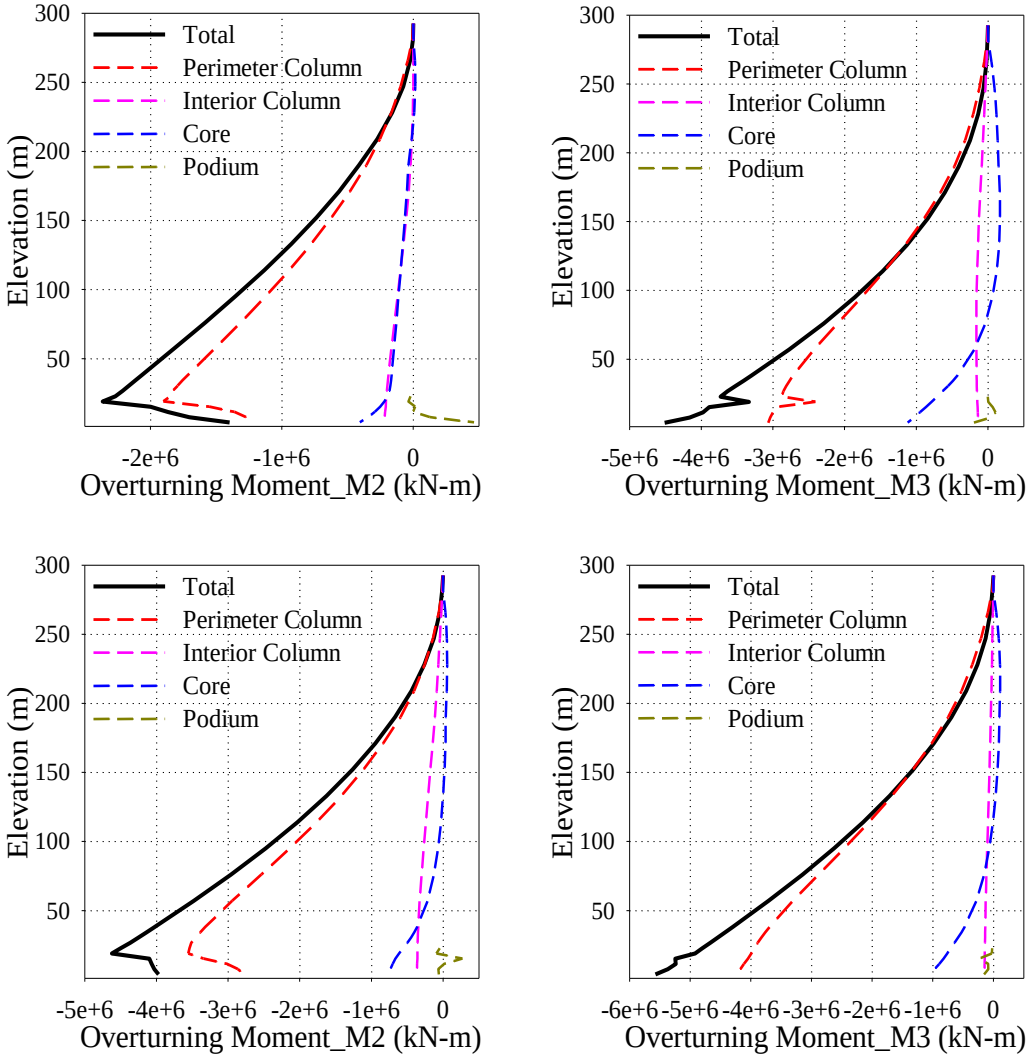

Figure 4.36. Distribution of overturning moments for twisting (on top) and prismatic (on bottom) structures in X (left panels) and Y (right panels) axes

Furthermore, frame members of structural analysis models are verified by design check feature of ETABS software. All columns of twisting structure passed the design check but only one column just above the shear walls of podium levels on prismatic structure failed (story 5) among 3428 columns. To preserve the compatibility between twisting and prismatic models (since frame sections of prismatic case are taken as same with the twisting structure) the prismatic model with one barely failed column among 3428 columns is used. Another consideration related with the frame members is internal forces. Figure 4.37 represents a detailed section of shear stresses (on left) and moment (on right) on the stepped perimeter columns and link beams (Figure 3.18; beam part 2) of twisting structure.

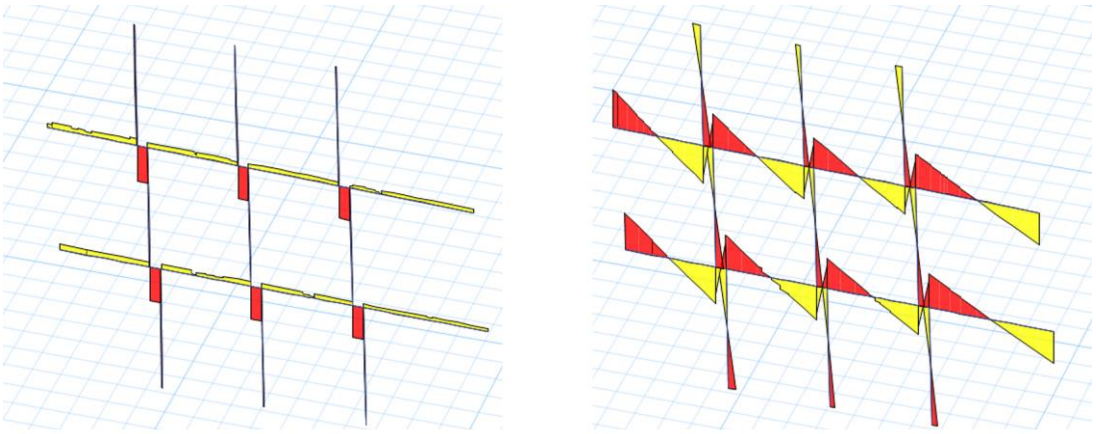

Figure 4.37. Shear force 2-2 diagram (left) and moment 3-3 diagram (right) on stepped perimeter columns and link beams of twisting structure

Referring to the Figure 4.37, it can be stated that, although stepped perimeter column approach reduces torsion and lateral drift due to self-weight of the twisting structure (Figure 3.4), local stress accumulation is obtained on link beams due to stress path discontinuity which might results in further design calculations and applications (such as coupling beam design and reinforcement etc.) on those specific structural elements.

CHAPTER 5

CONCLUSION

The whole research is summarized at the beginning of this chapter. Then, main outcomes related to objectives of the study are listed briefly. Afterwards, limitations of the research are outlined. The chapter is concluded with the future study recommendations in the light of obtained information.

5.1. Summary of the Work

The objective of this research is to investigate the aerodynamic and structural response characteristics of twisting tall buildings with respect to conventional prismatic forms. After introducing the necessary background information, existing literature is surveyed comprehensively in order to understand the possible potentials and challenges related to those structures. According to previous studies and existing examples, it is deduced that, twisting tall buildings are advantageous in terms of aerodynamic form, but their load carrying capacities can be relatively less due to their rotating structural system. Despite several studies mainly focused either on advantages or challenges of twisting buildings, clear and comprehensive analyses on their superiority and inferiority are missing in the existing literature. Regarding this research problem an existing twisting tall building was selected, and its conventional prismatic counterpart has been generated. A series of comparative HFBB and synchronous pressure measurement tests have been conducted to examine the base moments, static forces and surface pressure distributions for both forms. Tests were performed for each 15° angle to understand the effect of wind direction. Acquired wind tunnel data is used for static wind load analyses. Consequently, comparative results are evaluated in terms of base shear forces, story displacements and torsion.

5.2. Summary of the Results

Tall building design, particularly supertall building design is governed by the stiffness rather than strength. Thus, relatively less story displacement compared to higher values of torsion and secondary moments can be preferable in twisting tall building design. Furthermore, following conclusions can be stated from this research;

- Both forms can be advantageous in terms of mean moments according to wind direction. It is the impact of rectangular plan of the tower when compared to square plan.
- Background moment of the twisting form is smaller, which especially differentiated about 25% in across-wind direction.
- Resonant moments of the twisting form are relatively constant for both directions, variation on prismatic form is on a larger scale depending on the wind direction. Due to sharp edged form of prismatic building, vortex shedding characteristics are different for each angle of attack, whereas twisting form have a smoother response depending on the shape.
- Although twisting model is subjected to lesser base bending moments, localized surface pressure can be observed especially around twisting edges. Accordingly, it might bring additional complexities for cladding design of twisting form.
- Since the twisting building - under investigation - is subjected to lesser resultant base moment, lesser story displacement and lesser shear forces it can be declared as superior compared to the its prismatic twin in terms of aerodynamic form. On the other hand, almost 3 times larger torsion due to wind loads and significant degree of torsion due to gravity loads is observed for the twisting form. This variance becomes much larger under the combination of gravity and wind loads. Consequently, both advantages and disadvantages of twisting form should be taken into consideration.

- In aggregate, twisting form under investigation is aerodynamically better due to less wind loads both for along and across wind directions. Besides, it is also competitor in terms of shear forces and maximum story displacements but subjected to higher torsion. Since elimination of top displacement is a critical challenge and it effects the inhabitants (serviceability), higher torsion can be approached feasibly. Thus, considering gravity and wind loads only, twisting structural form can be preferable with respect to prismatic form in design of tall buildings.

5.3. Limitations of the Study

As usual, this research houses a number of limitations and assumptions. The major limitation of the study was drawn by the case study itself. Comparative tests and analyses were conducted for a building with a height of 300 m approximately.

Comparative response analyses have been scrutinized according to framed tube structural system only. In addition, adaptive structural system of the building is designed for a non-seismic region. Therefore, earthquake or combined loads which might amplify the torsion are not studied.

Relying on to the linear mode shape assumption of HFBB technique, the structural analyses that have been performed through this study and corresponding results are limited to linear mode shape compatible story wind loads.

Depending on the 1/750 model scale, maximum 45 pressure taps could be used for all surfaces in total. Thus, the density of pressure taps is relatively low. Although corresponding forces and moments show consistency with the CFD results, a degree of deviation is observed at specific angles.

5.4. Future Study Recommendations

Outcomes of this study is acquired from a selected existing twisting building. In the simplest terms, limitations of this research can be converted to recommendations for future studies. Similar procedure can be followed for the buildings with different heights such as “megatall” ones (over 600 m height). Also, the study can be expanded to other structural systems that are used for supertall buildings or with different twist angles. To summarize; other structures, existing or generic buildings can be used to compare twisting and prismatic forms in different heights, structural system and floor plan shapes.

In addition, reason behind the difference between the results of synchronous measurement tests and CFD analysis for specific angles can be investigated by additional studies.

Furthermore, investigation of earthquake loads, combined loads or the wake flow field can be studied comprehensively in order to scrutinize the trade-off between twisting and prismatic forms.

The last future study recommendation is related to methodology. Wind tunnel tests can be implemented on models with larger scale than 1/750. This way, extensive statements can be deducted from synchronous pressure measurement tests by increasing the density of pressure taps. Since elasticity has an effect on building responses (e.g., top displacement) much more realistic behavior can be observed if aeroelastic tests are conducted. Moreover, not only fundamental mode shapes, but also higher mode shapes can be investigated more elaborately.

REFERENCES

ACI Committee 318. (2014). *Building code requirements for structural concrete (ACI 318-14) : an ACI standard and commentary on building code requirements for structural concrete (ACI 318R-14) : an ACI report*. Farmington Hills, Michigan: American Concrete Institute.

Alaghmandan, M., Bahrami, P., & Elnimeiri, M. (2014). The Future Trend of Architectural Form and Structural System in High-Rise Buildings. *Architecture Research*, *4*(3), 55–62. https://doi.org/10.5923/j.arch.20140403.01

Alhatti, A. (2013). Ahmed Alhatti Chairman Cayan Group Interview CCTV The skyscraper with a twist Dubai's Cayan Tower [YouTube Video]. Retrieved from https://www.youtube.com/watch?v=n4nXF7OCHrc

Ali, M. M., & Moon, K. S. (2007). Structural Developments in Tall Buildings: Current Trends and Future Prospects. *Architectural Science Review*, *50*(3), 205–223.

Aly, A. M. (2013). Pressure integration technique for predicting wind-induced response in high-rise buildings. *Alexandria Engineering Journal*, *52*(4), 717–731. https://doi.org/10.1016/j.aej.2013.08.006

Aminmansour, A., & Moon, K. S. (2010). Integrated Design and Construction of Tall Buildings. *Journal of Architectural Engineering*, *16*(2), 47–53. https://doi.org/10.1061/(asce)1076-0431(2010)16:2(47)

Anderson, J. D. (2011). *Fundamentals of aerodynamics*. New York: Mcgraw-Hill.

Arabian Construction Company (2009). Al Bidda Tower | Arabian Construction Company. Retrieved April 18, 2019, from Arabian Construction Company website: https://www.accsal.com/projects/al-bidda-tower/

Arquitectobra. (2013, July 10). Torre F&F (Revolution Tower). Retrieved April 13, 2018, from http://arquitectobra.blogspot.com/2013/07/proyecto-destacado-torre-f-revolution.html

Arthitectural. (2011). GHD Global Pty Ltd Al Bidda Tower. Retrieved April 27, 2019, from https://www.arthitectural.com/ghd-global-pty-ltd-al-bidda-tower/

ASCE. (1999). *Wind Tunnel Studies of Buildings and Structures*. Reston, Va: American Society of Civil Engineers.

ASCE/SEI. (2017). *Minimum design loads and associated criteria for buildings and other structures: ASCE/SEI 7-16.* Reston, Virginia American Society of Civil Engineers.

AskariNejad, P. (2014). From "O" to "L" Design Challenges, Gazprom Tower. *CTBUH 2014 Shanghai Conference Proceedings, 556-562*.

Ay, B. Ö., Sezer-Uzol, N., Bilgen, S., & Orbay, E. (2018). *Burgulu Yüksek Binaların Taşıyıcı Sistem ve Aerodinamik Özelliklerinin İncelenmesi*. Middle East Technical University, Office of Scientific Research Projects Coordination.

Baker, W. F. (2017, September 21). *Building the world's tallest skyscraper, the Burj Khalifa* (A. Williams, Interviewer). Retrieved from https://newatlas.com/william-baker-interview-burj-khalifa/50751/

Baker, W. F., Brown, C. D., Young, B. S., & Zachrison, E. (2010). Infinity Tower, Dubai, UAE. *Structures Congress 2010*, 3078–3087.

Beedle, L. S., Ali, M. M., & Armstrong, P. J. (2007). *The skyscraper and the city: design, technology, and innovation / 1*. Lewiston: Mellen.

Bennett, D. (1995). *Skyscrapers: form & function*. New York: Simon And Schuster.

Bloomberg. (2014). Tallest U.S. Skyscraper Dream Kept Alive by Irish Builder. *Bloomberg.Com*. Retrieved from https://www.bloomberg.com/news/articles/2014-04-30/tallest-u-s-skyscraper-dream-kept-alive-by-irish-builder

Brownjohn, J. M. W., & Pan, T. C. (2001). Response of tall buildings to weak long distance earthquakes. *Earthquake Engineering & Structural Dynamics*, *30*(5), 709–729. https://doi.org/10.1002/eqe.32

Bunyan Program - Dubai TV. (2014). Cayan Tower Journey revealed by Bunyan Program- Dubai TV [YouTube Video]. Retrieved from https://www.youtube.com/watch?v=lQ-9vH1gdkI&t=33s

Cermak, J. E. (2003). Wind-tunnel development and trends in applications to civil engineering. *Journal of Wind Engineering and Industrial Aerodynamics*, *91*(3), 355–370. https://doi.org/10.1016/s0167-6105(02)00396-3

Clark, M., & Scott, D. M. (2010). New Songdo International City, Block D24, an Iconic and Efficient Twisted Tall Building Structure. *2010 Structures Congress ASCE*, 3066–3077.

CTBUH. (2016). Tall Buildings in Numbers: Twisted Tall Buildings. *CTBUH Journal*, (Issue III), 46–47.

CTBUH. (2019). CTBUH Height Criteria | Council on Tall Buildings and Urban Habitat. Retrieved 4, 2019, from Ctbuh.org website: http://www.ctbuh.org/criteria/

Çelebi, M. (2017, April). *Motion from Distant Earthquakes Can Shake Tall Buildings* (Seismological Society of America, Ed.) [Annual Meeting]. Retrieved from https://www.seismosoc.org/news/motion-distant-earthquakes-can-shake-tall-buildings/

DeSimone, V., Ramirez, L., & Mohammad, A. (2015). Structural Challenges of Twisting Towers. *CTBUH 2015 New York Conference, 478-484*.

Dubai Wind Code. (2013). Dubai Municipality.

Dutari, L. G. (2011). Facebook pagina Ingeniería LUIS GARCIA DUTARI - F&F Tower (Revolution). Retrieved from Luisgarciadutari.es.tl website: https://luisgarciadutari.es.tl/F%26F-Tower-k1-Revolution-k2-.htm

Duthinh, D., & Simiu, E. (2011). The Use of Wind Tunnel Measurements in Building Design. In *Wind Tunnels and Experimental Fluid Dynamics Research* (pp. 281–301). Rijeka: In Tech.

Efstathiou, G., & Baker, W. (2014). *The World's Tallest Twisting Tower: Cayan Tower, Dubai*. Presented at the CTBUH Awards 2014, 13th Annual Awards, Nowember 6, 2014.

Eurocode 1. (2005). *Eurocode 1: Actions on structures - Part 1-4: General actions - Wind actions*. Brussels: European Committee for Standardization.

Fu, F. (2018). *Design and analysis of tall and complex structures*. Kidlington, Oxford, United Kingdom: Butterworth-Heinemann, An Imprint of Elsevier.

Gamble, S. (2003, November). Wind Tunnel Testing. *Structure Magazine*, 24–27.

Gane, V., & Haymaker, J. (2007). Conceptual Design of High-Rises with Parametric Methods. *Predicting the Future [25th ECAADe Conference Proceedings / ISBN 978-0-9541183-6-5] Frankfurt Am Main (Germany) 26-29 September 2007*, 293–301.

Gensler. (2013). Gensler Design Update | Shanghai Tower. Retrieved May 12, 2018, from Gensler Design Update website: http://du.gensler.com/vol6/shanghai-tower/

Gerometta, M. (2009). The History of Measuring Tall Buildings | Council on Tall Buildings and Urban Habitat. Retrieved April 29, 2018, from Ctbuh.org website: http://www.ctbuh.org/about/measuringtall/

Golasz-Szolomicka, H., & Szolomicki, J. (2019). Architectural and Structural Analysis of Selected Twisted Tall Buildings. *IOP Conference Series: Materials Science and Engineering*, *471*, 052050. https://doi.org/10.1088/1757-899x/471/5/052050

Groesbeck, C., DeVries, J., Klemencic, R., & McDonald, J. F. (2012). Tall Buildings in Future Development of Metropolitan Universities. *CTBUH 2012 9th World Congress, Shanghai*.

Günel, M. H., & Ilgın, H. E. (2014). *Tall Buildings: Structural Systems and Aerodynamic Form* (1st ed.). London: Routledge.

Harbert, L. (2002). Home Insurance Building—The First Skyscraper. *Journal of American Society of Civil Engineers (ASCE)*, *43*(2), 3–4.

Hernandez, M. A. G., Lopez, A. I. M., Jarzabek, A. A., Perales, J. M. P., Wu, Y., & Xiaoxiao, S. (2013). Design Methodology for a Quick and Low-Cost Wind Tunnel. *Wind Tunnel Designs and Their Diverse Engineering Applications*. https://doi.org/10.5772/54169

Holmes, J. (2015). *Wind Loading of Structures, Third Edition*. Crc Press.

IABSE. (2019). Mode Gakuen Spiral Towers. Retrieved January 13, 2019, from https://www.iabse.org/Images/Outstanding%20Structure%20Awards%20PDFs/Spiral_Towers.pdf

Irwin, P. A. (2009). Wind Engineering Challenges of the New Generation of Super-Tall Buildings. *Journal of Wind Engineering and Industrial Aerodynamics*, *97*, 328–334.

Kayışoğlu, B. (2011). *Investigation of Wind Effects on Tall Buildings Through Wind Tunnel Testing* (Master Thesis). Middle East Technical University, Ankara, Turkey.

Kim, Y. C., Bandi, E. K., Yoshida, A., & Tamura, Y. (2015). Response characteristics of super-tall buildings – Effects of number of sides and helical angle. *Journal of Wind Engineering and Industrial Aerodynamics*, *145*, 252–262. https://doi.org/10.1016/j.jweia.2015.07.001

Kurç, Ö., Kayışoğlu, B., Shojaee, S. M. N., & Uzol, O. (2012). Yüksek Binalarda Rüzgar Etkilerinin Rüzgar Tüneli Deneyleriyle Tespiti. *İMO Teknik Dergi*, (389), 6163–6186.

Lagendijk, B., Pignetti, A., & Vacilotto, S. (2012). Case Study: Absoute World Towers, Mississauga. *CTBUH Journal*, (Issue IV), 11–17.

Liu, Z., Zheng, C., Wu, Y., Flay, R. G. J., & Zhang, K. (2019). Wind tunnel simulation of wind flows with the characteristics of thousand-meter high ABL. *Building and Environment*, *152*, 74–86. https://doi.org/10.1016/j.buildenv.2019.02.012

METUWIND. (2019). Experimental Aerodynamics Laboratory | RÜZGEM (METUWIND). Retrieved January 4, 2019, from Metu.edu.tr website: https://ruzgem.metu.edu.tr/en/experimental-aerodynamics-laboratory#WTC3

Mohotti, D., Mendis, P., & Ngo, T. (2014). Application of Computational Fluid Dynamics (CFD) in Predicting the Wind Loads on Tall Buildings-A Case Study. *23rd Australasian Conference on the Mechanics of Structures and Materials (ACMSM23) Byron Bay, Australia, 9-12 December 2014*, 1–6.

Moon, K. S. (2015). Structural Design and Construction of Complex-Shaped Tall Buildings. *International Journal of Engineering and Technology*, *7*(1), 30–35. https://doi.org/10.7763/ijet.2015.v7.761

Orbay, E., Bilgen, S., Sezer-Uzol, N., Ay, B. Ö., & Ostovan, Y. (2017). Numerical and Experimental Investigation of Aerodynamic Loads for Tall Buildings with Prismatic and Twisted Forms. *The International Conference on Wind Energy Harvesting, 20-21 April 2017, Coimbra, Portugal.*

Parker, D., & Wood, A. (2013). *The tall buildings reference book*. London; New York: Routledge, Cop.

Prohasky, D. J., Castro, R. M., Watkins, S., & Burry, J. (2016). Design Driven Physical Experimentation. *Living Systems and Micro-Utopias: Towards Continuous Designing, Proceedings of the 21st International Conference of the Association for Computer-Aided Architectural Design Research in Asia CAADRIA 2016*, 239–248.

Rath, N. (Ed.). (2014, December 14). When Engineering gets a Creative "twist." *Extreme Engineering Magazine*.

RMJM. (2019a). Lakhta Center. Height Gain: Made of Steel and Concrete [YouTube Video]. Retrieved from https://www.youtube.com/embed/5CApvwV_Cv8

RMJM. (2019b, June 13). RMJM. Retrieved June 20, 2019, from RMJM website: https://www.rmjm.com/lakhta-centre-facts/

Safetravels196. (2018). cornichedoha Archives | Safetravels196. Retrieved September 22, 2019, from Safetravels196 website: https://safetravels196.com/ngg_tag/cornichedoha/#gallery/cornichedoha/2386

Santiago Calatrava Architects. (2019). Turning Torso / Malmö (Overview) - Santiago Calatrava – Architects & Engineers. Retrieved March 15, 2019, from Calatrava.com website: https://calatrava.com/projects/turning-torso-malmoe.html

Scott, D., Farnsworth, D., Jackson, M., & Clark, M. (2007). The effects of complex geometry on Tall Towers. *The Structural Design of Tall and Special Buildings*, *16*(4), 441–455. https://doi.org/10.1002/tal.428

Sev, A., & Başarır, B. (2011). A Recent Trend In Tall Building Design: Twisted Forms. *New World Sciences Academy Engineering Sciences*, *6*(4), 1603–1619.

Shapiro, G. F. (2013). Cayan Tower, Designed by Skidmore, Owings & Merrill. *The Journal of the American Institute of Architects*.

Skidmore, Owings & Merrill LLP. (2013, June 14). SOM's Cayan Tower Opens. Retrieved April 19, 2016, from SOM website: http://www.som.com/news/soms_cayan_tower_opens

Skyscrapercity. (2017). Discuss: Twisting Towers - Page 7 - SkyscraperCity. Retrieved September 22, 2019, from Skyscrapercity.com website: https://www.skyscrapercity.com/showthread.php?t=1785186&page=7

Taghizadeh, K., & Seyedinnoor, S. (2013). Super -Tall Buildings Forms Based on Structural Concepts and Energy Conservation Principles. *Architecture Research*, *3*(2), 13–19.

Tanaka, H., Tamura, Y., Ohkate, K., Nakai, M., Kim, Y. C., & Bandi, E. K. (2013). Aerodynamic and Flow Characteristics of Tall Buildings with Various Unconvantional Configurations. *International Journal of High-Rise Buildings*, *2*(3), 213–228.

Taranath, B. S. (1998). *Steel, concrete, and composite design of tall buildings*. New York; London: Mcgraw-Hill.

Taranath, B. S. (2010). *Reinforced concrete design of tall buildings*. Boca Raton: Crc Press.

Taşkın, G. N. (2019). *A Comparative Study in Alternative Structural System Layouts of Twisted Tall Buildings* (Master Thesis). Middle East Technical University, Ankara, Turkey.

The Skyscraper Center. (2019a). 100 Tallest Under Construction Buildings in the World. *Skyscrapercenter.Com*. Retrieved from http://www.skyscrapercenter.com/buildings?list=tallest100-construction

The Skyscraper Center. (2019b). All Global Buildings, 2005-No Max. Year. *Skyscrapercenter.Com*. Retrieved from https://www.skyscrapercenter.com/quick-lists#q=&page=1&type=building&status=COM&status=UCT&status=STO&status=UC&min_year=2005&max_year=9999&region=0&country=0&city=0

The Skyscraper Center. (2019c). *Cayan Tower*. Retrieved from http://www.skyscrapercenter.com/building/cayan-tower/464

The Skyscraper Center. (2019d). Completed Buildings in the World, No Min. Year-No Max. Year. *Skyscrapercenter.Com*. Retrieved from https://www.skyscrapercenter.com/compare-data/submit?type%5B%5D=building&status%5B%5D=COM&base_height_range=4&base_company=All&base_min_year=1885&base_max_year=9999&skip_comparison=on&output%5B%5D=list

The Skyscraper Center. (2019e). F&F Tower. *Skyscrapercenter.Com*. Retrieved from https://www.skyscrapercenter.com/building/ff-tower/953

The Skyscraper Center. (2019f). *Ocean Heights*. Retrieved from https://www.skyscrapercenter.com/building/ocean-heights/446

The Skyscraper Center. (2019g). *Shanghai Tower*. Retrieved from http://www.skyscrapercenter.com/building/shanghai-tower/56

The Skyscraper Center. (2019h). *Turning Torso*. Retrieved from http://www.skyscrapercenter.com/building/turning-torso/1979

Tschanz, T., & Davenport, A. G. (1983). The base balance technique for the determination of dynamic wind loads. *Journal of Wind Engineering and Industrial Aerodynamics*, *13*(1–3), 429–439. https://doi.org/10.1016/0167-6105(83)90162-9

Vollers, K. (2001). *Twist & build: creating non-orthogonal architecure*. Rotterdam: 010 Publishers.

Vollers, K. (2009). The CAD-tool 2.0 morphological scheme of non-orthogonal high-rises. *CTBUH Journal*, (3), 38–49.

Vollers, K. J. (2005). High-Rise Buildings with Twisted Facades. *7th World Congress: Renewing the Urban Landscape, New York, 16-19 October*.

Watts, S., Kalita, N., & Maclean, M. (2007). The economics of super-tall towers. *The Structural Design of Tall and Special Buildings*, *16*(4), 457–470. https://doi.org/10.1002/tal.424

Wikipedia. (2004, October 6). Turning Torso. Retrieved July 5, 2019, from Wikipedia website: https://en.wikipedia.org/wiki/Turning_Torso

Wikipedia. (2019, September 23). Ocean Heights (Dubai). Retrieved September 25, 2019, from Wikipedia website: https://en.wikipedia.org/wiki/Ocean_Heights_(Dubai)

Wood, A. (2011). *Best tall buildings 2010: CTBUH international award winning projects*. Chicago: Routledge.

Xia, J., Poon, D., & Mass, D. C. (2010). Case Study: Shanghai Tower. *CTBUH Journal*, (Issue II).

Yılmaztük, S., & Sezer-Uzol, N. (2011). Investigation of Flow Field Around A High-Rise Building Model in Atmospheric Boundary Layer. *6. Ankara International Aerospace Conference 14-16 September 2011 - METU, Ankara, Turkey*, 1–12.

Yong, T. H., & Dol, S. S. (2015). Design and Development of Low-Cost Wind Tunnel for Educational Purpose. *IOP Conference Series: Materials Science and Engineering*, *78*, 012039. https://doi.org/10.1088/1757-899x/78/1/012039

Zhao, R., Xu, A., Sun, W., & Lan, X. (2017). Model shape correction method for high-frequency force balance technique. *Journal of Vibroengineering*, *19*(3), 1665–1679. https://doi.org/10.21595/jve.2017.17938

Zhou, Y., Kijewski, T., & Kareem, A. (2003). Aerodynamic Loads on Tall Buildings: Interactive Database. *Journal of Structural Engineering*, *129*(3), 394–404. https://doi.org/10.1061/(asce)0733-9445(2003)129:3(394)

Zhu, Y., Poon, D., Zhou, S., & Fu, G. (2012). Structural Design Challenges of Shanghai Tower. *CTBUH 2012 9th World Congress, Shanghai*.

APPENDICES

A. BLOCKAGE RATIOS FOR TWISTING AND PRISMATIC MODELS

Table A.1. *Blockage ratios for twisting and prismatic models*

	PRISMATIC MODEL (1/750 SCALE)		**TWISTING MODEL (1/750 SCALE)**	
ANGLE	MAXIMUM MODEL CROSS- SECTIONAL AREA (cm^2)	BLOCKAGE RATIO (%)	MAXIMUM MODEL CROSS- SECTIONAL AREA (cm^2)	BLOCKAGE RATIO (%)
0	215.6079	2.24	241.5742	2.52
15	244.5944	2.55	244.013	2.54
30	260.5329	2.71	246.8422	2.57
45	260.5467	2.71	248.1205	2.58
60	244.8534	2.55	247.5555	2.58
75	213.4125	2.22	244.6089	2.55
90	183.3624	1.91	239.6414	2.50
105	212.1964	2.21	231.8855	2.41
120	246.1607	2.56	228.5949	2.38
135	263.7688	2.75	227.9961	2.37
150	264.4748	2.75	230.0369	2.40
165	248.157	2.58	235.0189	2.45
180	215.6079	2.24	241.4917	2.51
195	244.5944	2.55	244.0131	2.54
210	260.5329	2.71	246.8422	2.57
225	260.5467	2.71	248.1205	2.58
240	244.8534	2.55	247.5555	2.58
255	213.4125	2.22	244.6089	2.55
270	183.3624	1.91	236.6414	2.46
285	212.1964	2.21	231.8846	2.41
300	246.1607	2.56	228.5949	2.38
315	263.7688	2.75	227.9943	2.37
330	264.4748	2.75	230.0378	2.40
345	248.157	2.58	235.0203	2.45
WIND TUNNEL CROSS-SECTION AREA=9604 cm^2				

B. TIME SERIES AND FFT GRAPHS OF HFBB TESTS

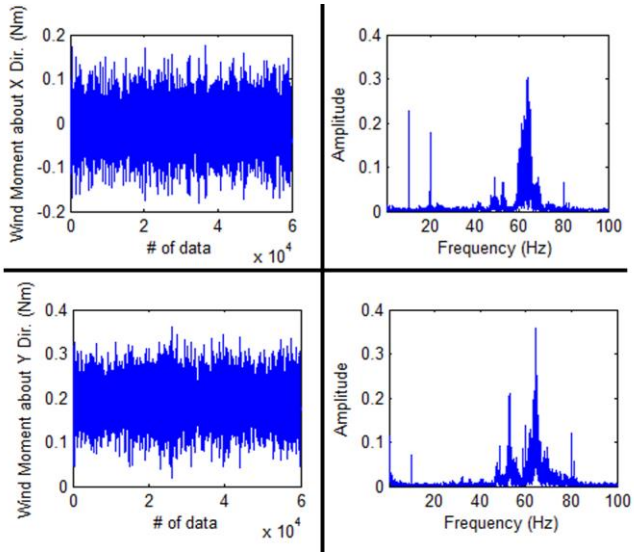

Figure B.1. Twisting model, 0° angle of attack; base bending moment and FFT graph in X (top) direction and Y (bottom) direction

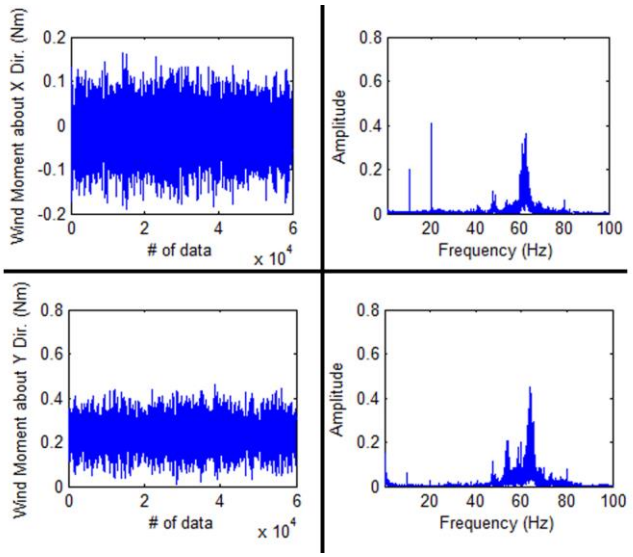

Figure B.2. Prismatic model, 0° angle of attack; base bending moment and FFT graph in X (top) direction and Y (bottom) direction

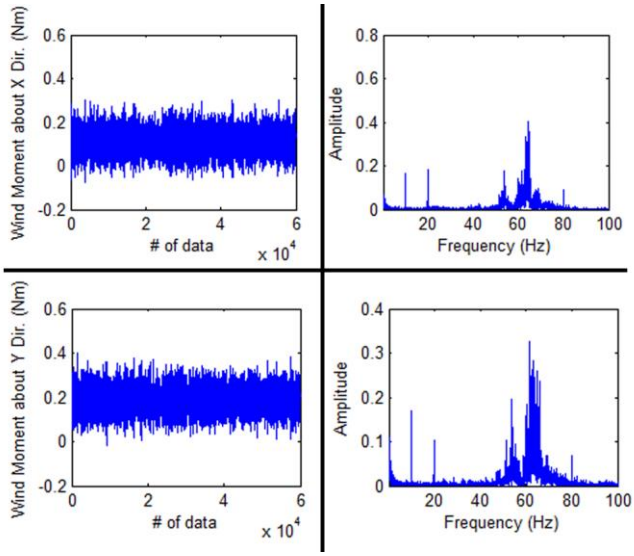

Figure B.3. Twisting model, 30° angle of attack; base bending moment and FFT graph in X (top) direction and Y (bottom) direction

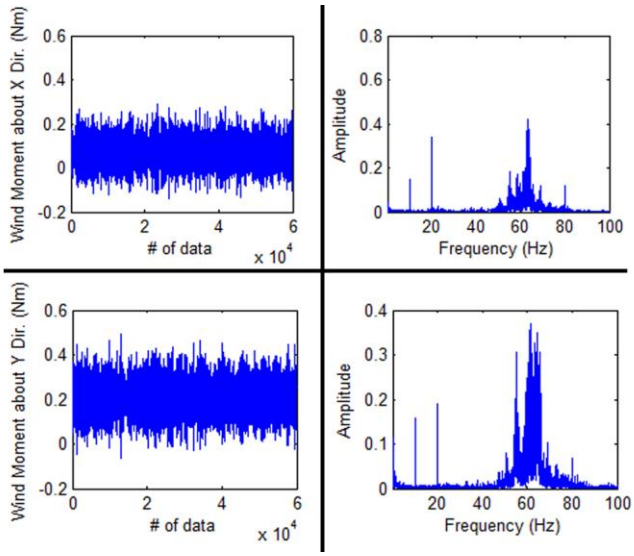

Figure B.4. Prismatic model, 30° angle of attack; base bending moment and FFT graph in X (top) direction and Y (bottom) direction

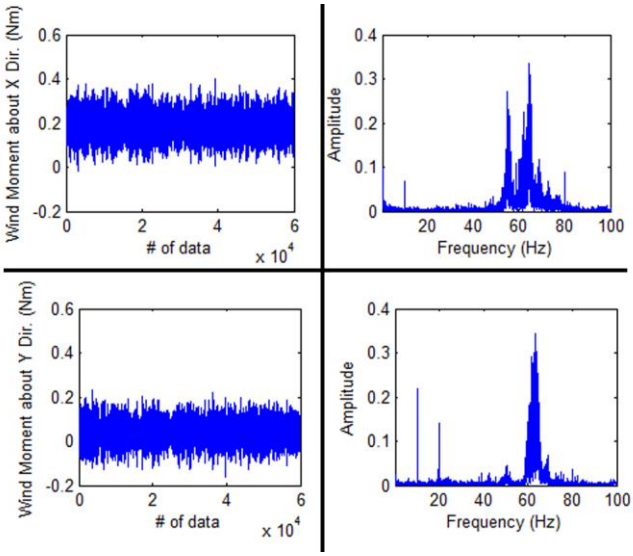

Figure B.5. Twisting model, 90° angle of attack; base bending moment and FFT graph in X (top) direction and Y (bottom) direction

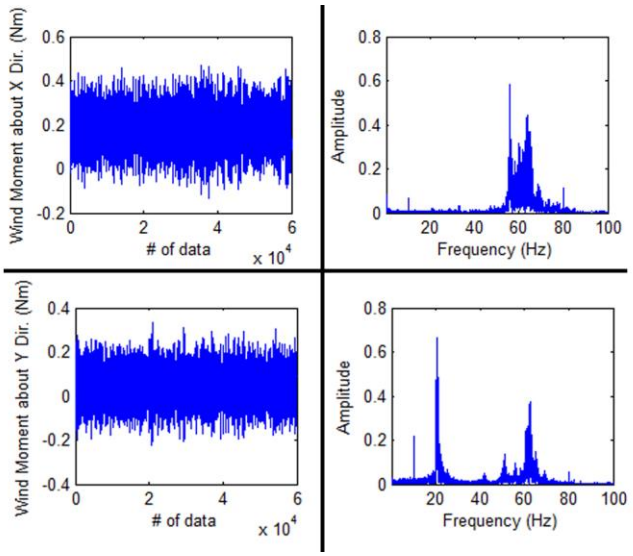

Figure B.6. Prismatic model, 90° angle of attack; base bending moment and FFT graph in X (top) direction and Y (bottom) direction

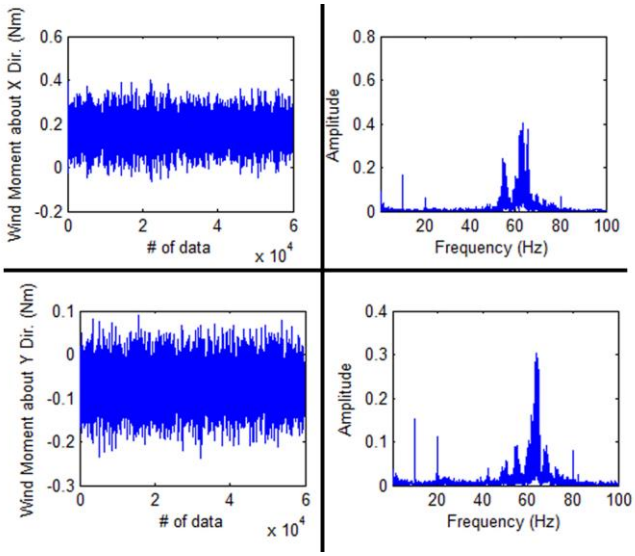

Figure B.7. Twisting model, 135° angle of attack; base bending moment and FFT graph in X (top) direction and Y (bottom) direction

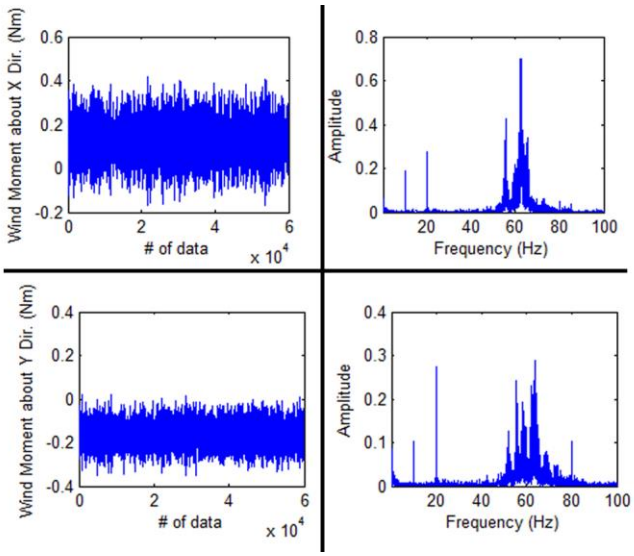

Figure B.8. Prismatic model, 135° angle of attack; base bending moment and FFT graph in X (top) direction and Y (bottom) direction

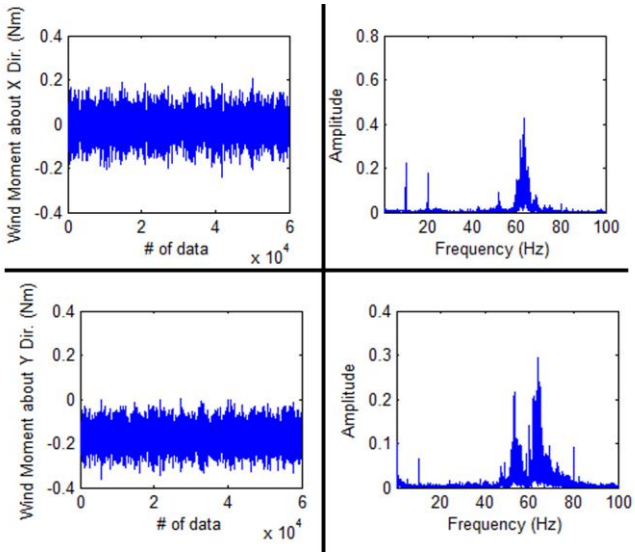

Figure B.9. Twisting model, 180° angle of attack; base bending moment and FFT graph in X (top) direction and Y (bottom) direction

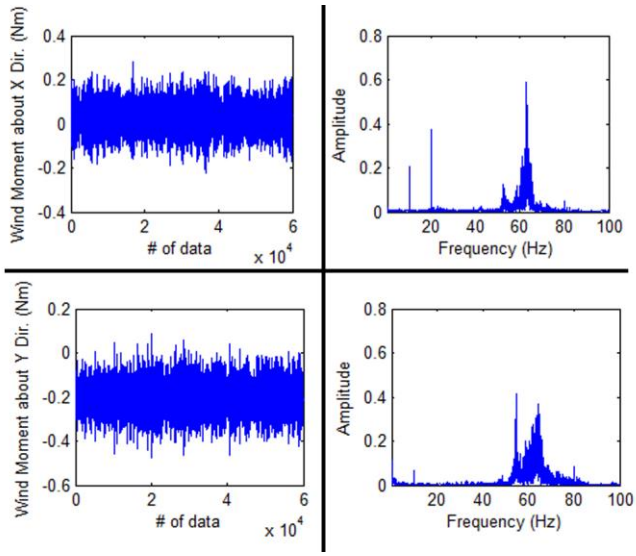

Figure B.10. Prismatic model, 180° angle of attack; base bending moment and FFT graph in X (top) direction and Y (bottom) direction

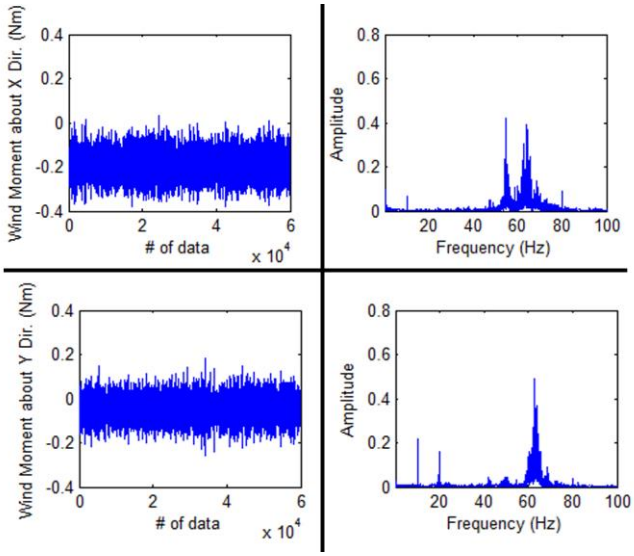

Figure B.11. Twisting model, 270° angle of attack; base bending moment and FFT graph in X (top) direction and Y (bottom) direction

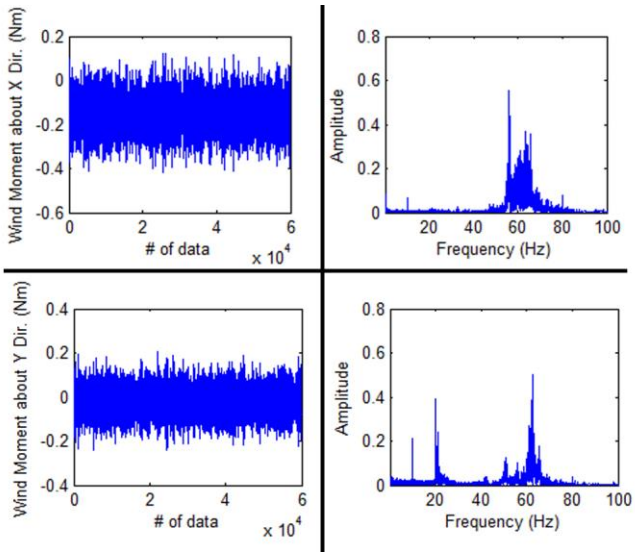

Figure B.12. Prismatic model, 270° angle of attack; base bending moment and FFT graph in X (top) direction and Y (bottom) direction